Heavy Ions with the ATLAS Experiment

Helena Santos

LIP, FCUL

https://www.youtube.com/watch?v=g4n-VGTus_o

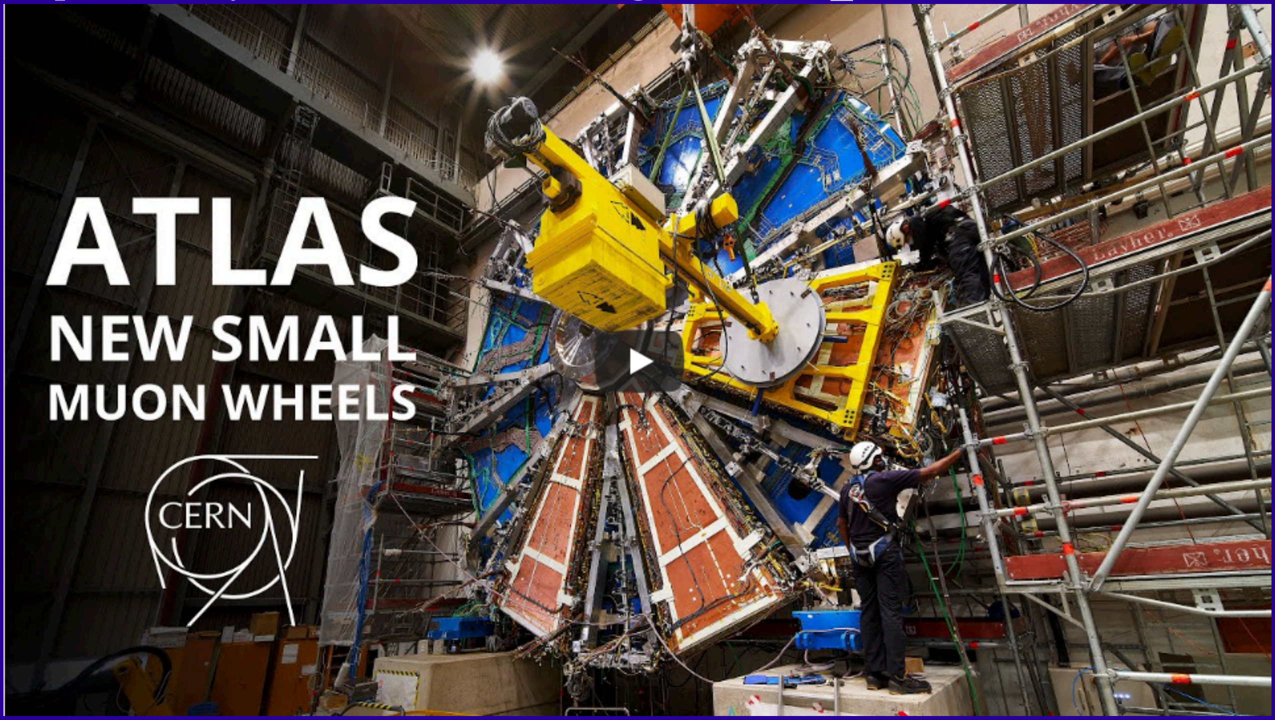

In Memoriam Stephanie Zimmermann

LIP 2020, 11 November, Coimbra

Heavy Ion Physics

- Introduction to the HI physics
- Global observables
- Electroweak probes
- Hard probes
- An 80 years old prediction
- Summary

Heavy Ion Physics

Goal is to understand QCD in extreme conditions of temperature and density
→ study distinct phases of matter: hadronic vs. partonic deconfined system (a plasma of quarks and gluons - the QGP)

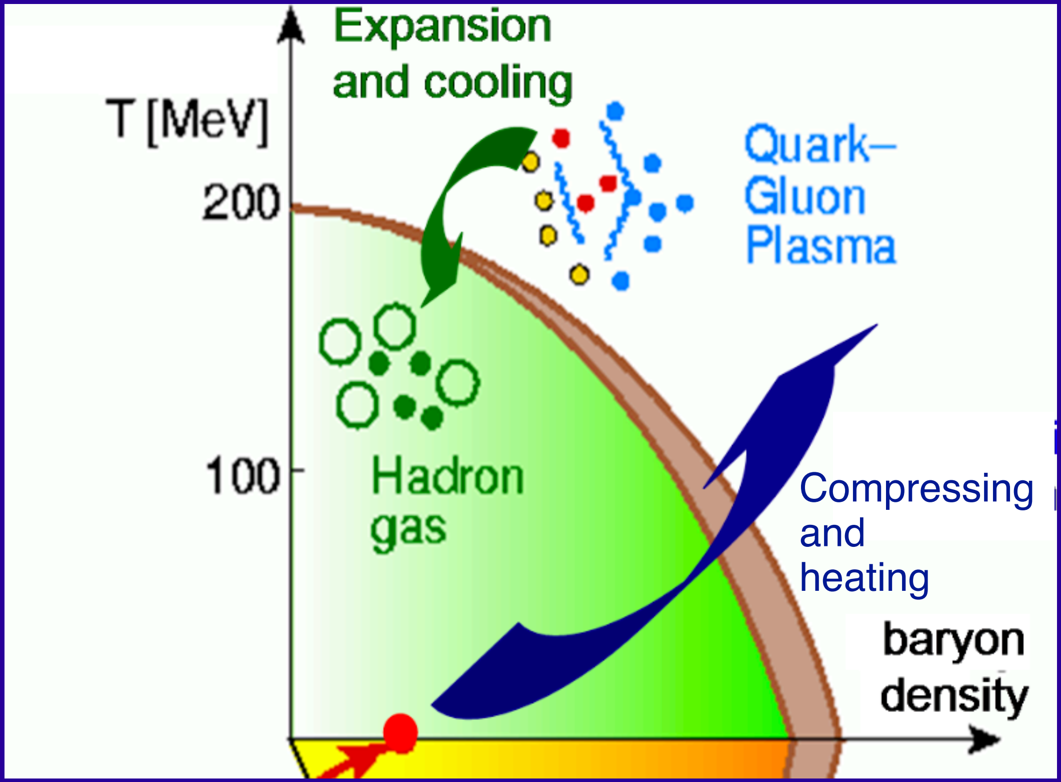

nuclei ($n_B = 0.14/fm^3$)

Heavy Ion Physics

Time evolution of heavy-ion (HI) collisions:

- Initial state
- QGP state
- Hadronic state

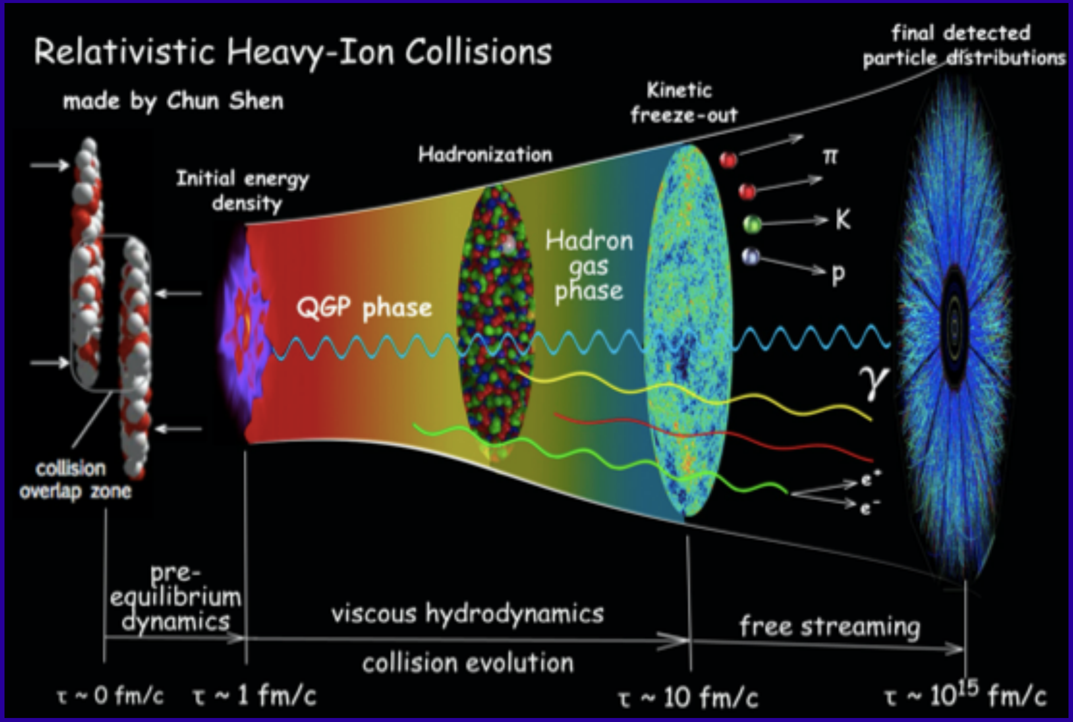

Heavy Ion Physics

Time evolution of heavy-ion (HI) collisions:

Initial state

QGP state

Hadronic state

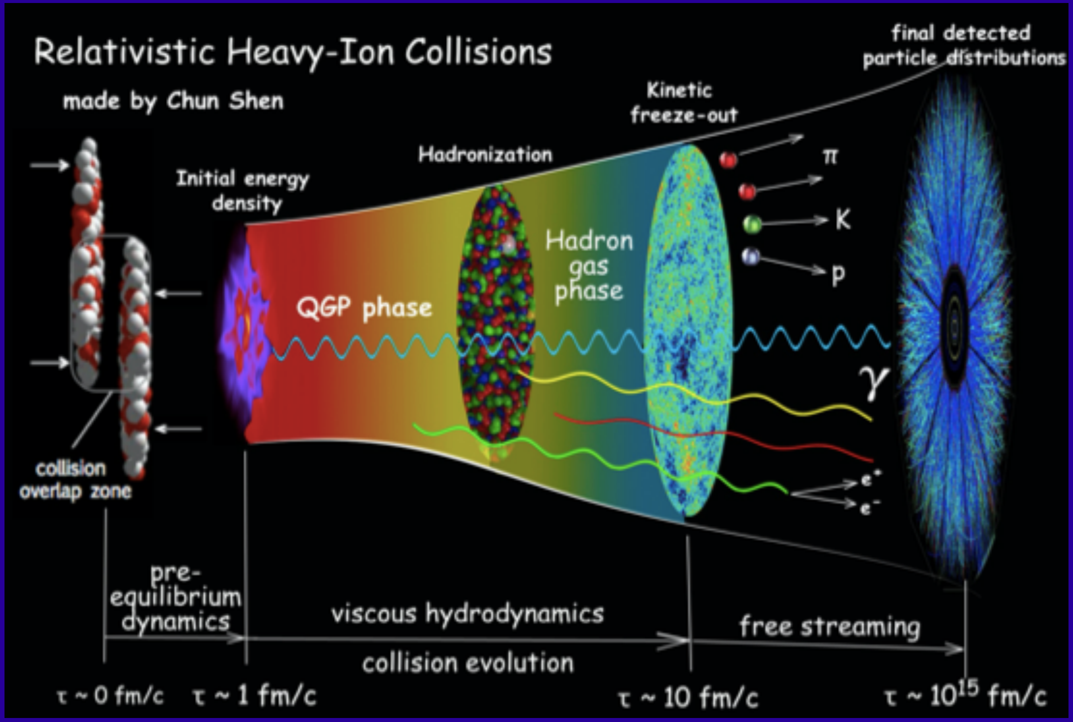

How to understand the different stages?

Heavy Ion Collisions

How to understand the different stages?

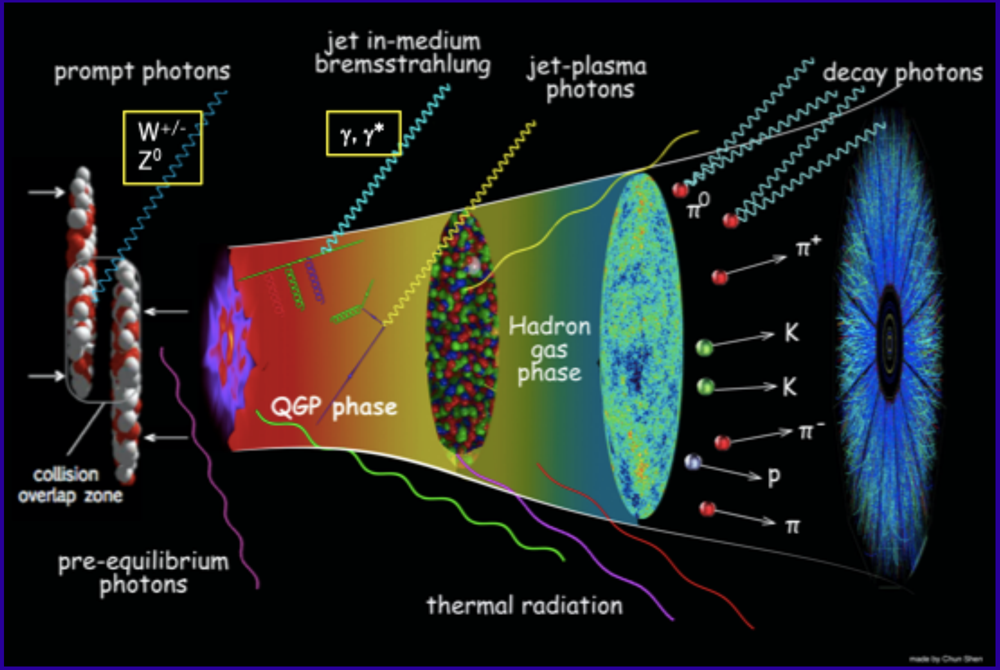

Use probes emitted during these stages:

- Initial conditions, collisions geometry: electroweak bosons; particle correlations, collective behaviour
- QGP and hadronic state: hadrons, jets, quarkonia

The ATLAS Detector

An excellent detector for the LHC Heavy-Ion program, with enourmous trigger capabilities

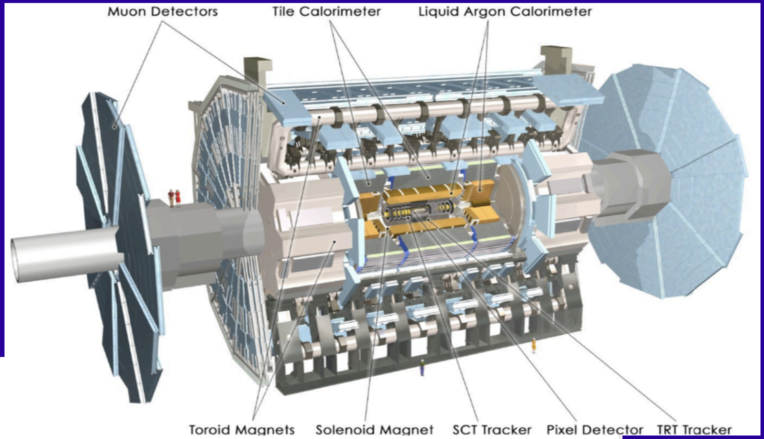

Full azimuthal coverage

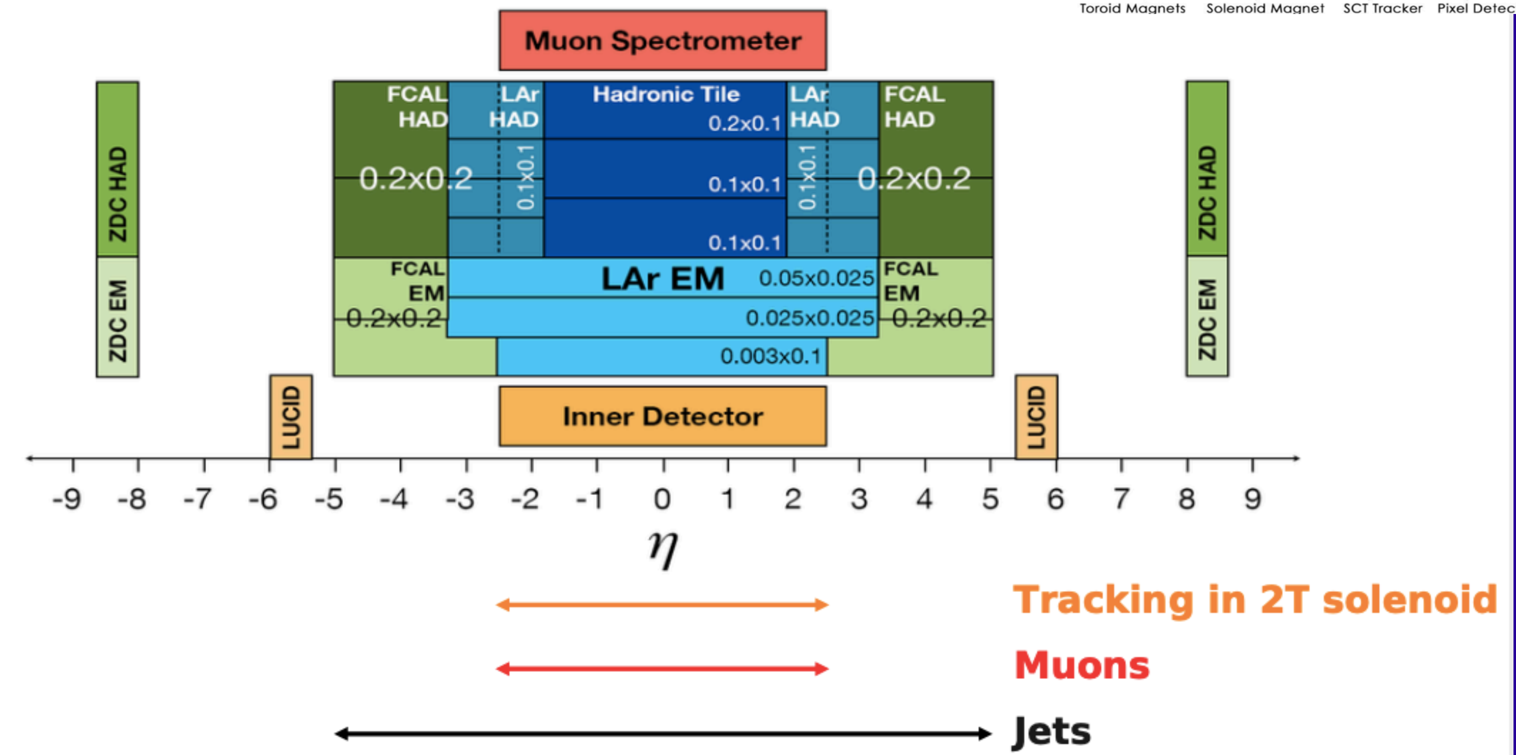

Cesar L. Silva (LANL)
HP2020

An excelle

Heavy-Ion

trigger cap

Full azimu

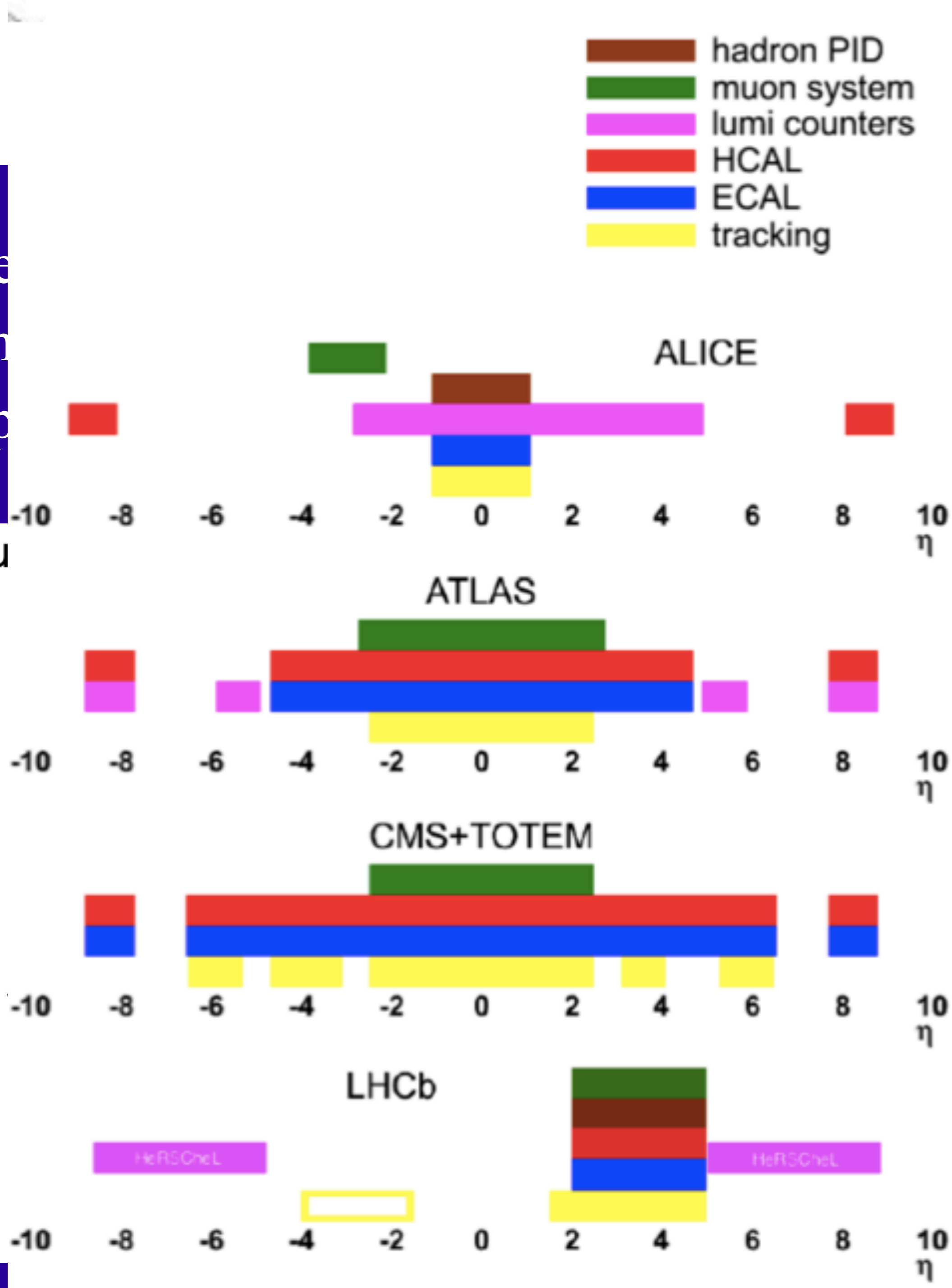

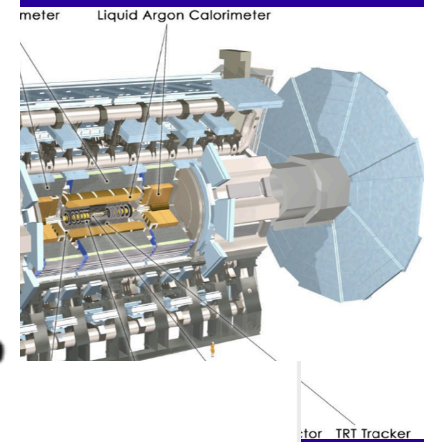

Collisions Centrality

HI collision's dynamics controlled by impact parameter "*b*"

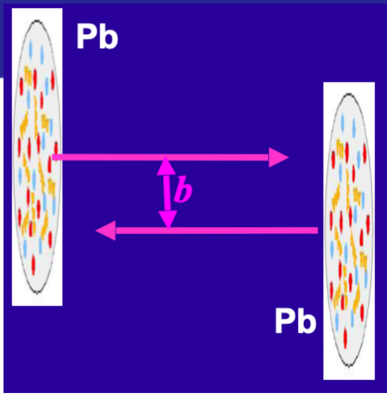

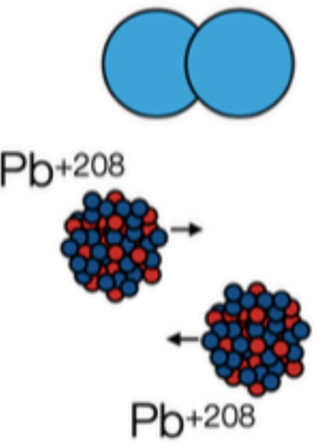

Peripheral collision

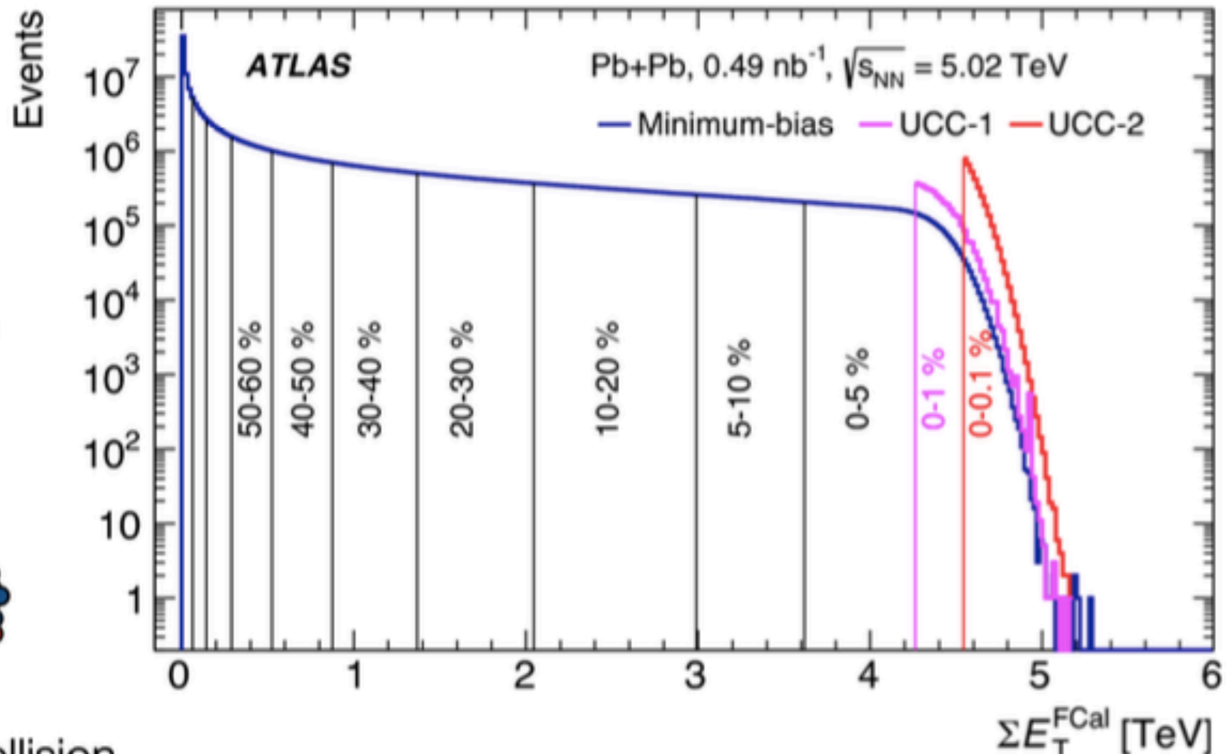

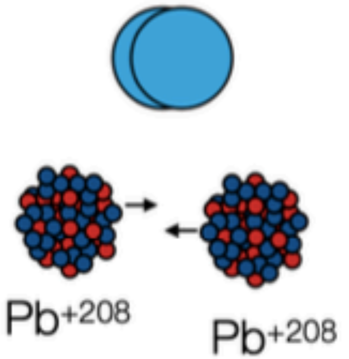

Central collision

Centrality is parametrized using the energy deposited in the Forward calorimeter (|η|>3.2)

Flow

Anisotropic collective motion is described by a Fourier expansion of particle distribution in azimuthal angle ϕ

$$\frac{\mathrm{d}N}{\mathrm{d}\phi} \propto 1 + 2\sum_{n=1}^{\infty} v_n \cos n(\phi - \Phi_n)$$

High order coefficients are associated with fluctuations of nucleon positions in the overlap

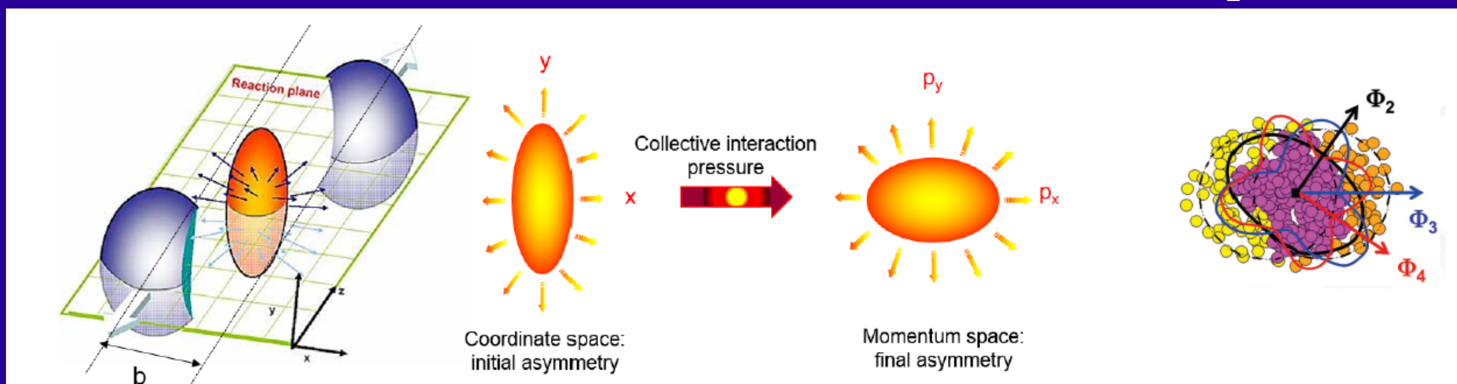

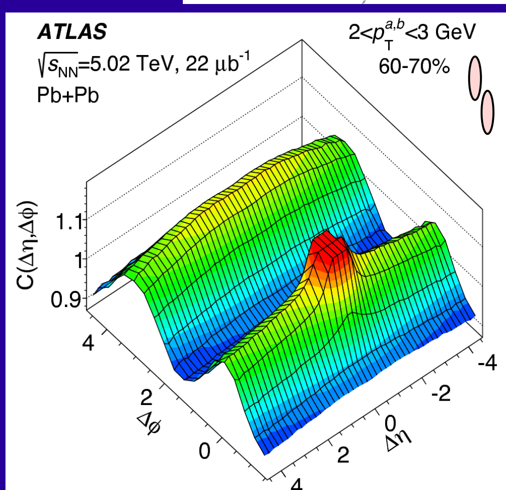

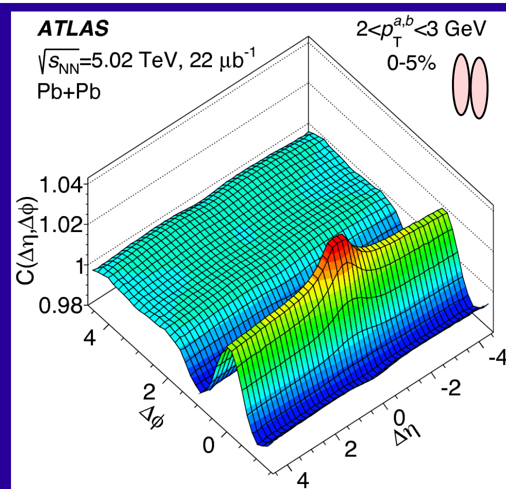

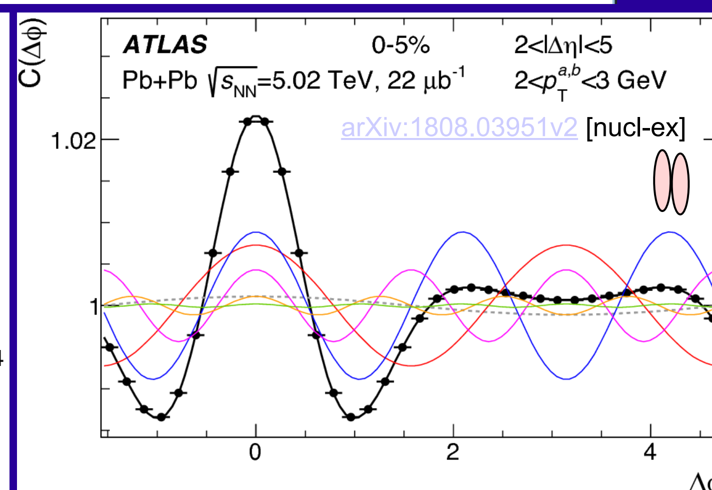

v_n in Xe+Xe and Pb+Pb collisions

Phys. Rev. C 101 (2020) 024906

Xe is smaller than Pb

→ larger EbyE fluctuations → larger eccentricities
→ larger viscous effects (1711.08499)

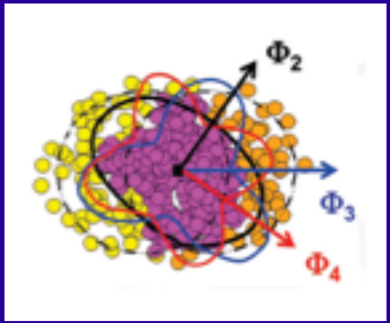

v_n in Xe+Xe and Pb+Pb collisions

Phys. Rev. C 101 (2020) 024906

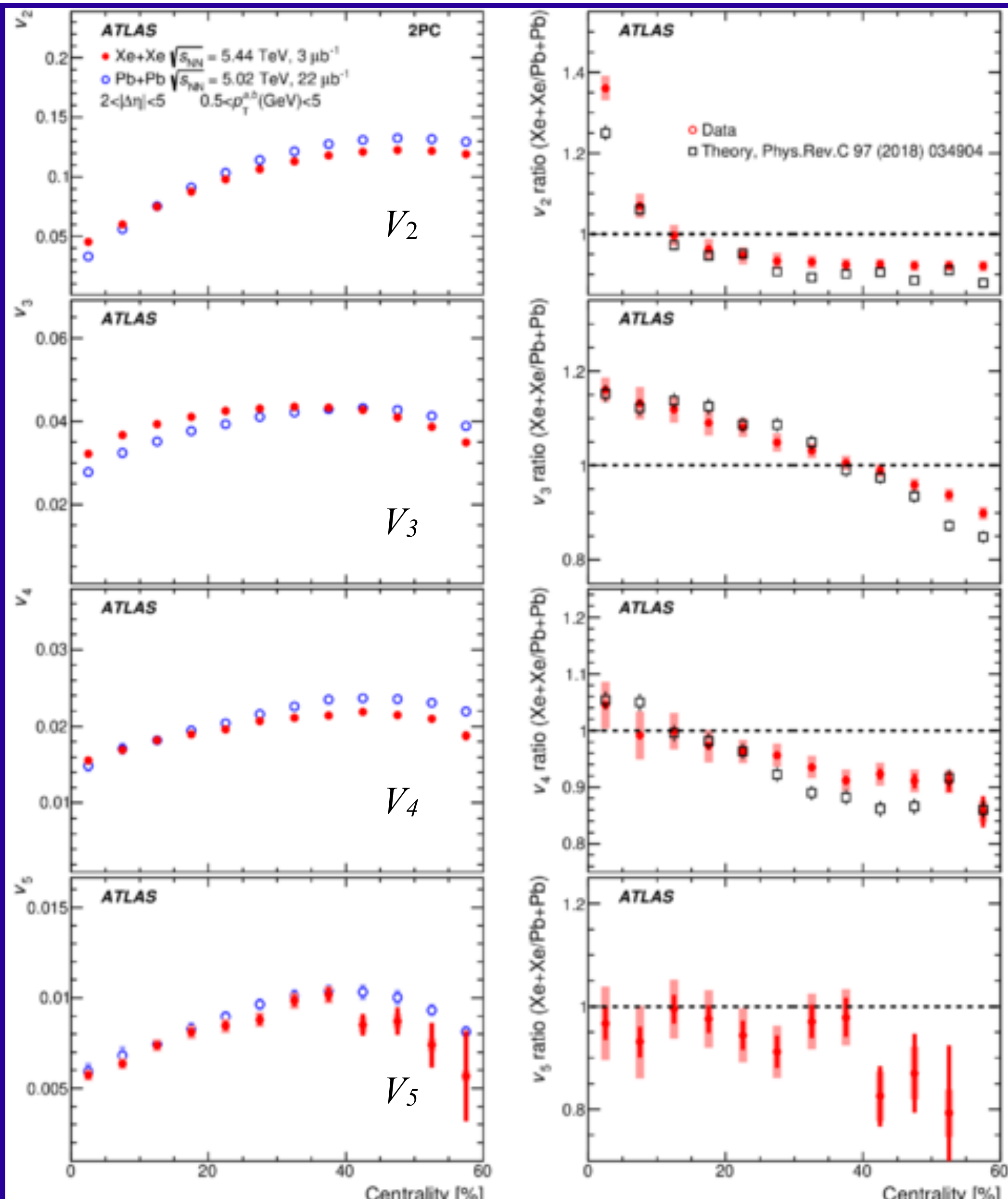

Xe is smaller than Pb

→ larger EbyE fluctuations → larger eccentricities

→ larger viscous effects (1711.08499)

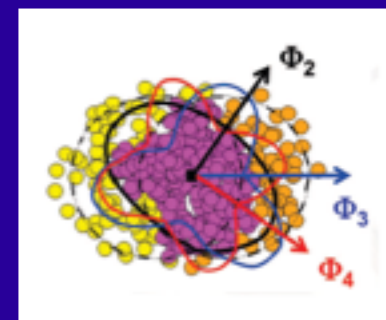

- v_n increases from central to peripheral collisions, peaking around mid-central collisons.

v_n in Xe+Xe and Pb+Pb collisions

Phys. Rev. C 101 (2020) 024906

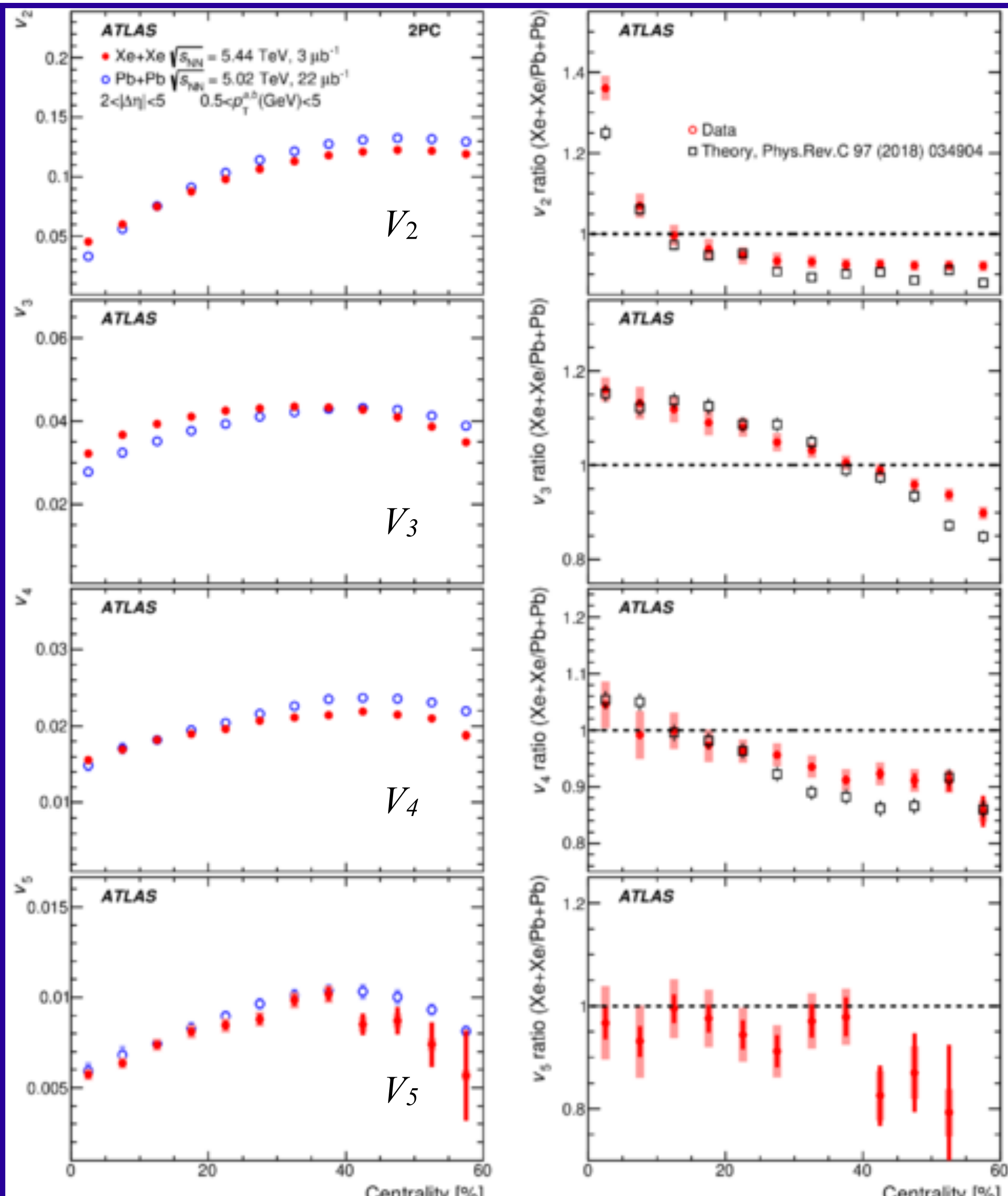

Xe is smaller than Pb

→ larger EbyE fluctuations → larger eccentricities

→ larger viscous effects (1711.08499)

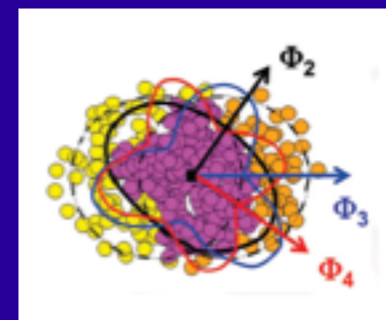

- v_n increases from central to peripheral collisions, peaking around mid-central collisons.
- v_2 and v_3 are clearly larger in central Xe+Xe collisions.

v_n in Xe+Xe and Pb+Pb collisions

Phys. Rev. C 101 (2020) 024906

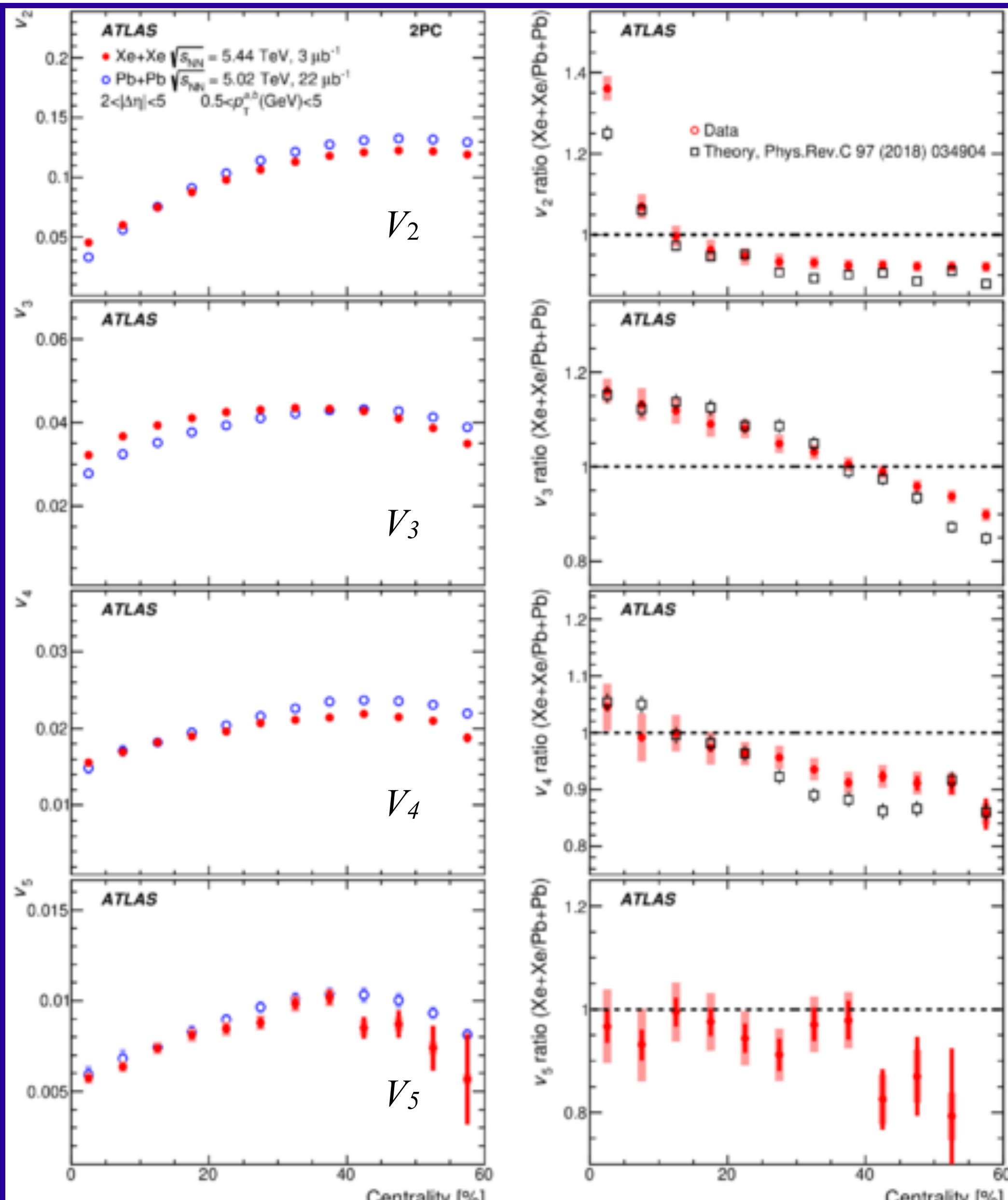

Xe is smaller than Pb

→ larger EbyE fluctuations → larger eccentricities
→ larger viscous effects (1711.08499)

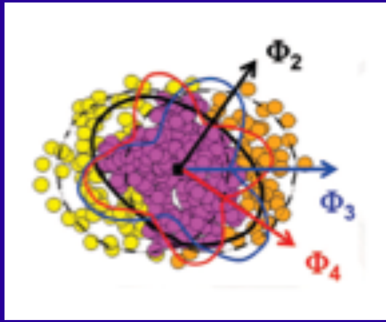

- v_n increases from central to peripheral collisions, peaking around mid-central collisons.
- v_2 and v_3 are clearly larger in central Xe+Xe collisions.
- Hydrodynamic predictions (1711.08499) describe data well.

Messages from flow

- Significant harmonic (v_2-v_4) observed in Pb+Pb collisions reflecting the nuclear overlap and fluctuations of the initial nucleon-nucleon positions.
- The long range “ridge” and “cone” structures in two-particle correlation at low p_T can be explained by flow effects.
- Hydrodynamics (also) describes flow in Xe+Xe collisions.

Electroweak probes

W/Z, photons, are not supposed to interact with QGP.

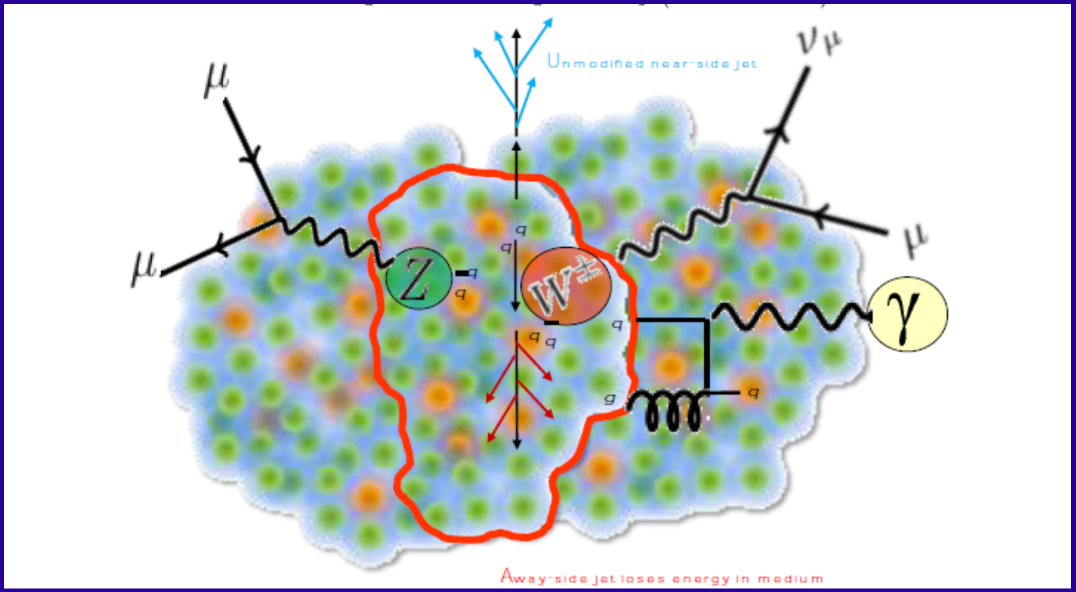

They are produced in HI collisions before QGP is formed:

- Production mechanisms sensitive to nuclear PDFs - initial stages.
- Can be used to check models of collision geometry (Glauber). Their production is expected to be proportional to the nuclear overlap.
- Provide calibration for jet energy loss in the QGP (photon-jet, Z-jet).

Nuclear Modification Factor - R_{AA}

$$R_{AA} = \frac{\boxed{N_{AA}}}{\boxed{\langle T_{AA} \rangle} \times \boxed{\sigma_{pp}}}$$

Yields in Pb+Pb collisions, (in medium)

Nuclear thickness function $<N_{coll}>/\sigma_{NN}$

Cross section in pp collisions (in vacuum)

- Nuclear thickness function accounts for the nuclear orverlap.
- Nuclear modification factor quantifies the change of yields, relatively to the production in vacuum.
- Any deviation from unity points to suppression or enhancement of the Pb+Pb yields.

Electroweak probes in Pb+Pb collisions – Z

Phys. Lett. B 802 (2020) 135262

Normalized Z boson yield as a function of rapidity

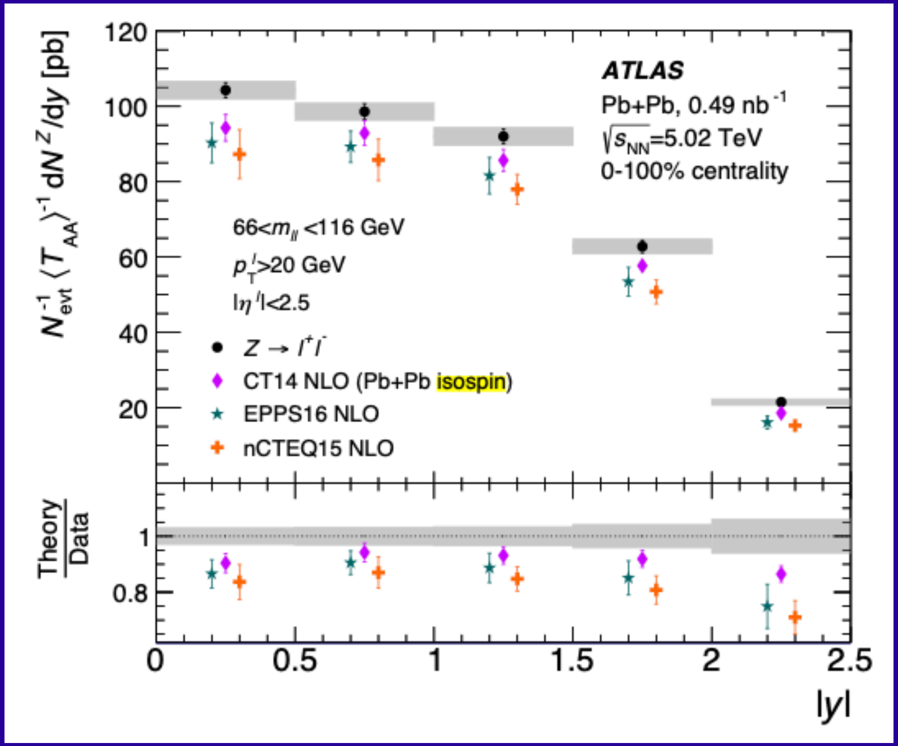

- (free-nucleon) CT14 NLO takes into account that Z production Xsection is higher in *nn* and *pn* collisions than in *pp* collisions.
- nuclear NLO PDFs EPPS16 and nCTEQ15 underestimate even more Z production by 1-3σ.
- Difference between data and theory increases towards forward rapidity.

Electroweak probes in Pb+Pb collisions – Z

Phys. Lett. B 802 (2020) 135262

$$R_{AA}(y) = \frac{1}{\langle T_{AA}\rangle N_{evt}} \frac{dN^Z_{Pb+Pb}/dy}{d\sigma^Z_{pp}/dy},$$

- R^Z_{AA} is expected to be greater than unity by about 2.5% due to isospin effect.

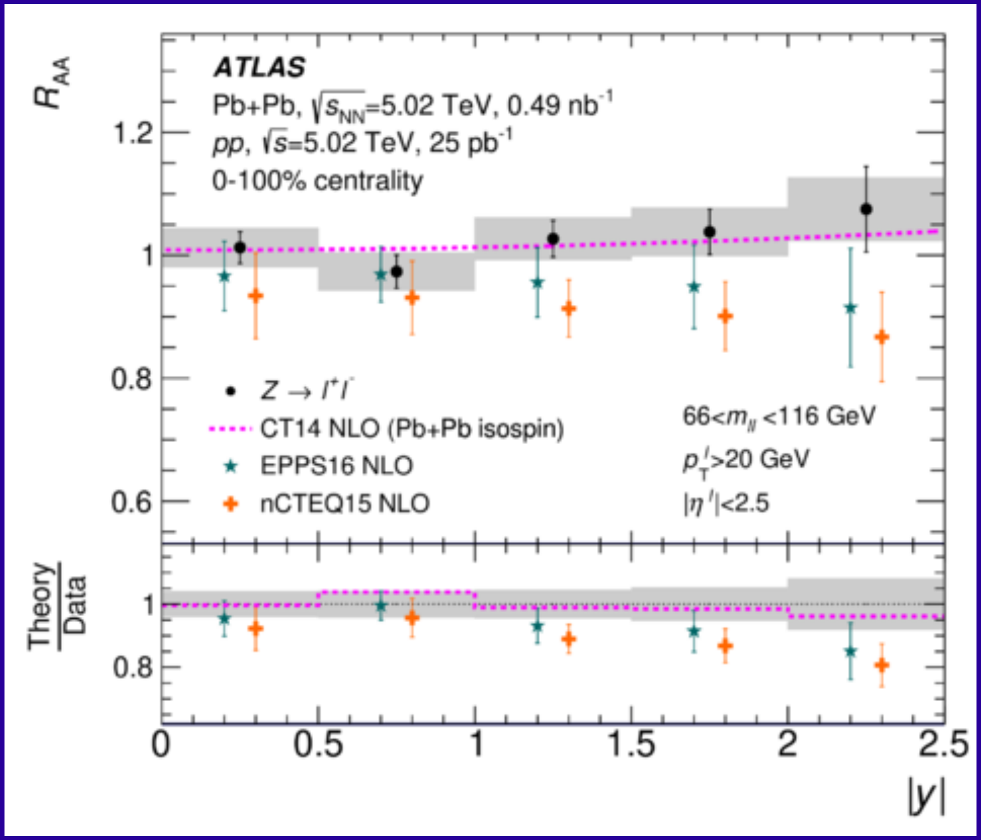

- R_{AA} is consistent with unity and agrees with CT14 NLO that accounts for Pb isospin.

Electroweak probes in Pb+Pb collisions – Z

Phys. Lett. B 802 (2020) 135262

$$R_{AA}(y) = \frac{1}{\langle T_{AA}\rangle N_{evt}} \frac{dN^Z_{Pb+Pb}/dy}{d\sigma^Z_{pp}/dy},$$

- R^Z_{AA} is expected to be greater than unity by about 2.5% due to isospin effect.

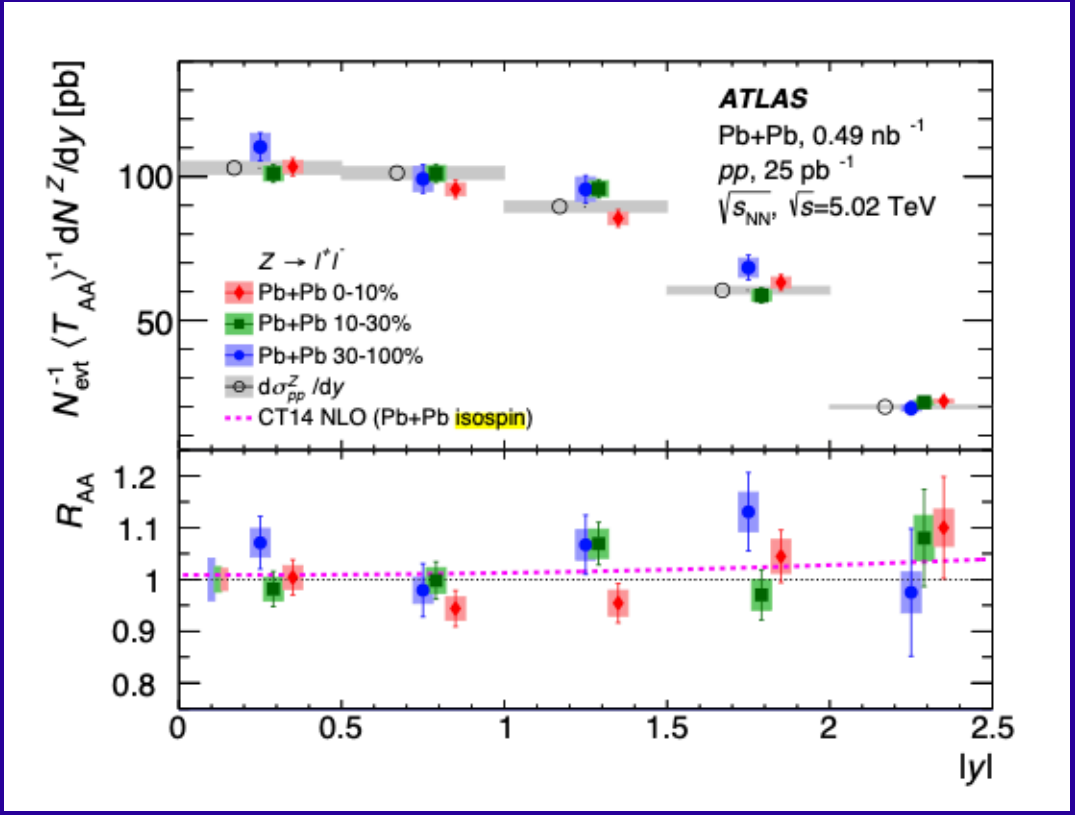

- R_{AA} is consistent with unity, independently on collisions centrality, and agrees with CT14 NLO that accounts for Pb isospin.

Electroweak probes in Pb+Pb collisions - $W^{\pm}$

Eur. Phys. J. C 79 (2019) 935

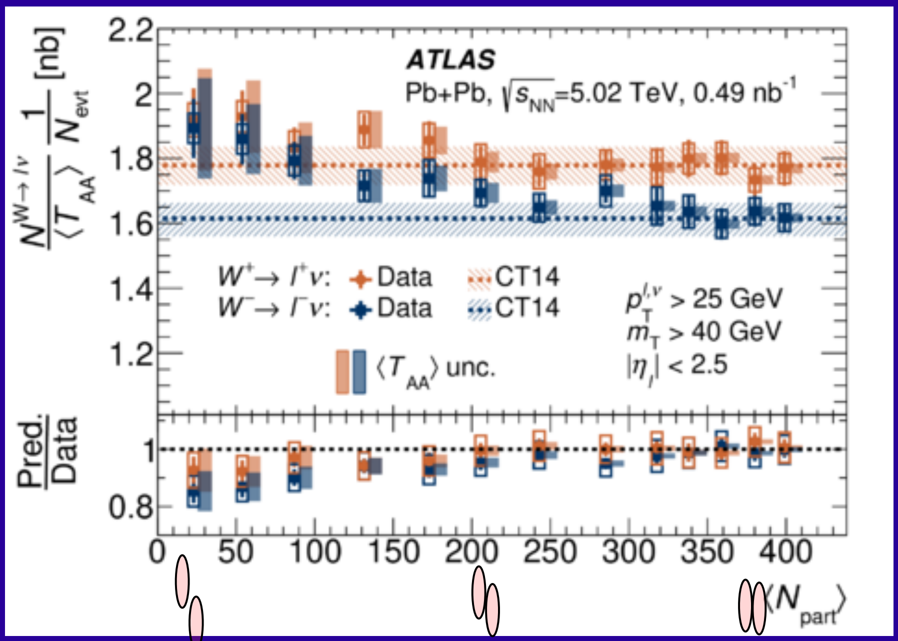

- $W^{+} \to \mu^{+}\nu$ yields are systematically ~10% larger than $W^{-} \to \mu^{-}\nu$ yields.
- Theory understimates W boson yields in peripheral collisions.

Electroweak probes in Pb+Pb collisions - W±

Eur. Phys. J. C 79 (2019) 935

$$A_\ell(\eta_\ell) = \frac{dN_{W^+\to\ell^+\nu}/d\eta_\ell - dN_{W^-\to\ell^-\bar{\nu}}/d\eta_\ell}{dN_{W^+\to\ell^+\nu}/d\eta_\ell + dN_{W^-\to\ell^-\bar{\nu}}/d\eta_\ell}$$

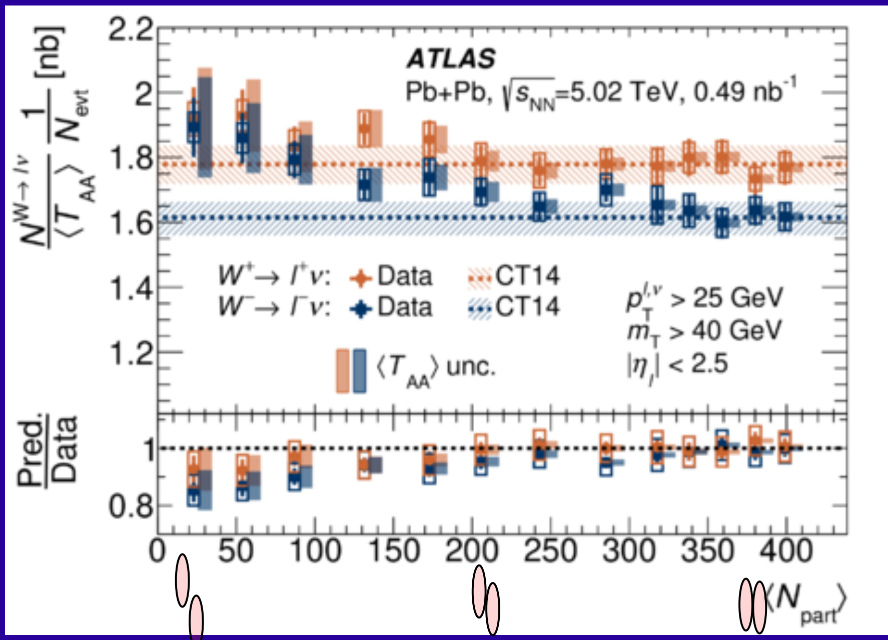

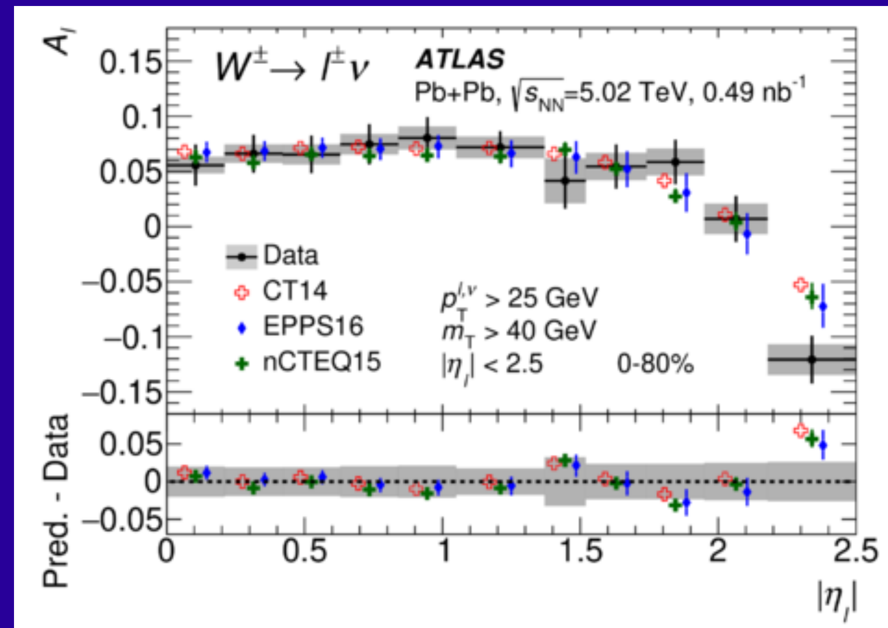

- $W^+ \to \mu^+\nu$ yields are systematically ~10% larger than $W^- \to \mu^-\nu$ yields.
- Theory understimates W boson yields in peripheral collisions.
- Good agreement with predictions, both that ascribe free-nucleon PDF and nPDF, for $|\eta_\mu| < 1.4$. Three sigma at forward. All PDFs account for isospin. Asymmetry changes sign for $|\eta| > 2$.

Quarkonia

Quarkonia suppression is predicted by lattice QCD calculations

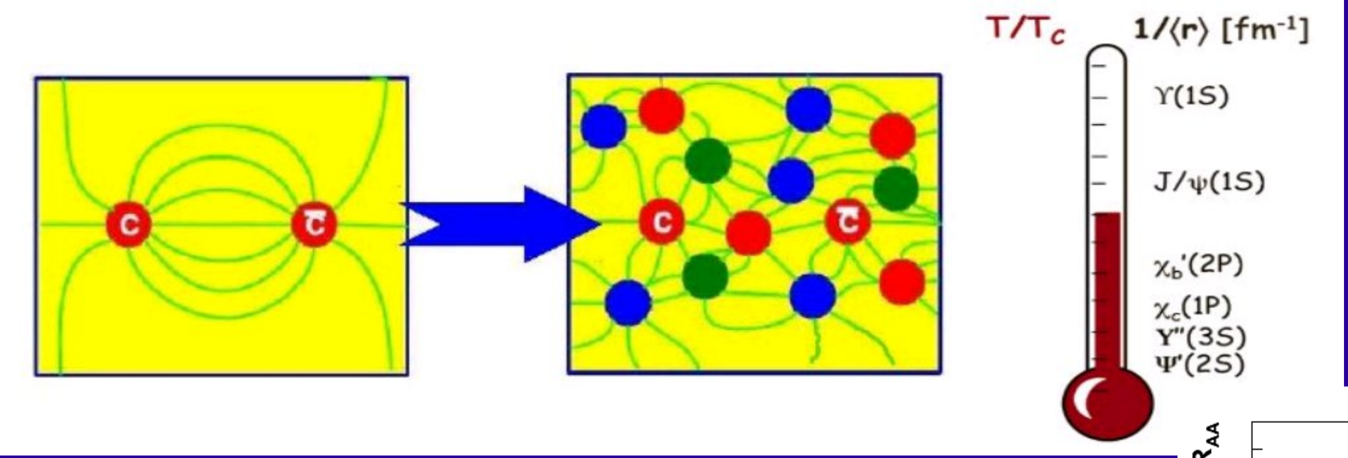

J/psi anomalous suppression by Debye colour screening (Matsui and Satz, 1986)

⟶ One of the most striking signatures for the QGP

⟶ A major contribution from LIP

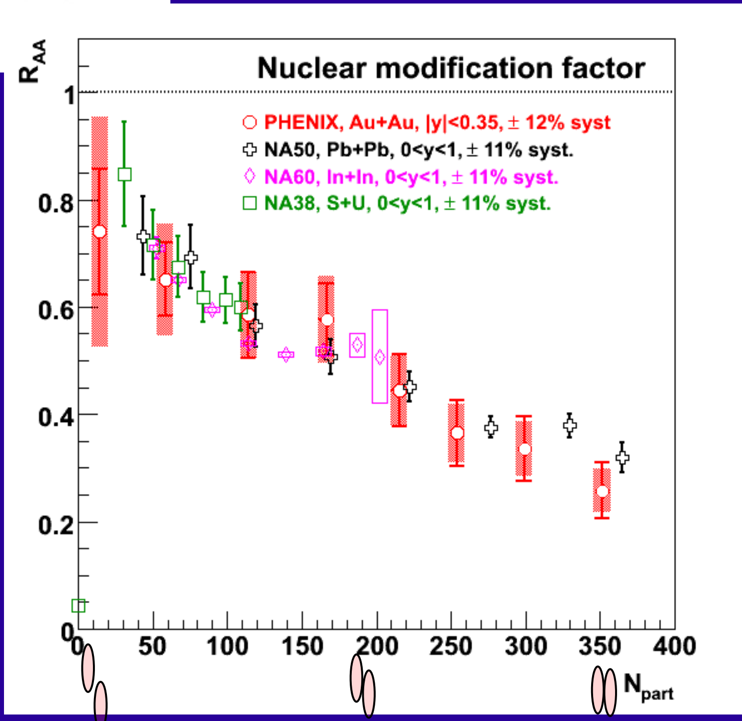

Prompt and Non-prompt Charmonia in Pb+Pb

Dimuon invariant mass

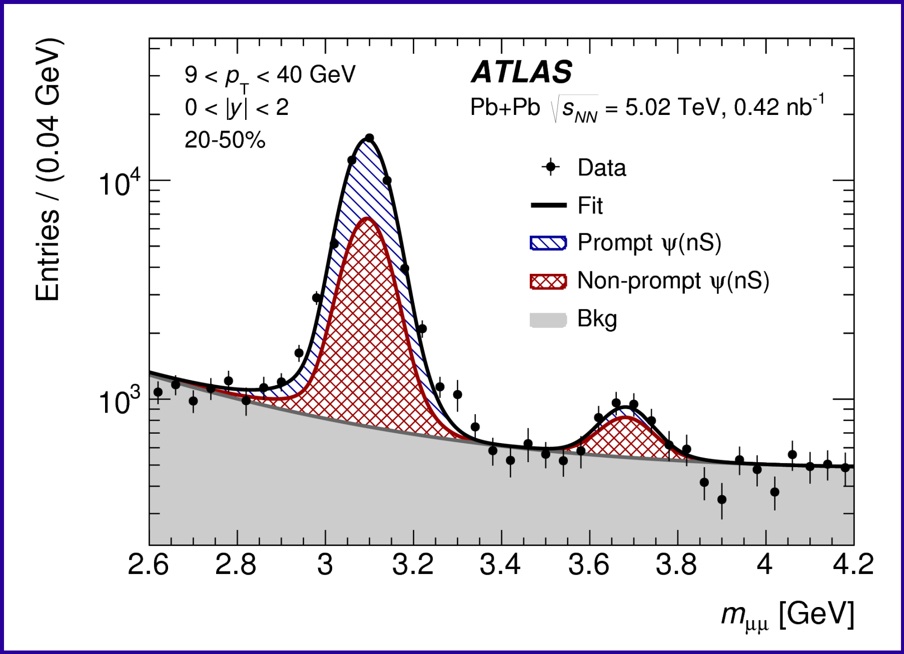

Dimuon pseudo-proper time

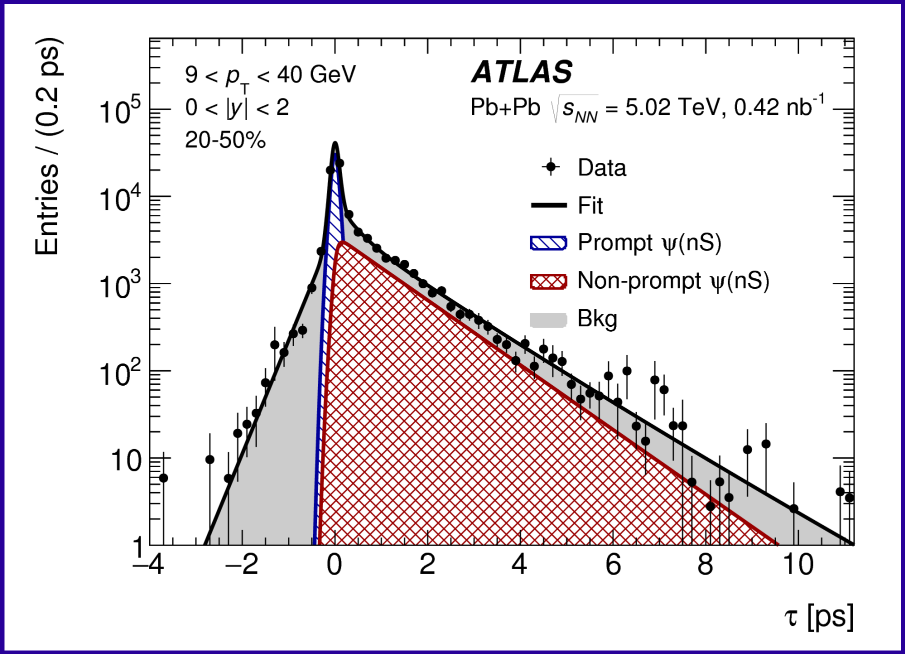

Prompt J/ψ: direct production; feed-down from excited states.

Modified by colour screening and regeneration in the QGP.

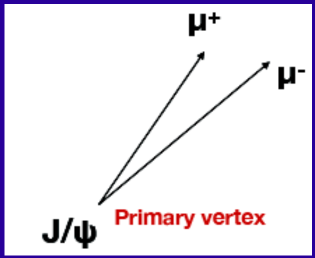

Non-prompt J/ψ: decays from B-hadrons

Energy loss of the b-quarks in the QGP.

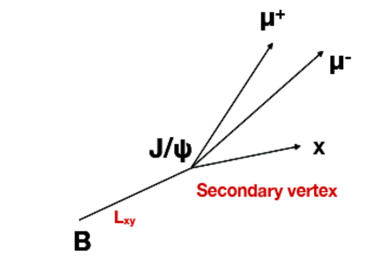

$$\tau = \frac{L_{xy} m_{\mu\mu}}{p_T^{\mu\mu}},$$

J/ψ R_{AA} as a function of N_{part}

$$R_{AA} = \frac{\boxed{N_{AA}}}{\boxed{\langle T_{AA}\rangle} \times \boxed{\sigma_{pp}}}$$

Eur. Phys. J. C 78 (2018) 762

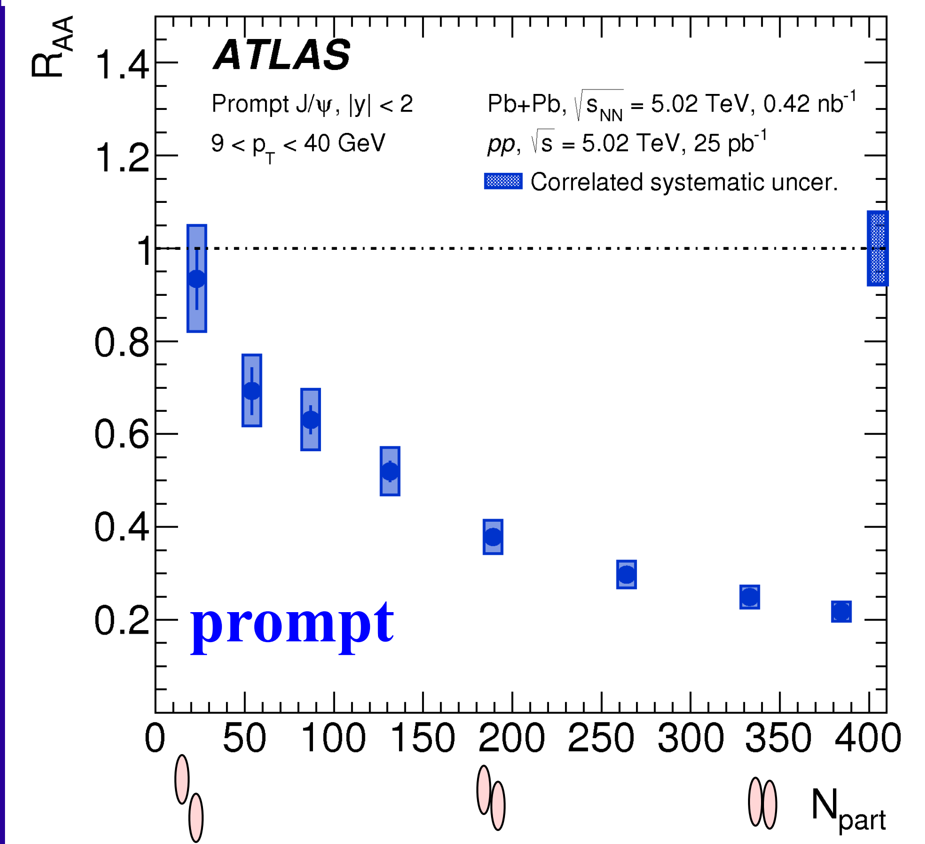

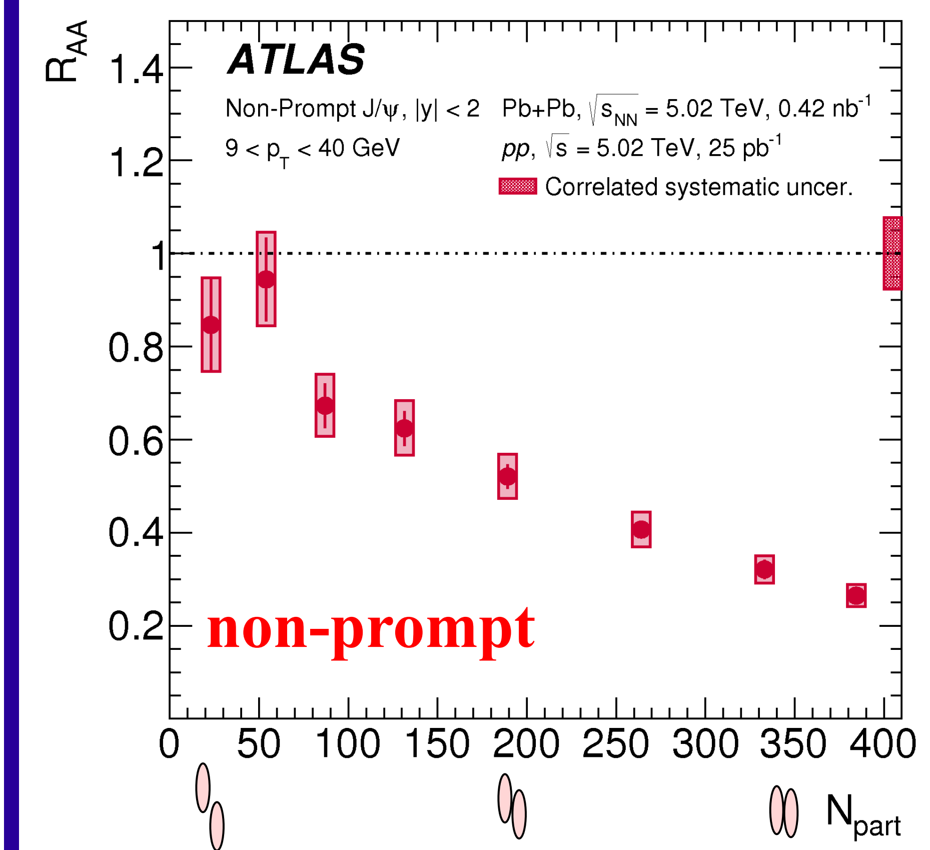

Strong centrality dependence for both **prompt** and **non-prompt** J/ψ, with similar suppression pattern.

ψ(2S) to J/ψ as a function of N_{part}

Eur. Phys. J. C 78 (2018) 762

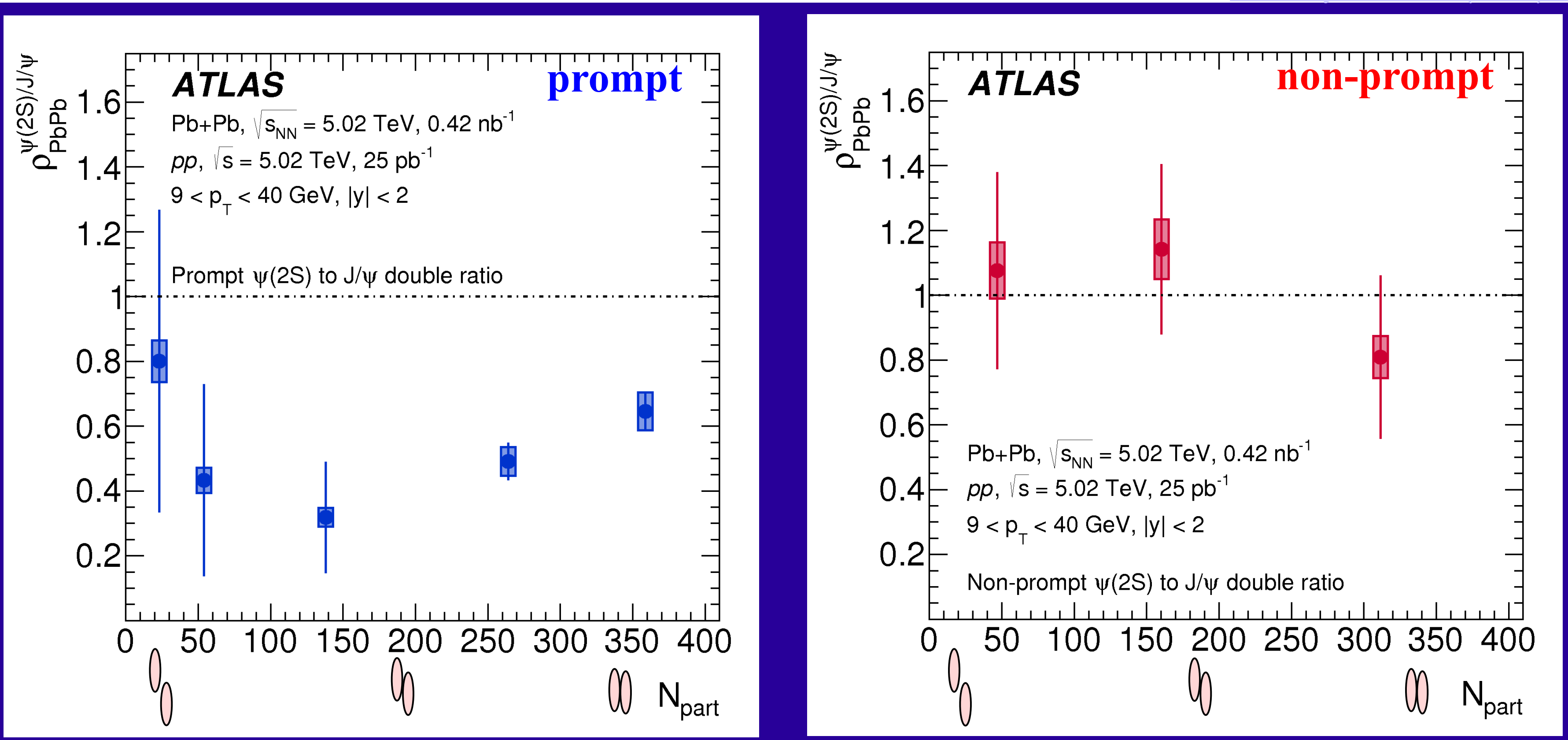

- Prompt ψ(2S) to J/ψ ratio increases in central collisions, supporting the hypothesis of ψ(2S) being produced by regeneration. More data is needed.
- Non-prompt ψ(2S) to J/ψ ratio is consistent with unity, suggesting that both mesons originate from b-quarks hadronising outside the QGP.

Prompt J/ψ R_{AA} as a function of p_T

Eur. Phys. J. C 78 (2018) 762

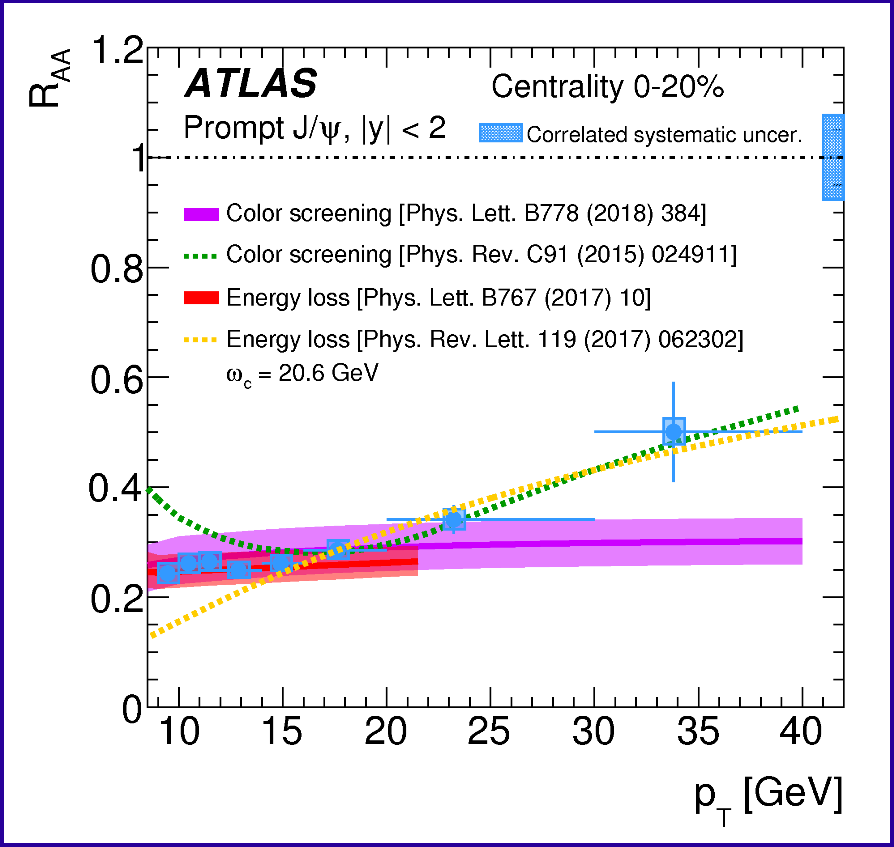

Data at high p_T well described by **color screening** and **energy loss** scenarios, but they miss low p_T.

Different models on **color screening** and **energy loss** agree at low p_T, but fail at high p_T.

Prompt ψ(2S) to J/ψ as a function of N_{part}

Eur. Phys. J. C 78 (2018) 762

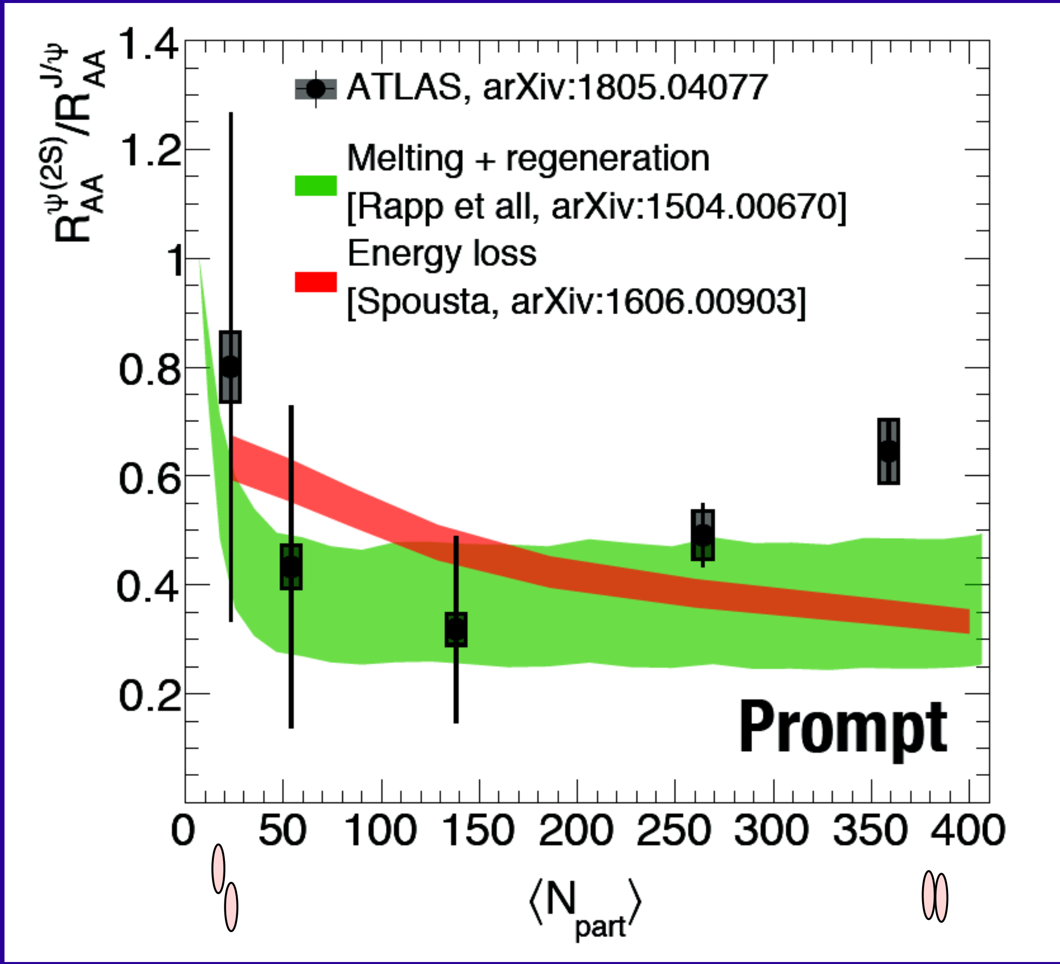

Both models foresee the decrease in the double ratio, but fail in describing simultaneously all centralities.

Messages from Quarkonia

- Strong centrality dependence, and with similar suppression, for both prompt and non-prompt J/ψ.
- Modest dependence on |y| (in backup). Different p_T dependence.
- Data at high p_T well described by color screening and energy loss models. But these miss low p_T.
- Indications of prompt ψ(2S) regeneration in central collisions.
- Non-prompt ψ(2S) to J/ψ ratio is consistent with unity.

Jets in HI collisions

First insight of jets produced at LHC indicated a large dijet asymmetry

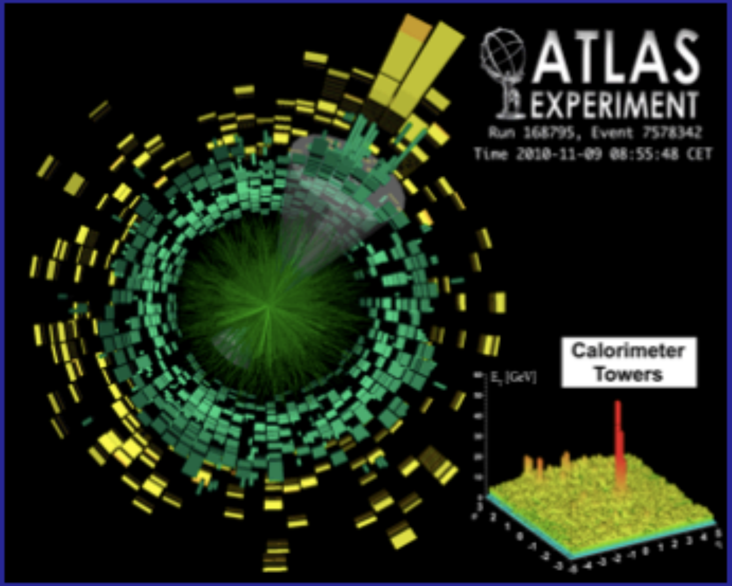

Jets in HI collisions

First insight of jets produced at LHC indicated a large dijet asymmetry

$x_J = p_{T2}/p_{T1}$

ATLAS-CONF-2020-017

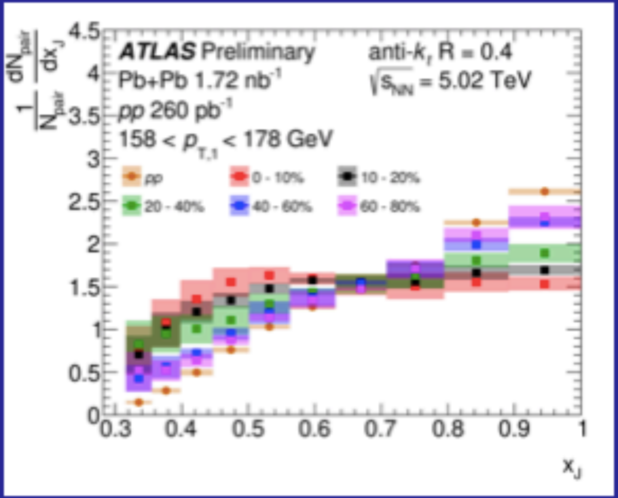

- The dijet momentum-balance in peripheral collisions is well compatible with pp collisions.
- Imbalance increases with increasing centrality.

Jets in HI collisions

First insight of jets produced at LHC indicated a large dijet asymmetry

$x_J = p_{T2}/p_{T1}$

ATLAS-CONF-2020-017

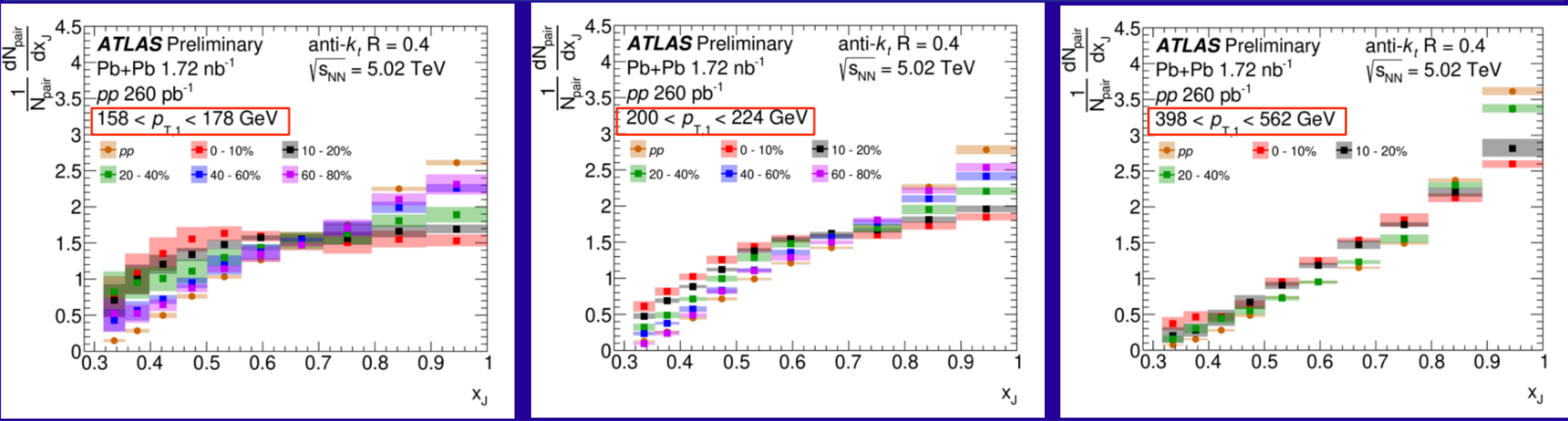

- The momentum-balance in peripheral collisions is well compatible with pp collisions.
- Imbalance increases with increasing centrality.
- The imbalance is weaker with increasing leading jet p_T.

Inclusive jet production in Pb+Pb

$$R_{\mathrm{AA}} = \frac{\boxed{N_{\mathrm{AA}}}}{\boxed{\langle T_{\mathrm{AA}} \rangle} \times \boxed{\sigma_{pp}}}$$

Yields in Pb+Pb collisions, (in medium)

Nuclear thickness function <N_{coll}>/σ_{NN}

Cross section in *pp* collisions (in vacuum)

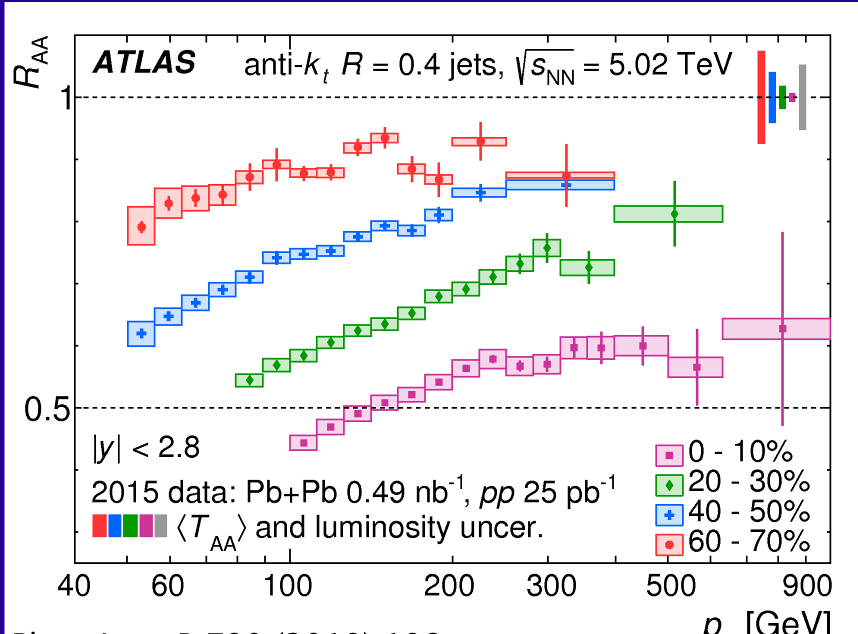

Phys. Lett. B 790 (2019) 108

- Nuclear modification factor quantifies the change of yields, w.r.t. the production in vacuum.
- Any deviation from unity indicates suppression or enhancement of yields.

Jets are suppressed by a factor of two in central Pb+Pb collisions with clear dependence on transverse momentum, p_T.

Path length dependence of quenching

ATLAS-CONF-2020-019

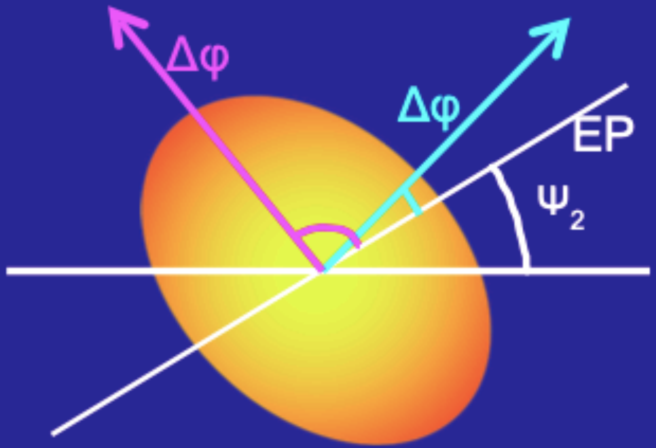

Unequal path lengths of the showers in the medium

$$\frac{\mathrm{d}N}{\mathrm{d}\phi} \propto 1 + 2\sum_{n=1}^{n} v_n \cos(n(\phi - \Psi_n)),$$

Path length dependence of quenching

ATLAS–CONF–2020–019

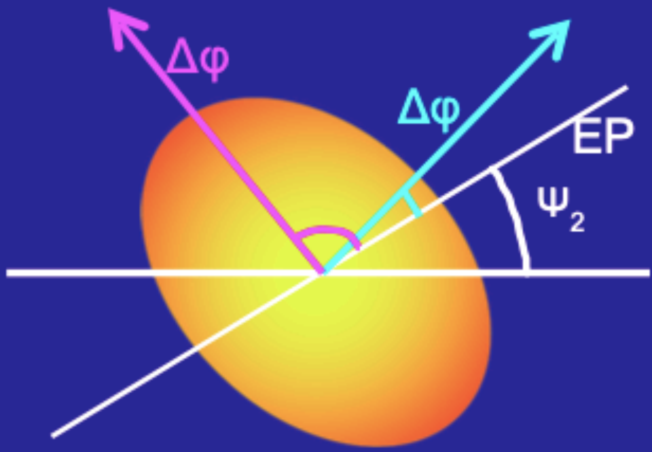

Unequal path lengths of the showers in the medium

$$\frac{dN}{d\phi} \propto 1 + 2\sum_{n=1}^{n} v_n \cos(n(\phi - \Psi_n)),$$

R=0.2 jets with
$100 < p_T < 126$ GeV
Unfolded in p_T and $\Delta\varphi_n$

Angular distribution of jets with respect to Ψ_2

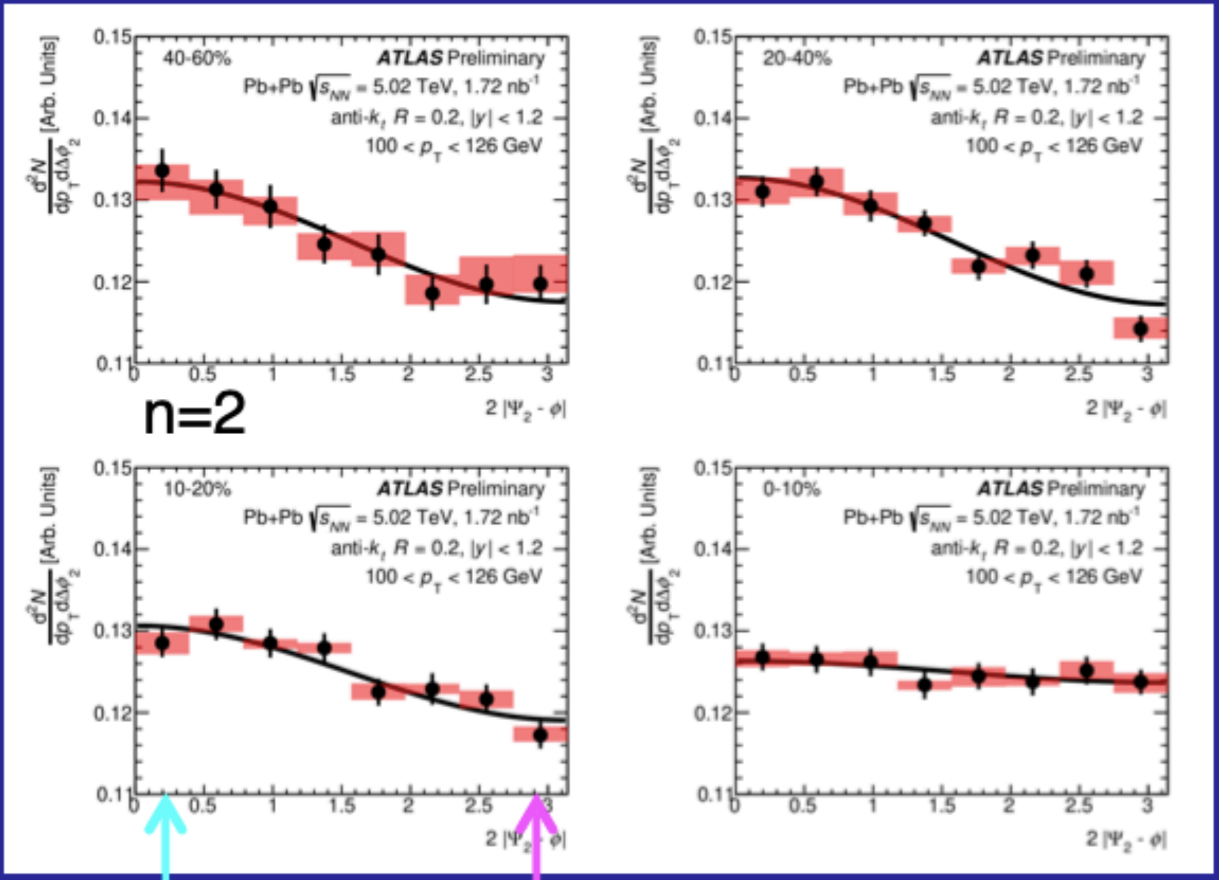

Jets produced in the direction of the event–plane are less suppressed

Path length dependence of quenching

ATLAS-CONF-2020-019

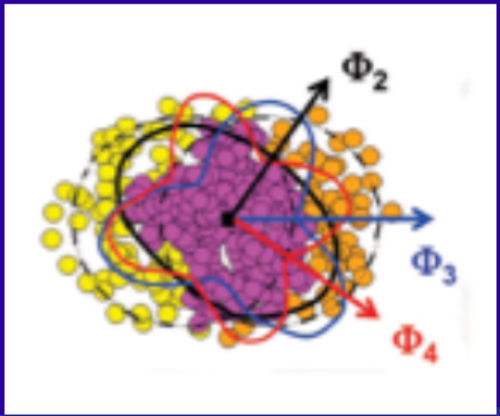

Unequal path lengths of the showers in the medium

$$\frac{dN}{d\phi} \propto 1 + 2\sum_{n=1}^{n} v_n \cos(n(\phi - \Psi_n)),$$

R=0.2 jets with
$100 < p_T < 126$ GeV
Unfolded in p_T and $\Delta\varphi_n$

Angular distribution of jets with respect to Ψ_3

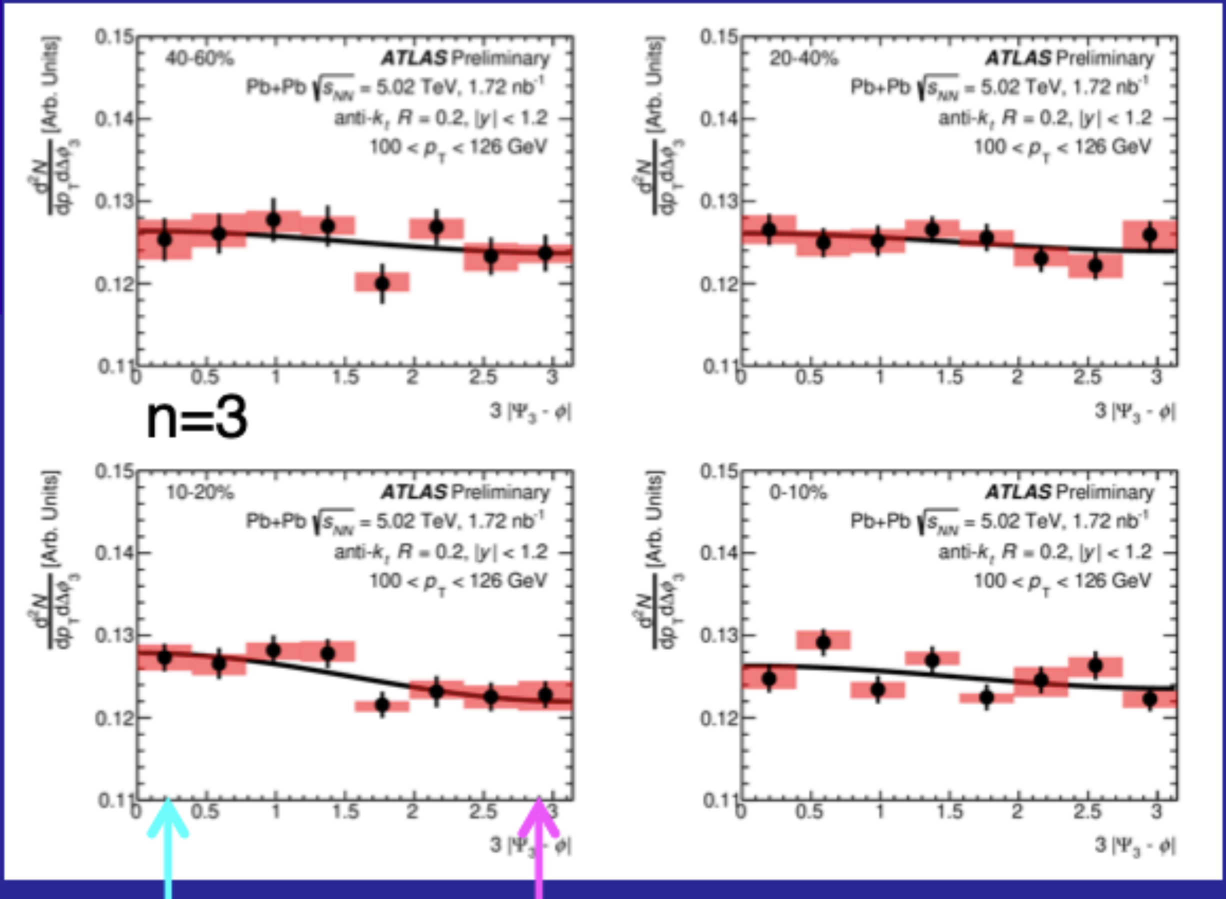

Smaller effect for n=3

A deeper insight

How is the parton shower modified in the hot and dense QCD medium?

What is the resolution scale of the quark-gluon plasma?

Does the jet suppression depend on substructure?

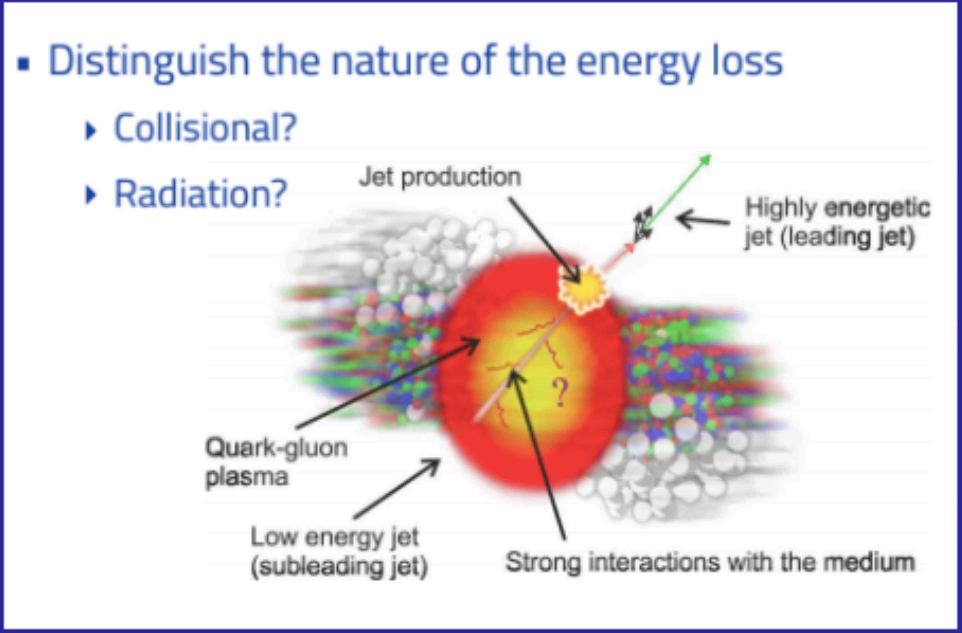

Inclusive fragmentation functions

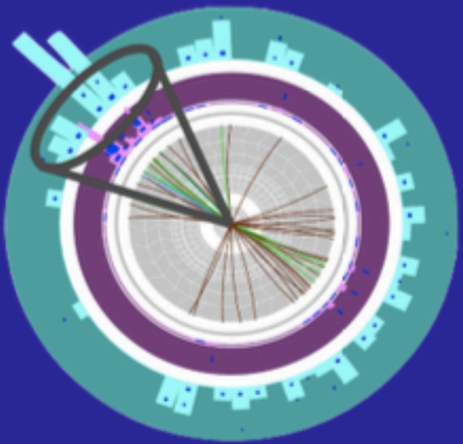

Does the jet suppression depend on jet structure?

$$D(z) = \frac{1}{N_{jet}} \frac{\mathrm{d}N}{\mathrm{d}z} \qquad D(p_T) = \frac{1}{N_{jet}} \frac{\mathrm{d}N}{\mathrm{d}p_T}$$

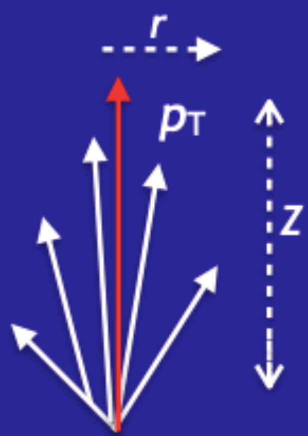

$z \equiv p_{\mathrm{T}} \cos \Delta R \,/\, p_{\mathrm{T}}^{\mathrm{jet}}$

Inclusive fragmentation functions

Does the jet suppression depend on jet structure?

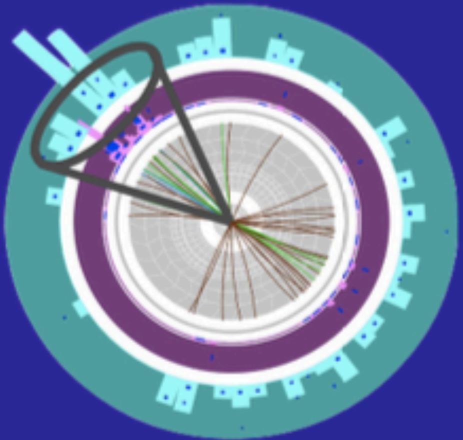

Shower in medium

$$R_{D(z)} \equiv \frac{D(z)_{\mathrm{PbPb}}}{D(z)_{pp}}$$

Shower in vacuum

Phys. Rev. C 98, (2018) 024908

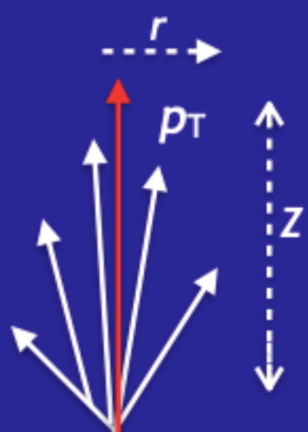

$$z \equiv p_T \cos \Delta R \,/\, p_T^{\mathrm{jet}}$$

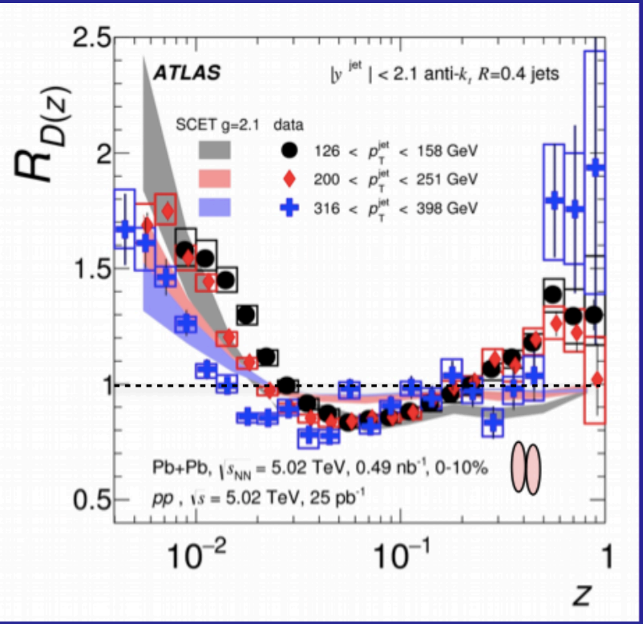

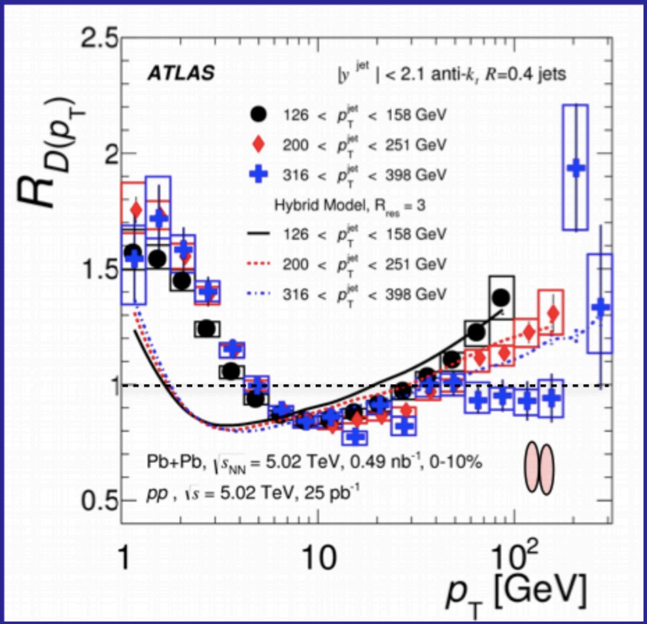

- Enhancement at low and high-z(p_T).
- Suppression at intermediate z(p_T).
- D(z,(p_T)) modifications do not scale with $p_{T,\mathrm{jet}}$ at low-z(high-p_T).

How do particles re-distribute within the jet and beyond?

Study *FF* as a function of the angular distance between the charged particle and the jet axis.

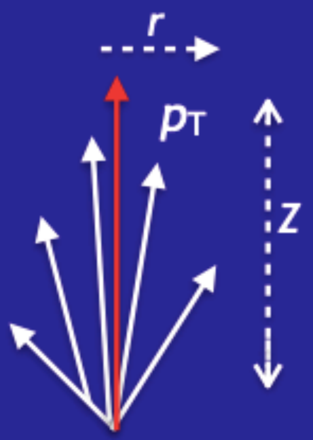

$$D(p_T, r) = \frac{1}{N_{jet}} \frac{1}{2\pi r} \frac{d^2 n_{ch}(r)}{dr\,dp_T}$$

$$r = \sqrt{\Delta\eta^2 + \Delta\phi^2}$$

How do particles re-distribute within the jet and beyond?

Study *FF* as a function of the angular distance between the charged particle and the jet axis.

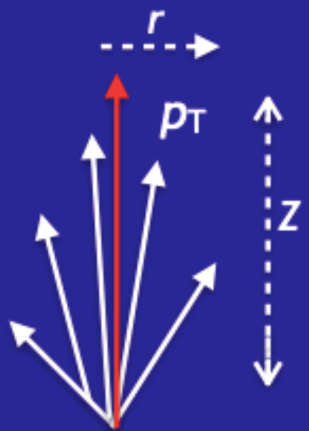

$$D(p_{\mathrm{T}}, r) = \frac{1}{N_{\mathrm{jet}}} \frac{1}{2\pi r} \frac{\mathrm{d}^2 n_{\mathrm{ch}}(r)}{\mathrm{d}r\,\mathrm{d}p_{\mathrm{T}}}$$

$$r = \sqrt{\Delta\eta^2 + \Delta\phi^2}$$

Shower in medium

$$R_{D(z)} = \frac{D(z)_{\mathrm{PbPb}}}{D(z)_{pp}}$$

Shower in vacuum

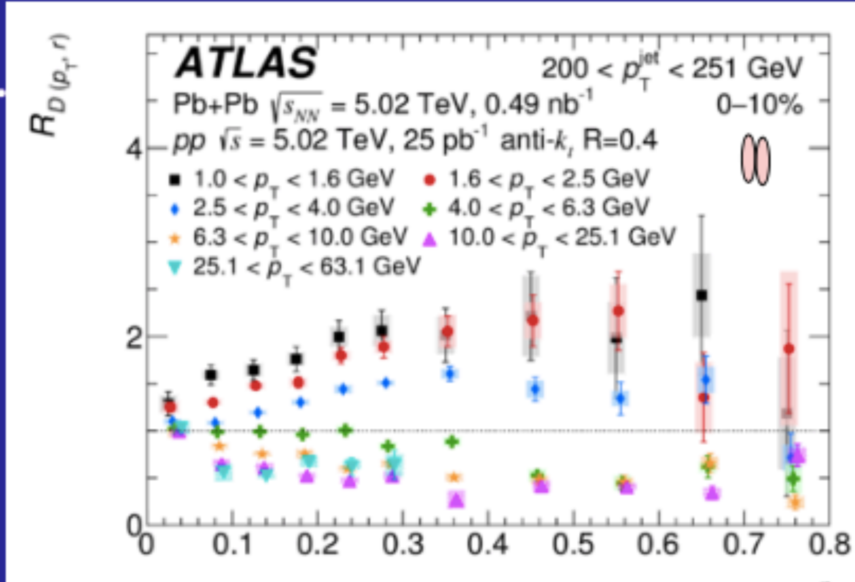

Phys. Rev. C 100 (2019) 064901

In central collisions $R_{D(p_{\mathrm{T}},r)}$ is above unity at all r for all $p_{\mathrm{T}} < 4$ GeV —> Energy lost by jets is being transferred to particles with $p_{\mathrm{T}} < 4$ GeV with larger radial distance.

How do particles re-distribute within the jet and beyond?

Study *FF* as a function of the angular distance between the charged particle and the jet axis.

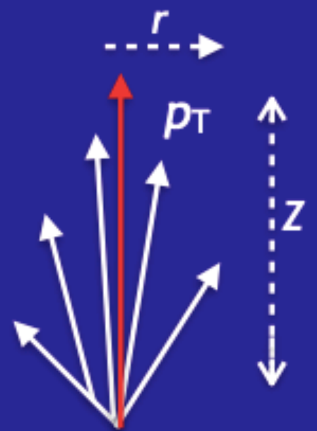

$$D(p_T, r) = \frac{1}{N_{jet}} \frac{1}{2\pi r} \frac{d^2 n_{ch}(r)}{dr\, dp_T}$$

$$r = \sqrt{\Delta\eta^2 + \Delta\phi^2}$$

Shower in medium

$$R_{D(z)} = \frac{D(z)_{PbPb}}{D(z)_{pp}}$$

Shower in vacuum

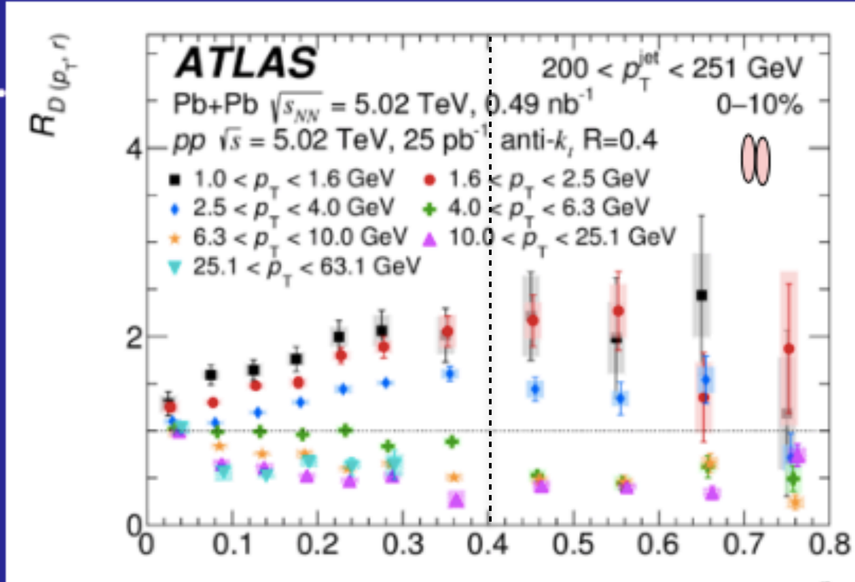

Phys. Rev. C 100 (2019) 064901

In central collisions $R_{D(p_T,r)}$ is above unity at all r for all p_T < 4 GeV —> Energy lost by jets is being transferred to particles with p_T < 4 GeV

How do particles re-distribute within the jet and beyond?

Study *FF* as a function of the angular distance between the charged particle and the jet axis.

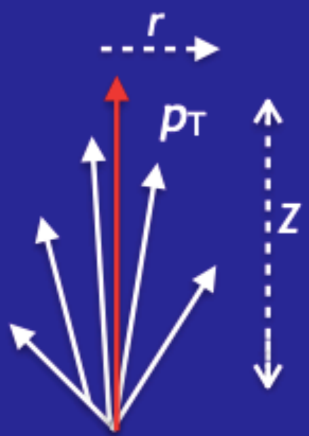

$$D(p_{\mathrm{T}}, r) = \frac{1}{N_{\mathrm{jet}}} \frac{1}{2\pi r} \frac{\mathrm{d}^2 n_{\mathrm{ch}}(r)}{\mathrm{d}r\,\mathrm{d}p_{\mathrm{T}}}$$

$$r = \sqrt{\Delta\eta^2 + \Delta\phi^2}$$

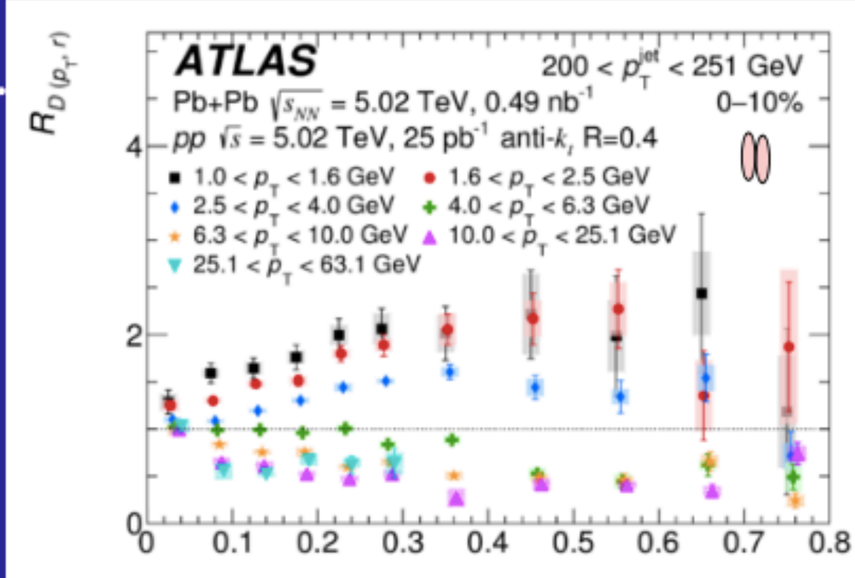

Phys. Rev. C 100 (2019) 064901

In central collisions $R_{D(p_{\mathrm{T}},r)}$ is above unity at all r for all $p_{\mathrm{T}} < 4$ GeV —> Energy lost by jets is being transferred to particles with $p_{\mathrm{T}} < 4$ GeV

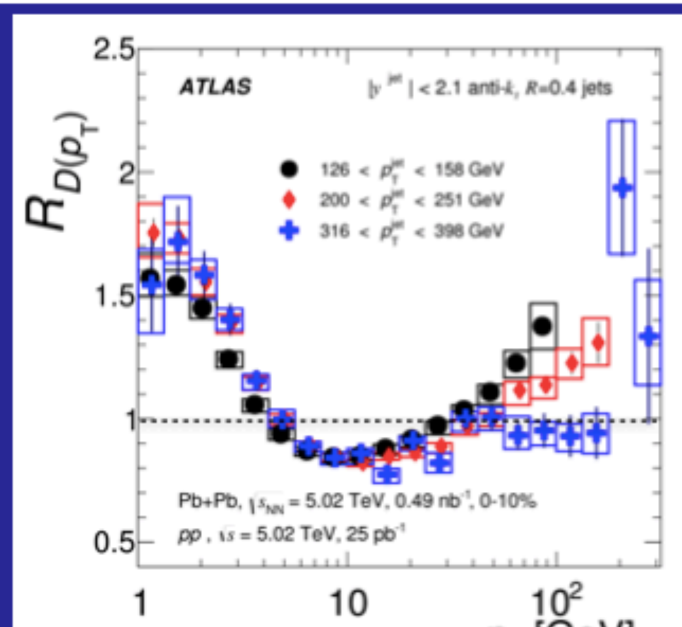

Phys. Rev. C 98, (2018) 024908

How do particles re-distribute within the jet and beyond?

Study *FF* as a function of the angular distance between the charged particle and the jet axis.

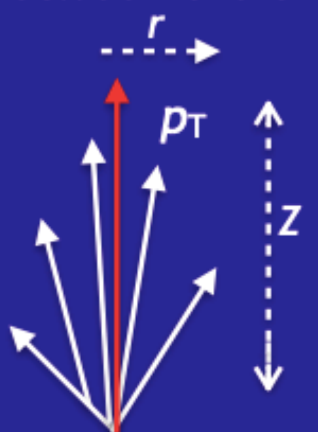

$$D(p_{\mathrm{T}}, r) = \frac{1}{N_{\mathrm{jet}}} \frac{1}{2\pi r} \frac{\mathrm{d}^2 n_{\mathrm{ch}}(r)}{\mathrm{d}r\, \mathrm{d}p_{\mathrm{T}}}$$

$$r = \sqrt{\Delta\eta^2 + \Delta\phi^2}$$

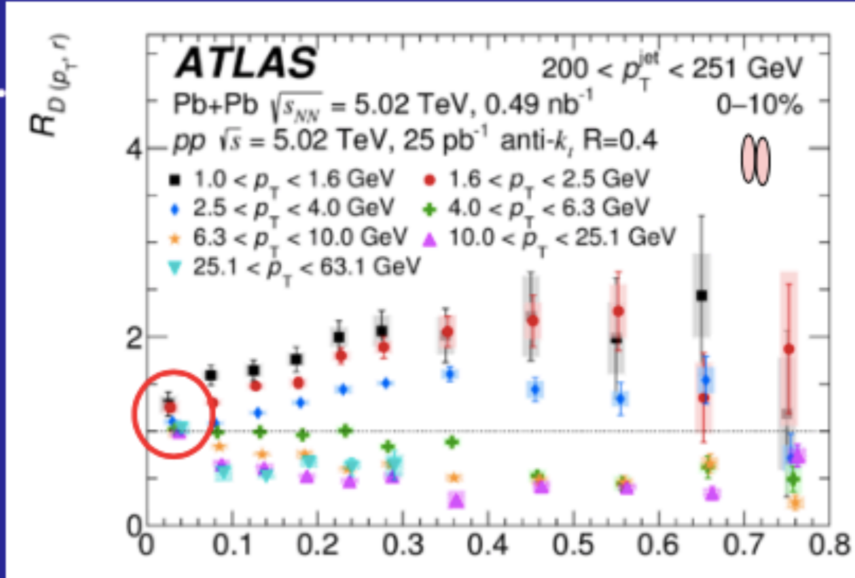

Phys. Rev. C 100 (2019) 064901

In central collisions $R_{D(p_T,r)}$ is above unity at all r for all $p_T < 4$ GeV —> Energy lost by jets is being transferred to particles with $p_T < 4$ GeV

Jet core remains unmodified.

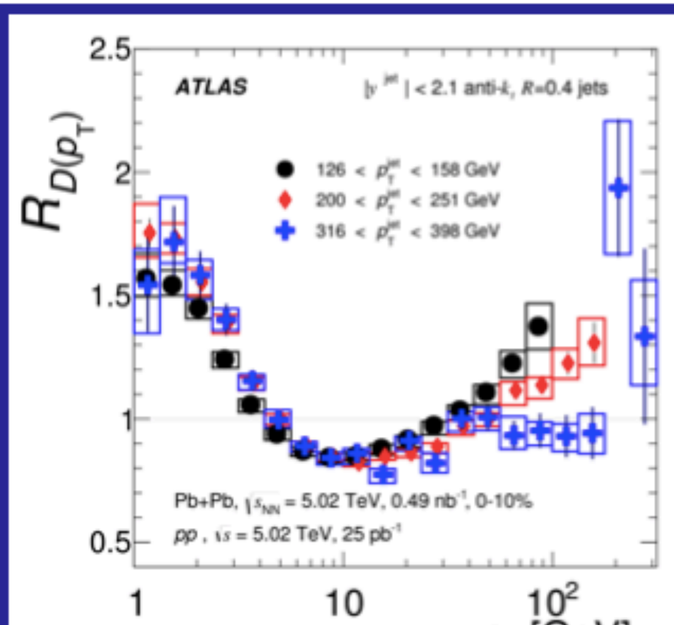

Phys. Rev. C 98, (2018) 024908

How do particles re-distribute within the jet and beyond?

Study *FF* as a function of the angular distance between the charged particle and the jet axis.

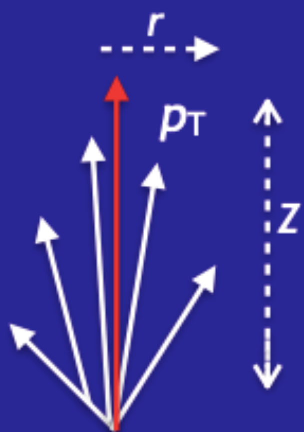

$$D(p_{\mathrm{T}}, r) = \frac{1}{N_{\mathrm{jet}}} \frac{1}{2\pi r} \frac{\mathrm{d}^2 n_{\mathrm{ch}}(r)}{\mathrm{d}r\,\mathrm{d}p_{\mathrm{T}}}$$

$$r = \sqrt{\Delta\eta^2 + \Delta\phi^2}$$

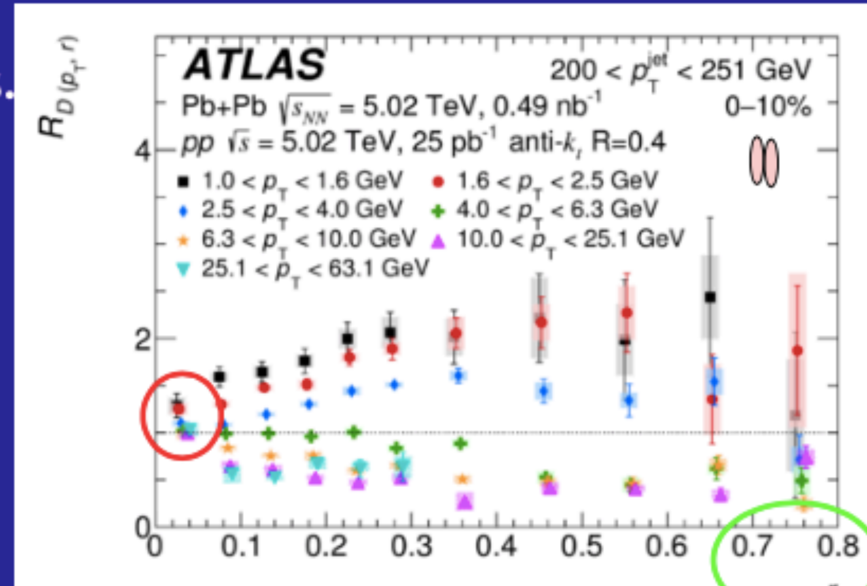

Phys. Rev. C 100 (2019) 064901

In central collisions $R_{D(p_T,r)}$ is above unity at all r for all $p_T < 4$ GeV —> Energy lost by jets is being transferred to particles with $p_T < 4$ GeV

Jet core remains unmodified.

Yield of soft particles starts to drop down when r –> 0.8.

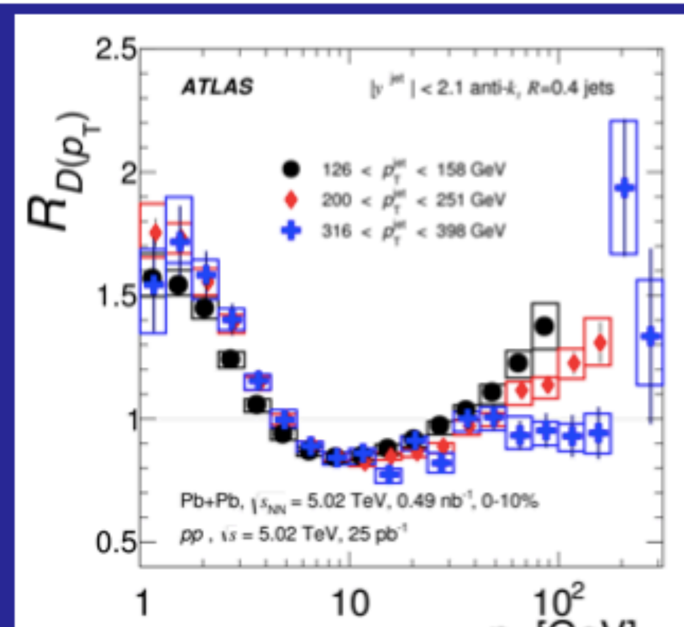

Phys. Rev. C 98, (2018) 024908

What can be learnt from large-R jets?

Measure jet R_{AA} as a function of jet sub-structure using sub-jets

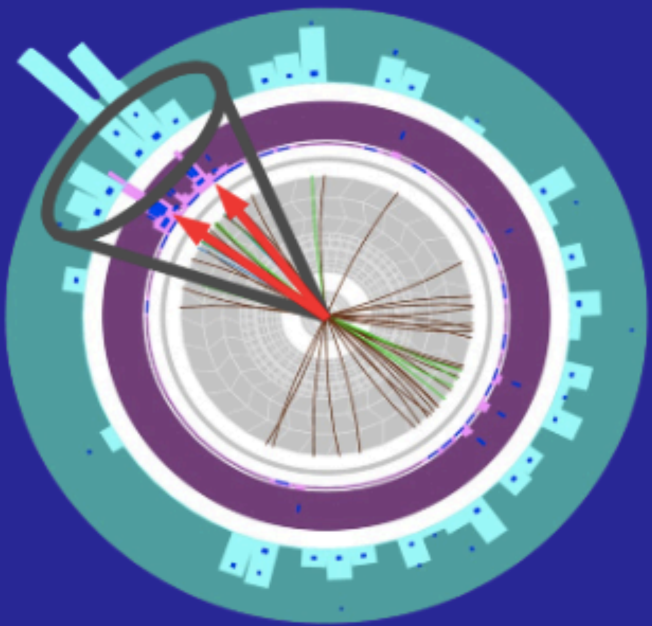

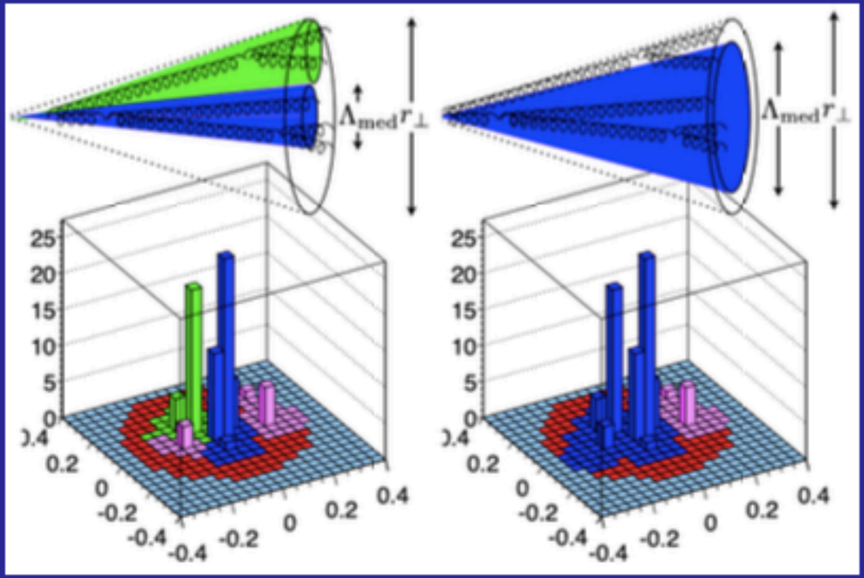

J. Casalderrey-Solana, Y. Mehtar-Tani, C. A. Salgado, K. Tywoniuk, Phys. Lett. B725 (2013) 357

What can be learnt from large-*R* jets?

Measure jet R_{AA} as a function of jet sub-structure using sub-jets

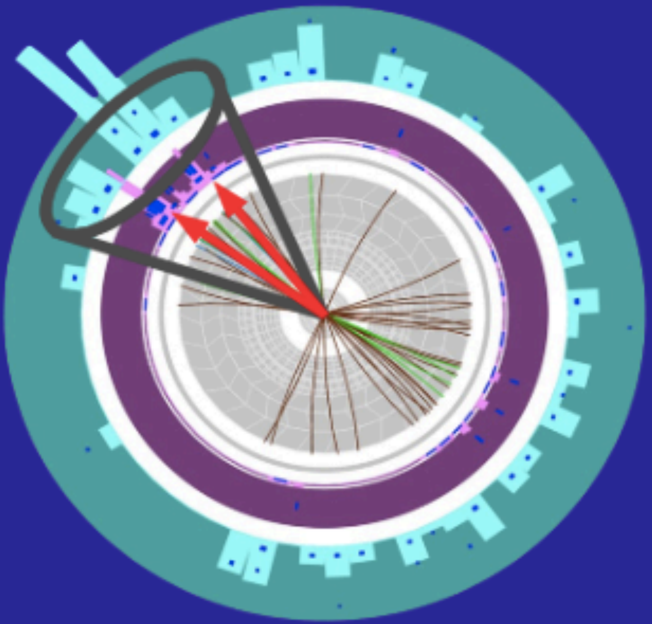

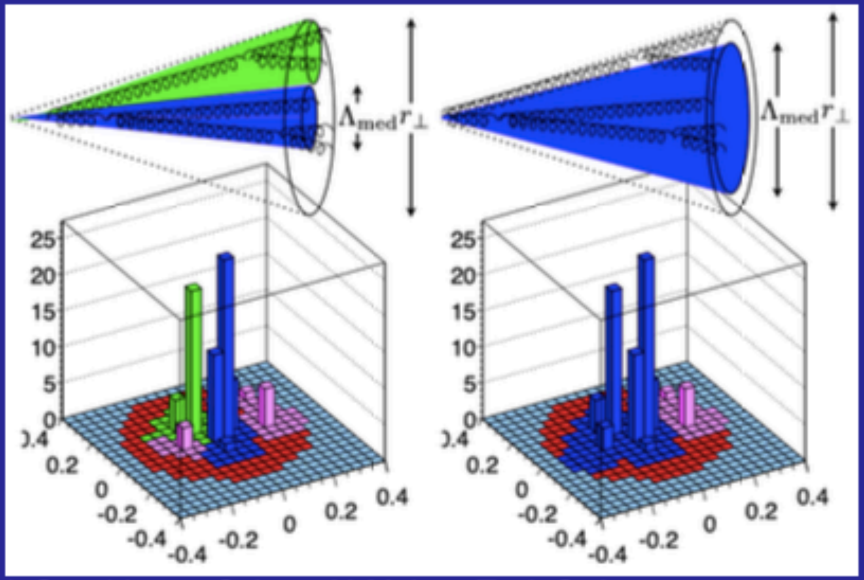

J. Casalderrey-Solana, Y. Mehtar-Tani, C. A. Salgado, K. Tywoniuk, Phys. Lett. B725 (2013) 357

recluster jets and remove soft contributions

$R = 0.2$ jets with $p_T > 35$ GeV

reclustered into anti-k_t $R = 1.0$

Allows the study of k_t sppliting scale

$$\sqrt{d_{12}} = \min(p_{T,1}, p_{T,2}) \cdot \Delta R_{12}$$

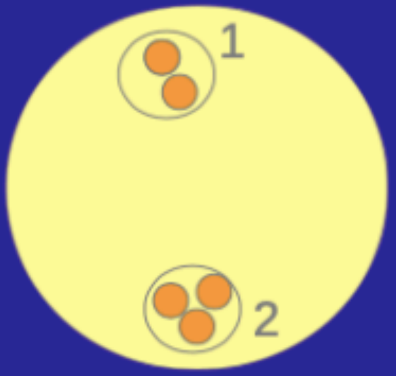

R_{AA} as a function of jet p_T

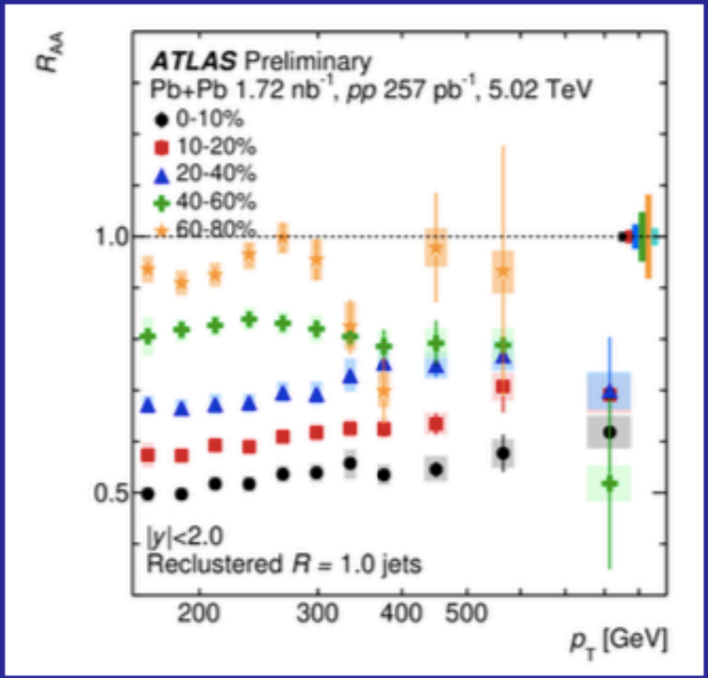

- Large-*R* (re-clustered with 0.2 jets and soft particles removed) jets are increasingly suppressed with centrality.

R_{AA} as a function of jet p_T

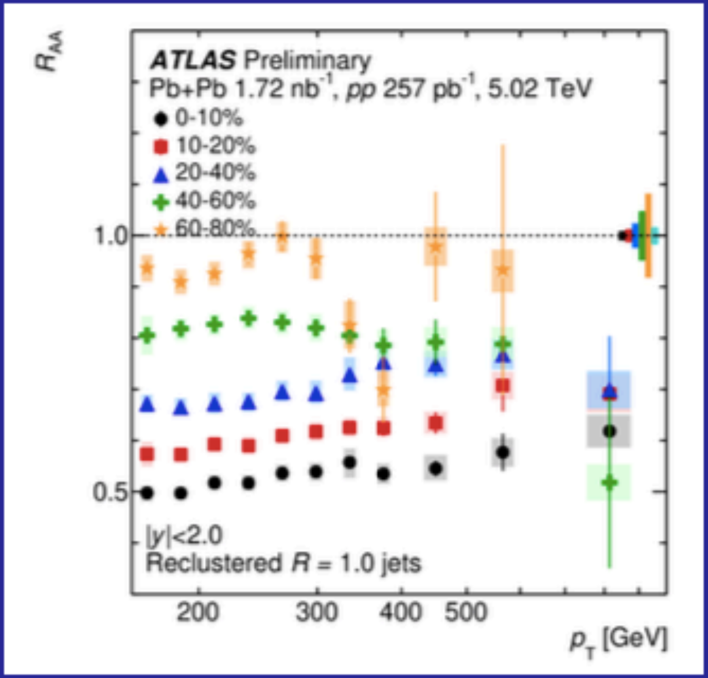

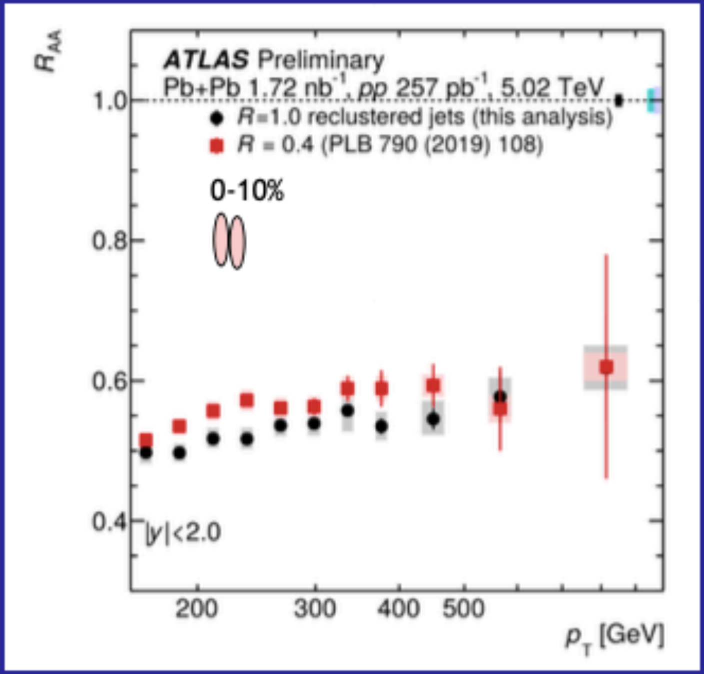

ATLAS-CONF-2019-056

- Large-*R* (re-clustered with 0.2 jets and soft particles removed) jets are increasingly suppressed with centrality.
- R = 0.4 jets slightly less suppressed, but trend is similar.

R_{AA} as a function of jet sub-structure

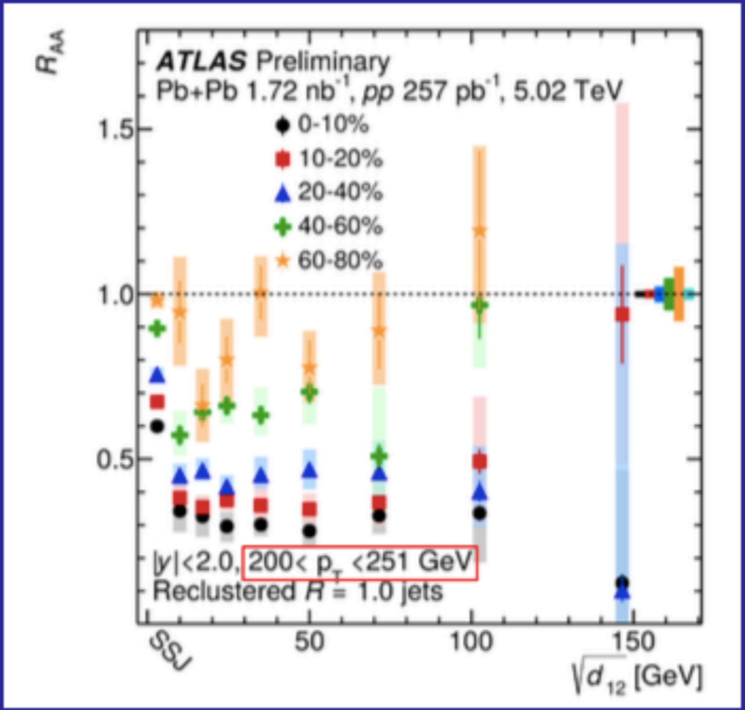

$$\sqrt{d_{12}} = \min(p_{T,1}, p_{T,2}) \cdot \Delta R_{12}$$

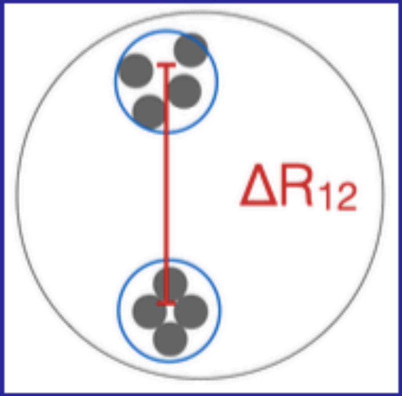

The lowest $\sqrt{d_{12}}$ interval is populated with jets with single "isolated" sub-jet - SSJ

- Significant change of the R_{AA} magnitude between jets with SSJ and those with more complex sub-structure.
- Then R_{AA} is not dependent on $\sqrt{d_{12}}$.

R_{AA} as a function of jet sub-structure

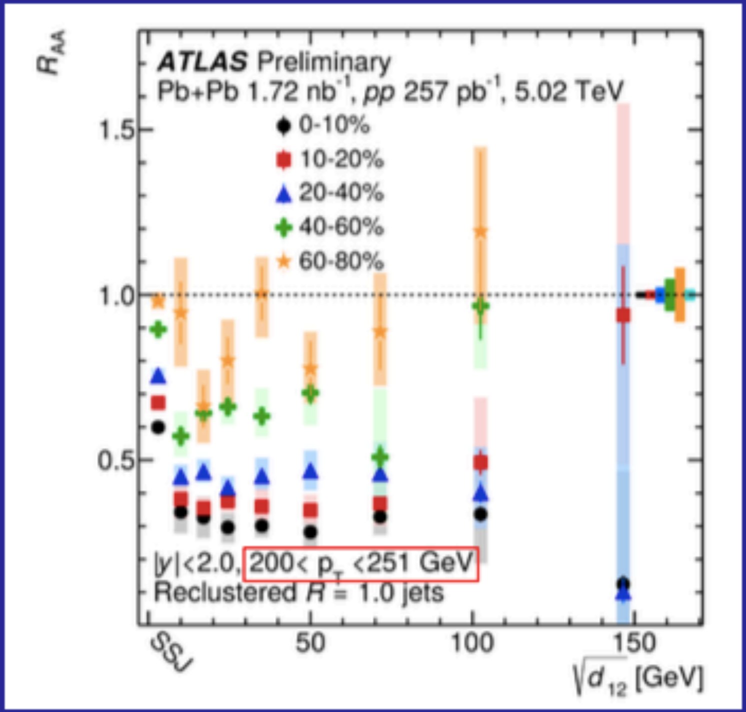

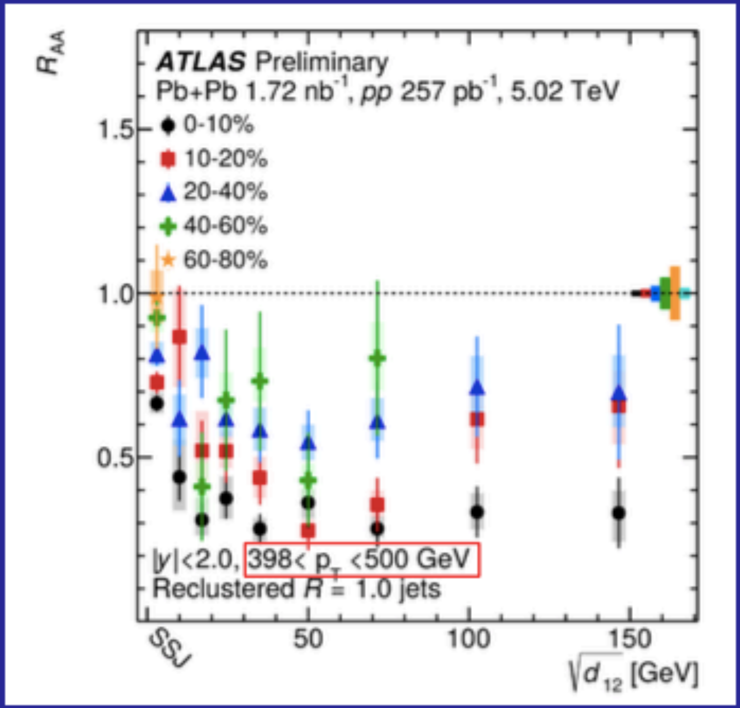

ATLAS-CONF-2019-056

The lowest $\sqrt{d_{12}}$ interval is populated with jets with single "isolated" sub-jet - SSJ

- Significant change of the R_{AA} magnitude between jets with SSJ and those with more complex sub-structure.
- Then R_{AA} is not dependent on $\sqrt{d_{12}}$.
- This behaviour is not dependent on jet p_T (up to 500 GeV).

Z-recoil particles

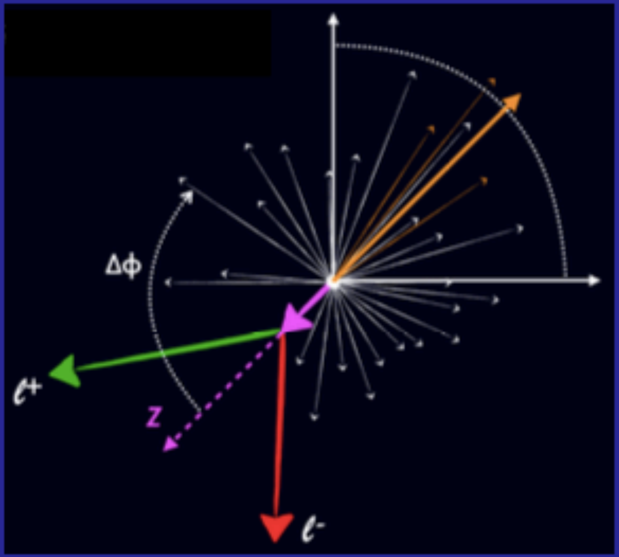

The Z boson tags the initial energy, direction, and flavour of the opposing parton before it starts to shower and propagate through the QGP.

Access to low-p_T ranges not reached by reconstructed jets —> precious for understanding the mechanisms of the parton energy loss.

Z-recoil particles

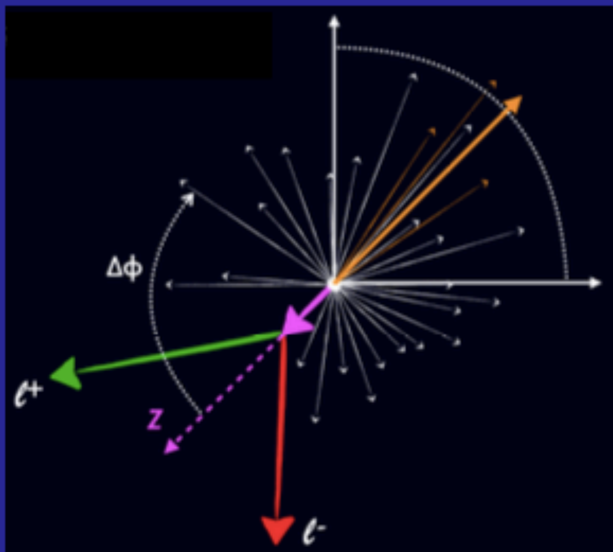

Charged particles

- p_T^{ch} > 1 GeV
- $|\Delta\varphi| > 3\pi/4$
- $|\eta| < 2.5$

p_T^{ch}-dependent enhancement/ suppression pattern

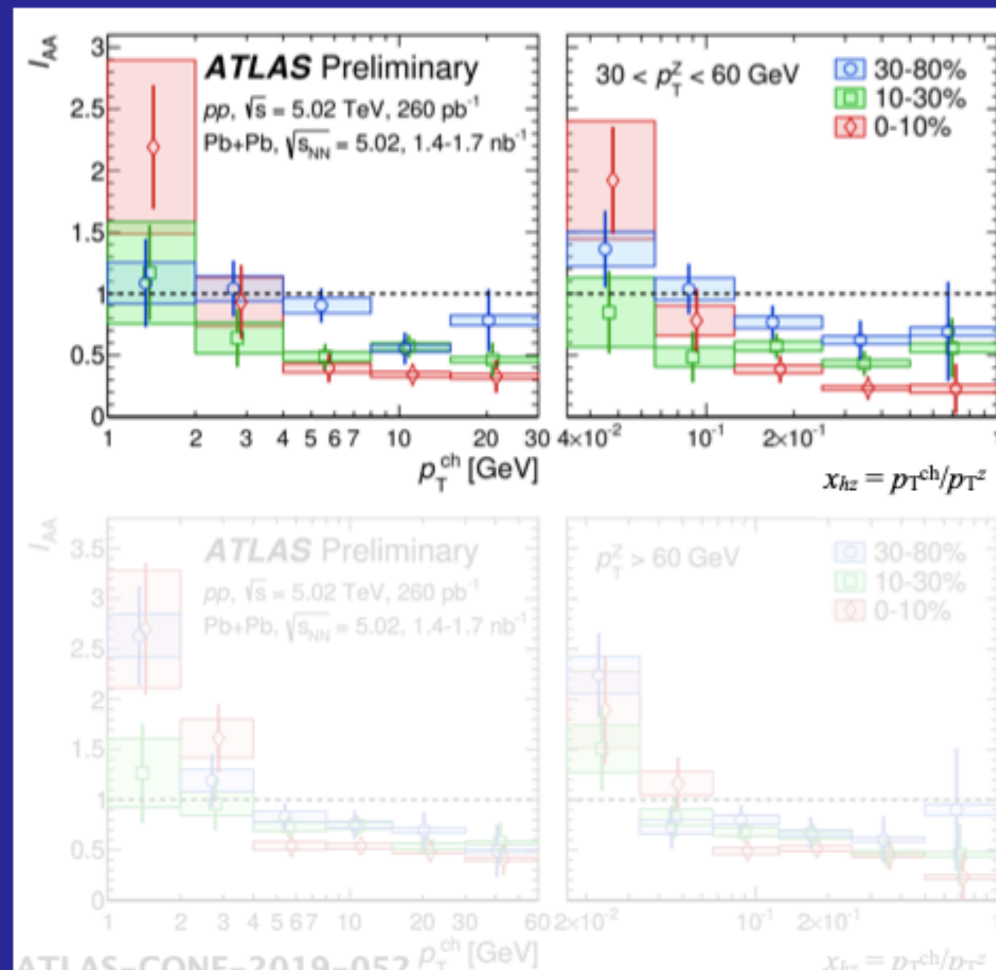

- $Z \rightarrow ee$ or $Z \rightarrow \mu\mu$
- $76 < m_Z < 106$ GeV
- $p_T^Z > 30$ GeV

Measure the average number of charged particles per Z

and

I_{AA} = yield in Pb+Pb / yield in *pp*

Z-recoil particles

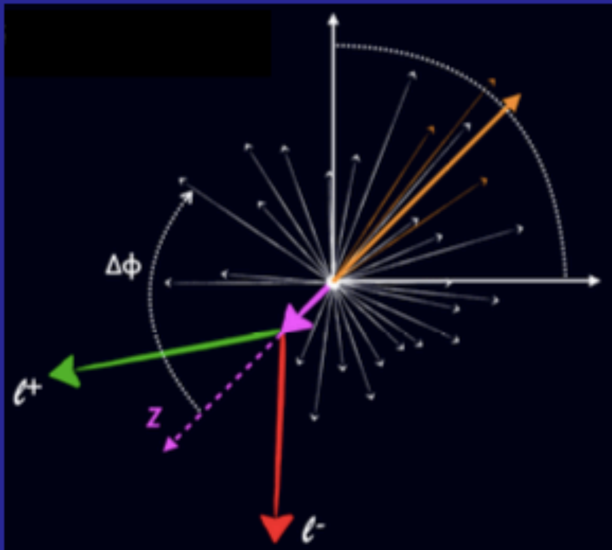

Charged particles
- p_T^{ch} > 1 GeV
- $|\Delta\varphi| > 3\pi/4$
- $|\eta| < 2.5$

p_T^Z plays a role in the enhancement/suppression pattern

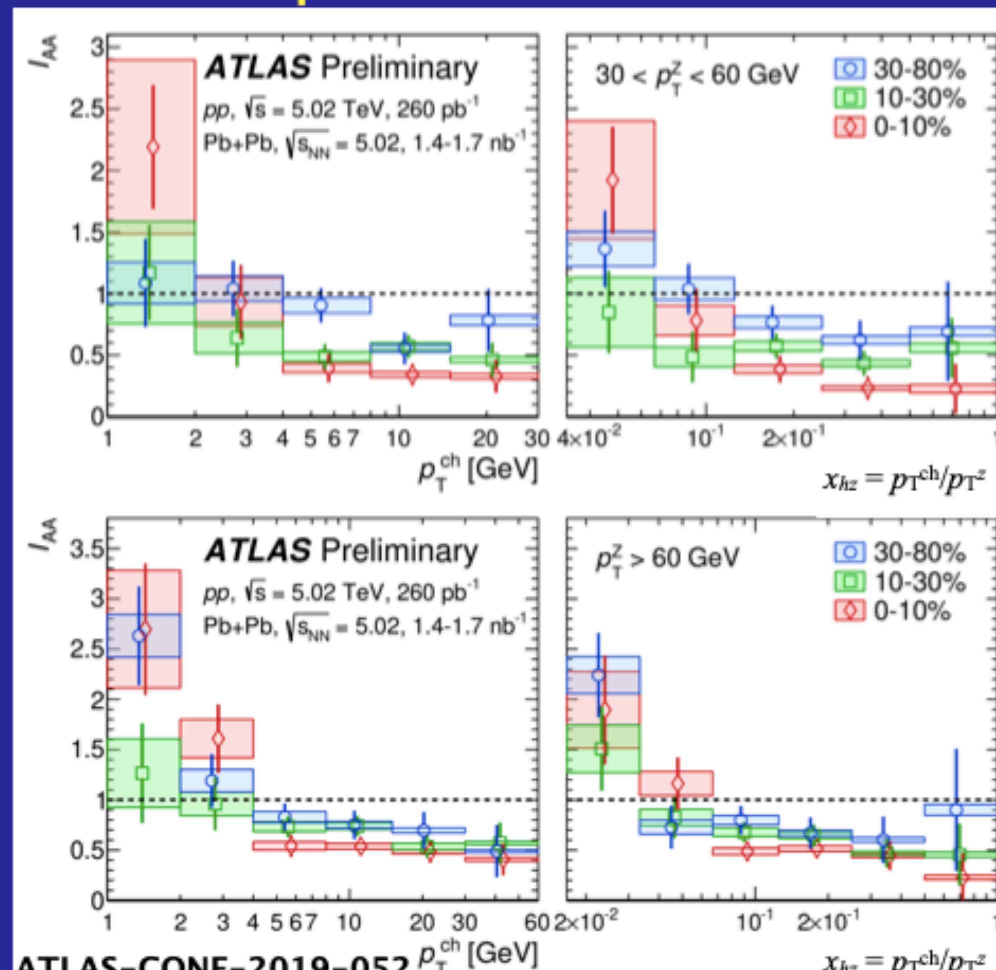

- $Z \rightarrow ee$ or $Z \rightarrow \mu\mu$
- $76 < m_Z < 106$ GeV
- $p_T^Z > 30$ GeV

Measure the average number of charged particles per Z and

I_{AA} = yield in Pb+Pb / yield in *pp*

Z-recoil particles

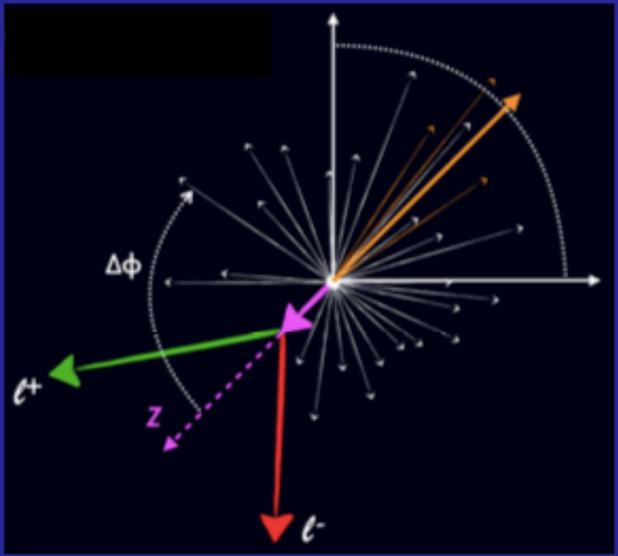

Charged particles

- $p_T^{ch} > 1$ GeV
- $|\Delta\varphi| > 3\pi/4$
- $|\eta| < 2.5$

- $Z \rightarrow ee$ or $Z \rightarrow \mu\mu$
- $76 < m_Z < 106$ GeV
- $p_T^Z > 30$ GeV

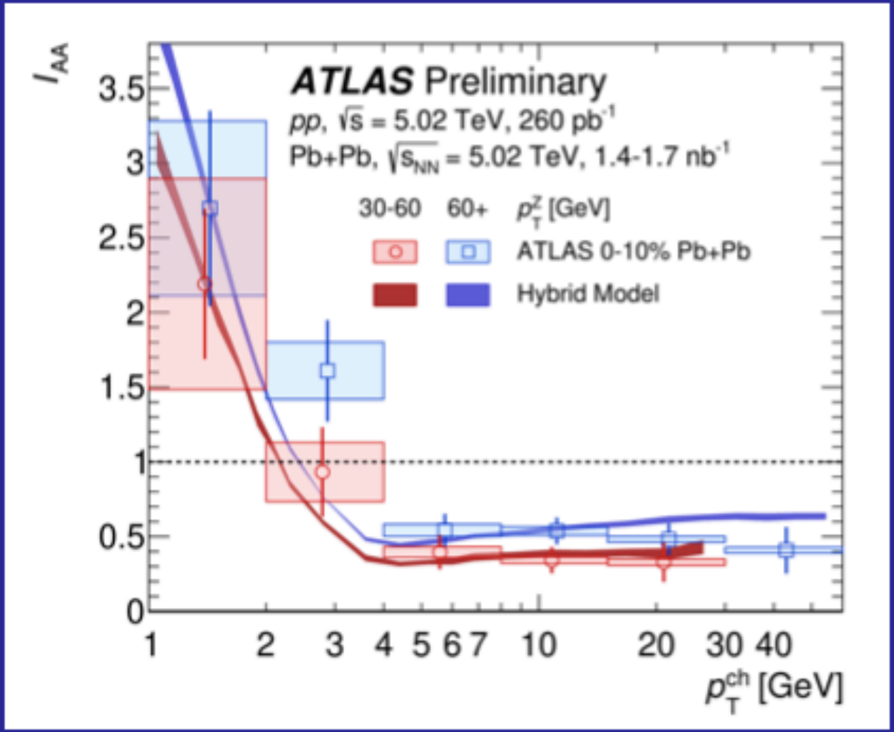

Measure the average number of charged particles per Z and

I_{AA} = yield in Pb+Pb / yield in *pp*

Good agreement with the predictions of the Hybrid model (JHEP 03 (2016) 053) in the entire p_T^{ch} range and for both p_T^Z selections.

Messages from Jets

- Inclusive jets in Pb+Pb are suppressed relatively to *pp* up to a factor of 2.
- Evidence of path length dependence of jet energy loss.
- Jet substructure strongly modified in Pb+Pb collisions with onset at 4 GeV.
- Reclustered R=1.0 jets with single sub-jet less quenched than those with more complex substructure.
- Suppression of high-p_T hadrons in Z-tagged hadron yields; enhancement at low-p_T.

An 80 years old prediction - LbyL

Heisenberg, W., Euler, H. Folgerungen aus der Diracschen Theorie des Positrons. *Z. Physik* **98,** 714–732 (1936). https://doi.org/10.1007/BF01343663

The fact that electromagnetic radiation can be transformed into matter and vice versa leads to modifications of the Maxwell's equations…

An 80 years old prediction - LbyL

Heisenberg, W., Euler, H. Folgerungen aus der Diracschen Theorie des Positrons. *Z. Physik* **98,** 714–732 (1936). https://doi.org/10.1007/BF01343663

The fact that electromagnetic radiation can be transformed into matter and vice versa leads to modifications of the Maxwell's equations…

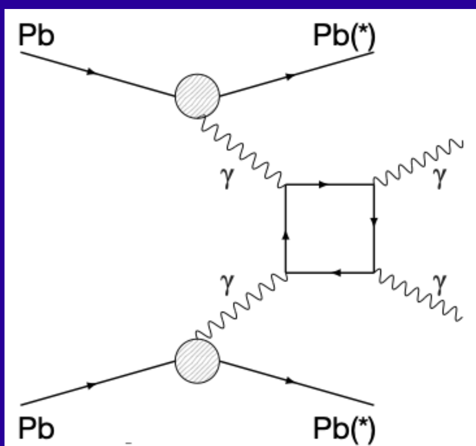

$-Q^2 < 1/R^2$

$\sigma(\gamma\gamma)$ scales with $\sim Z^4$

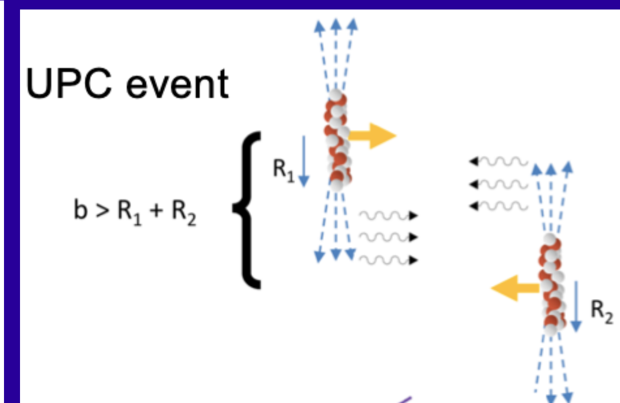

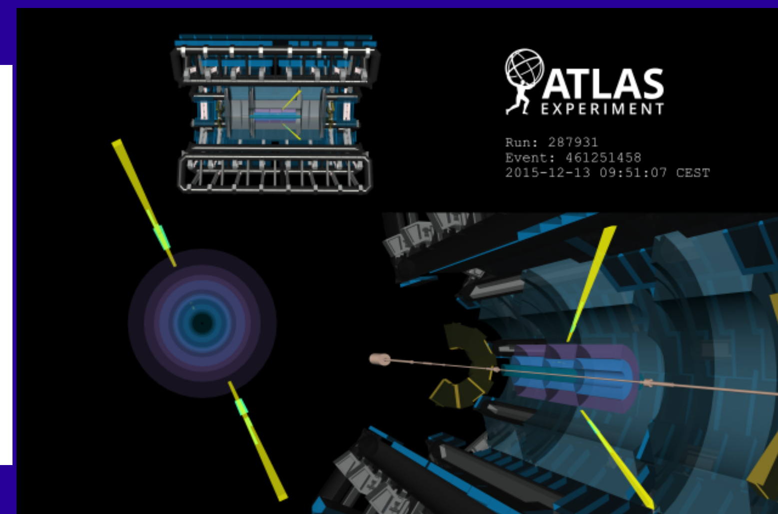

Evidence of LbyL scattering (Nature Physics 13, 852–858(2017)): 4.4 (3.8) σ

σ_{fid} = 70 ± 24 (stat) ± 17 (syst) nb, in agreement with SM predictions.

Noawdays perspective

Heisenberg, W., Euler, H. Folgerungen aus der Diracschen Theorie des Positrons. *Z. Physik* **98,** 714–732 (1936). https://doi.org/10.1007/BF01343663

The fact that electromagnetic radiation can be transformed into matter and vice versa leads to modifications of the Maxwell's equations…

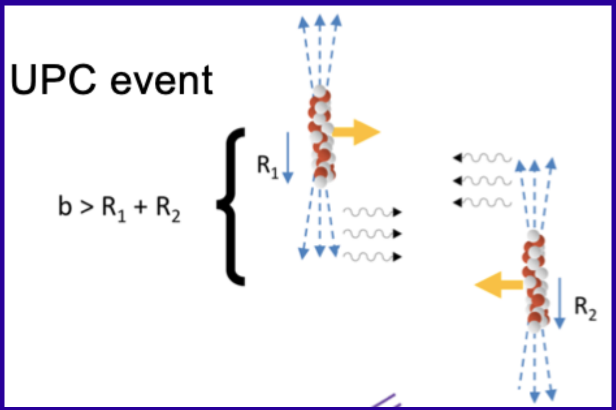

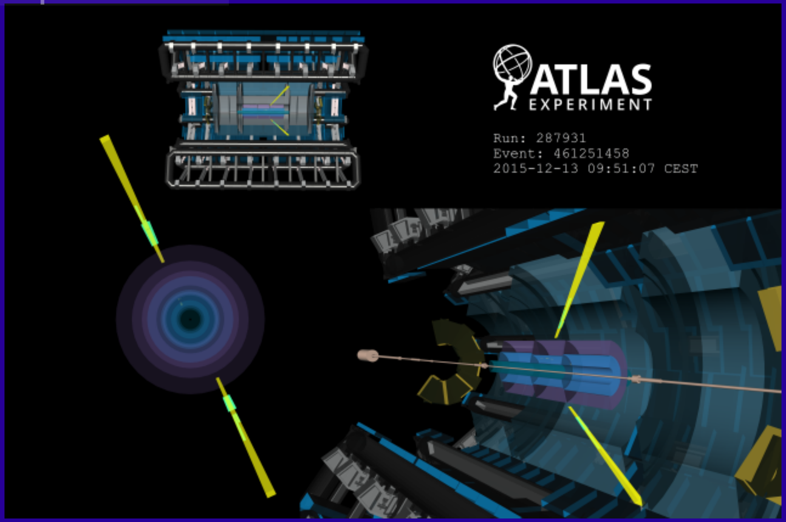

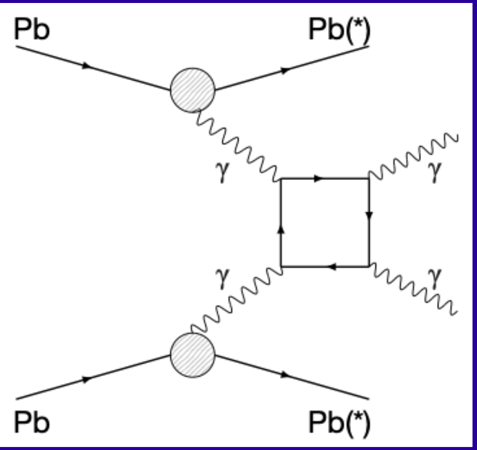

LbyL may be sensitive to BSM

- Exotic charged particles
- Extra dimensions
- **Axion-like particles - ALP**

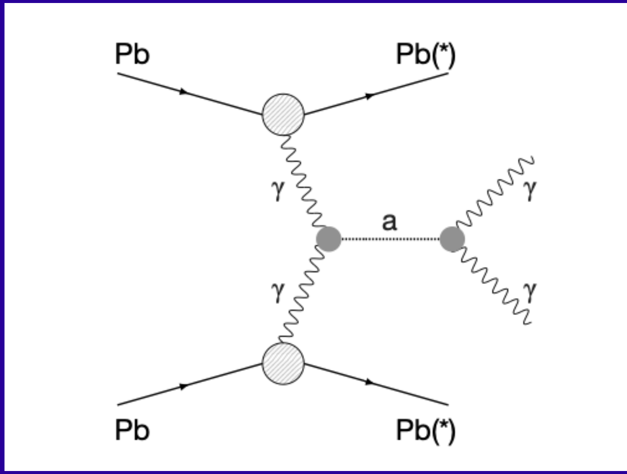

γγ→γγ in Ultra Peripheral Collisions

arXiv:2008.05355

Detector calibrated with $\gamma\gamma \to e^+e^-$

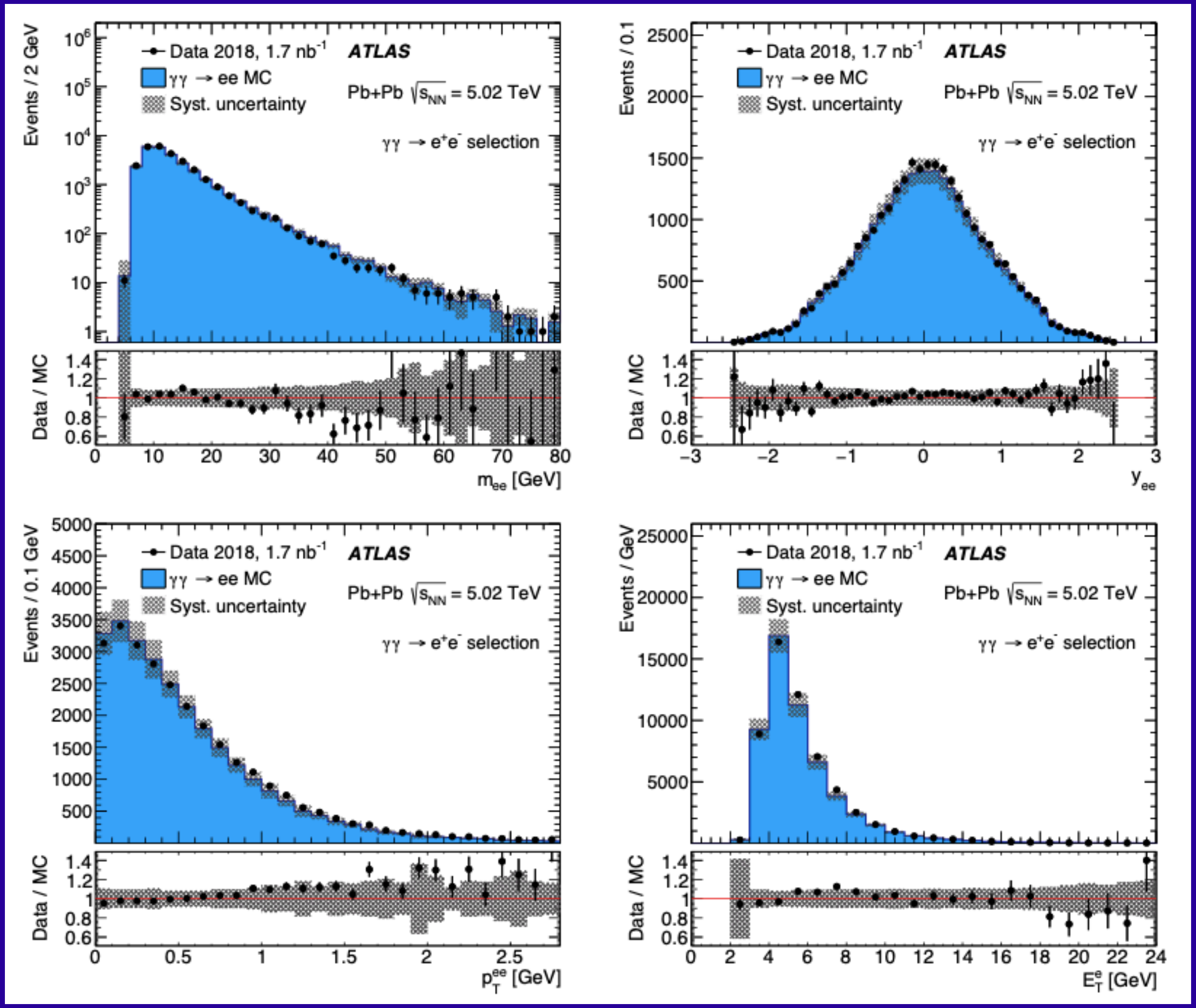

STARlight MC describe kinematics well, in general

γγ→γγ in UPC

arXiv:2008.05355

Acoplanartity, A_φ

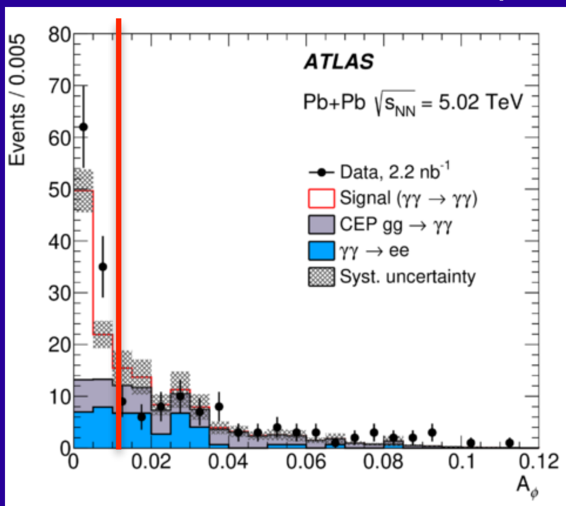

$$A_\phi = (1 - |\Delta\phi_{\gamma\gamma}|/\pi)$$

Signal plus non-negligible backgrounds

$A_\varphi < 0.01$ defined as the signal region

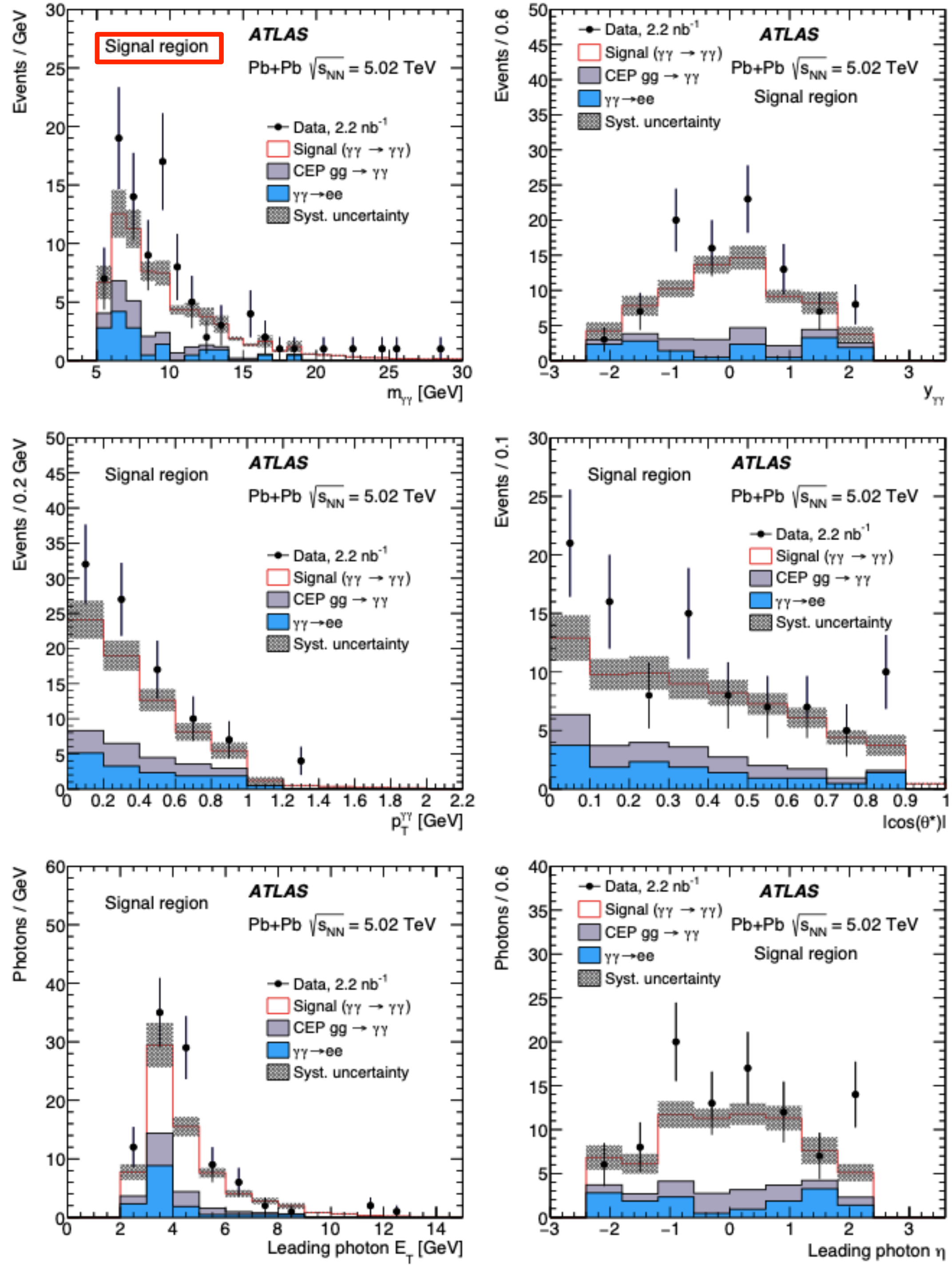

γγ→γγ in UPC

arXiv:2008.05355

Cross section for γγ→γγ

$$\sigma_{\text{fid}} = \frac{N_{\text{data}} - N_{\text{bkg}}}{C \times \int L dt},$$

$$\sigma_{\text{fid}} = 120 \pm 17\,(\text{stat.}) \pm 13\,(\text{syst.}) \pm 4\,(\text{lumi.})\ \text{nb}$$

predicted values of 80 ± 8 nb

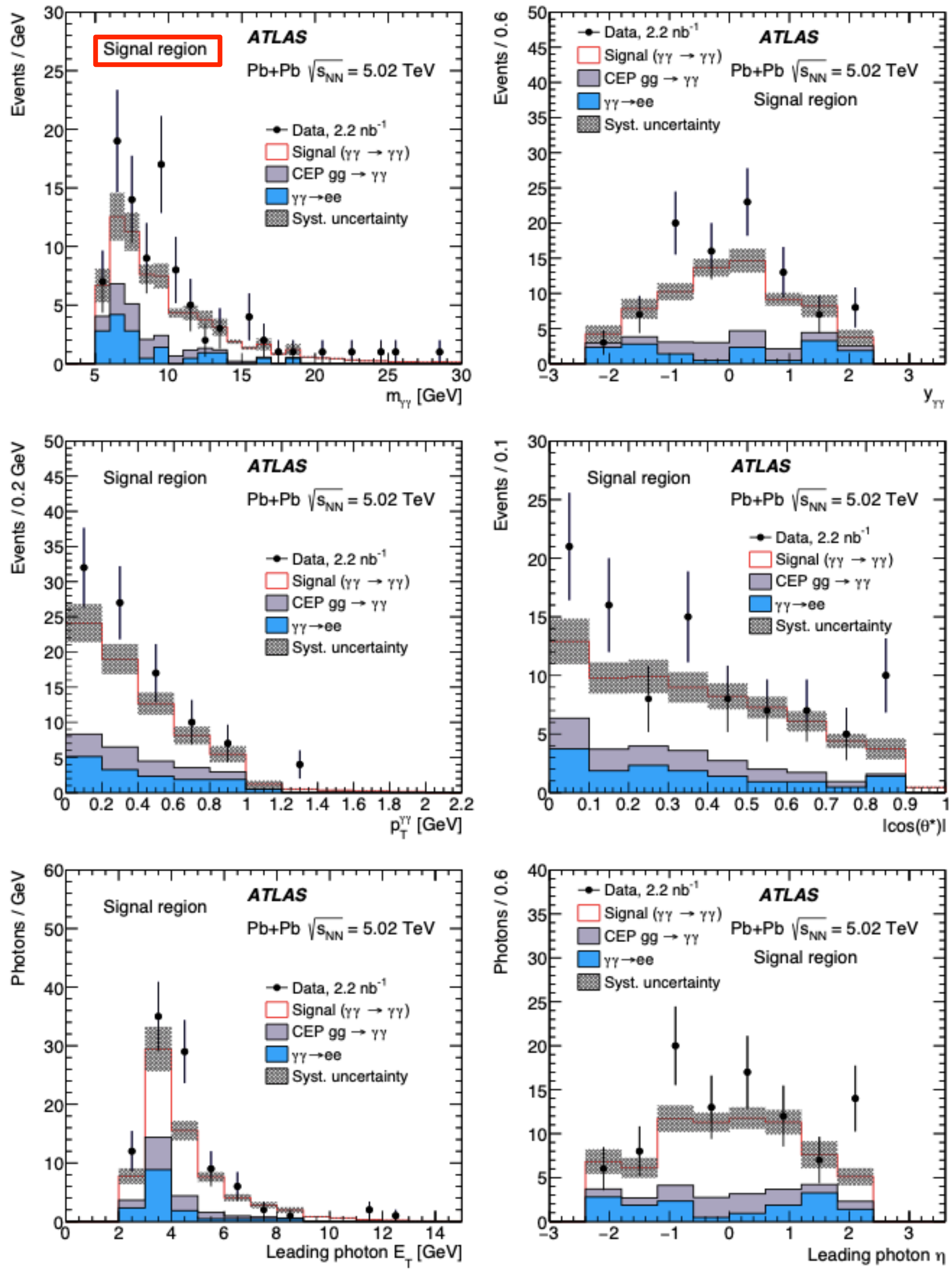

γγ→γγ in UPC - search for Axion-like particles

arXiv:2008.05355

95% CL upper for γγ→a→γγ

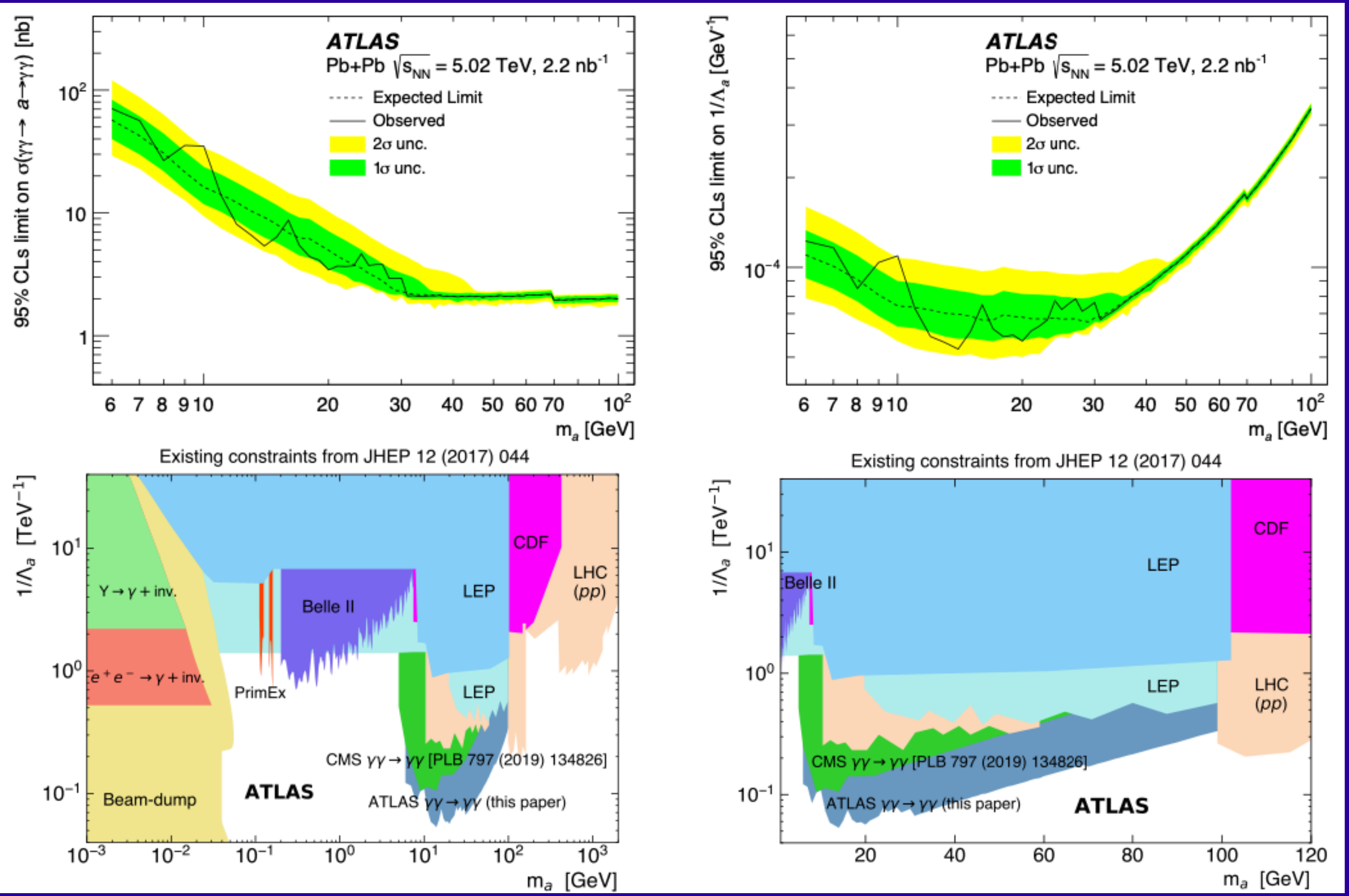

The exclusion limits from this analysis are the strongest so far for 6 < m_a < 100 GeV

Outlook

Stay tuned to data Run 3 data. Integrated luminosity will increase from 2.2 to 6 nb^{-1}. Heavy Flavour jets and Top quark studies will be a priority.

Many topics were not covered, but they are unmissable:
https://twiki.cern.ch/twiki/bin/view/AtlasPublic/HeavyIonsPublicResults

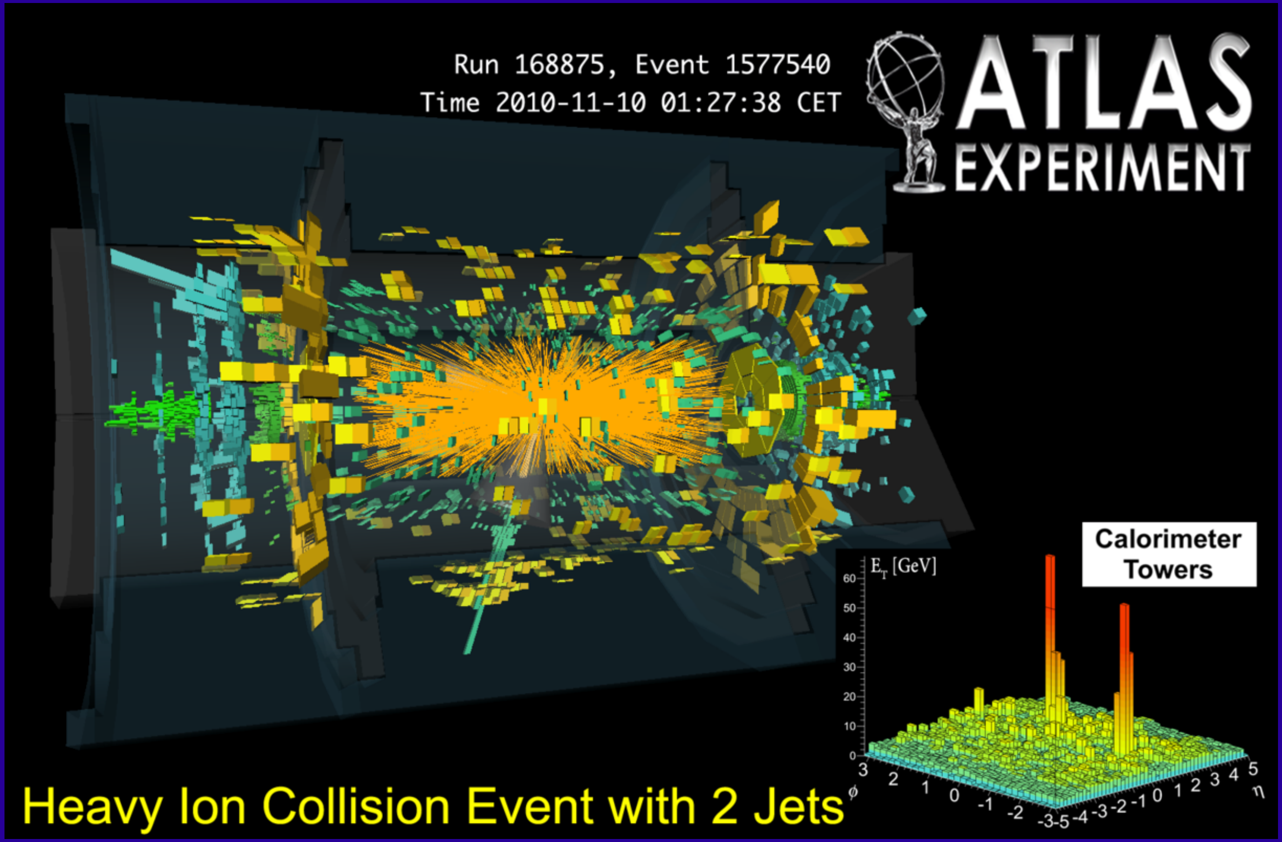

Backup

ATLAS Performance ($\gamma\gamma \to \gamma\gamma$ in UPC)

arXiv:2008.05355

Source of uncertainty	Detector correction (C)
	0.263 ± 0.021
Trigger efficiency	5%
Photon reco. efficiency	4%
Photon PID efficiency	2%
Photon energy scale	1%
Photon energy resolution	2%
Photon angular resolution	2%
Alternative signal MC	1%
Signal MC statistics	1%
Total	8%

Table 1: The detector correction factor, C, and its uncertainties for the integrated fiducial cross-section measurement.

γγ→γγ in Ultra Peripheral Collisions

arXiv:2008.05355

Cross section for γγ→γγ

$$\sigma_{\mathrm{fid}} = \frac{N_{\mathrm{data}} - N_{\mathrm{bkg}}}{C \times \int L dt},$$

$$\sigma_{\mathrm{fid}} = 120 \pm 17\ (\mathrm{stat.}) \pm 13\ (\mathrm{syst.}) \pm 4\ (\mathrm{lumi.})\ \mathrm{nb}$$

predicted values of 80 ± 8 nb

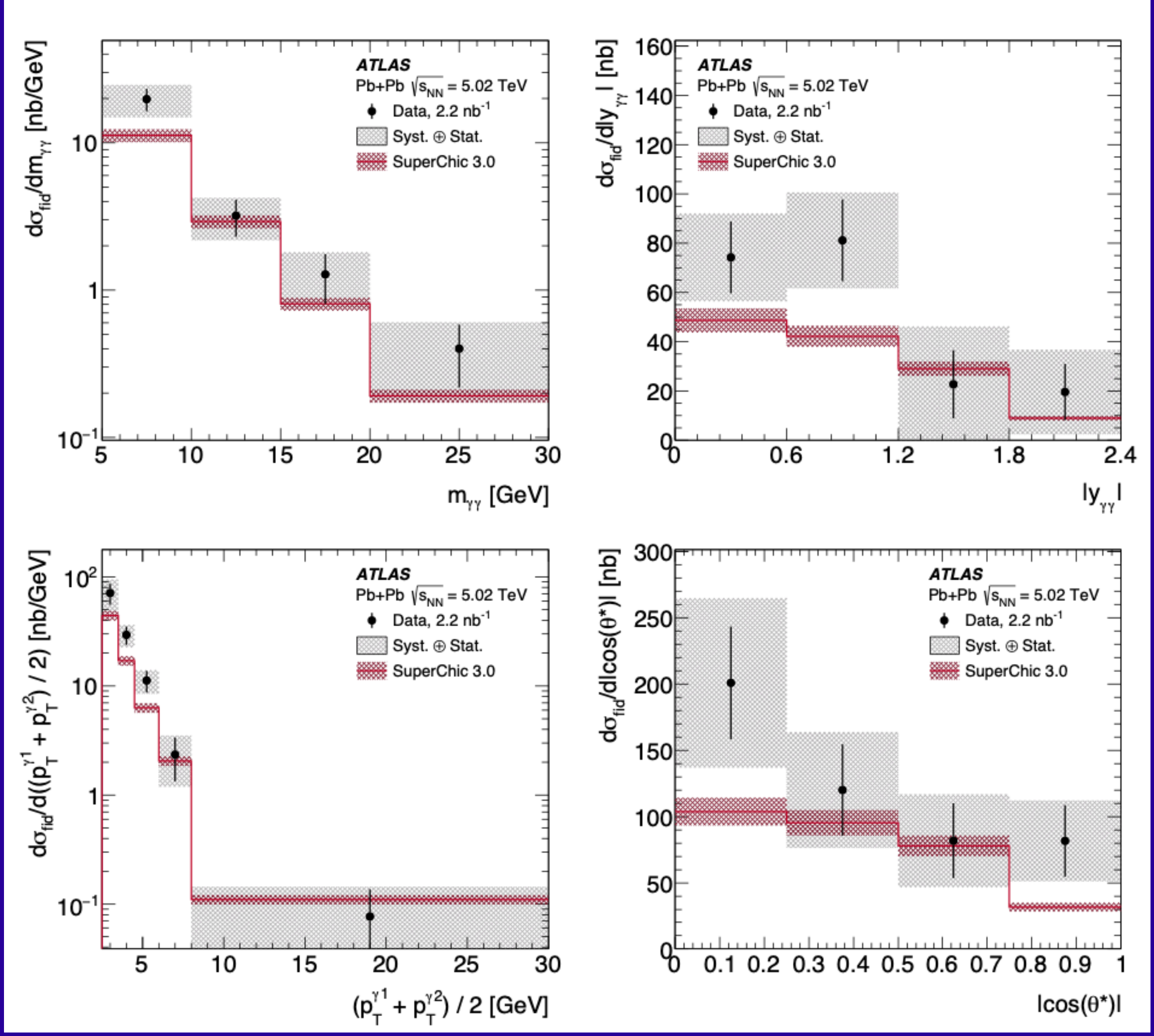

γγ→μ⁺μ⁻ in non-UPC

Phys. Rev. Lett. 121 (2018) 212301

Dimuon pairs resulting from photonuclear interactions occurring simultaneously with the hadronic collision.

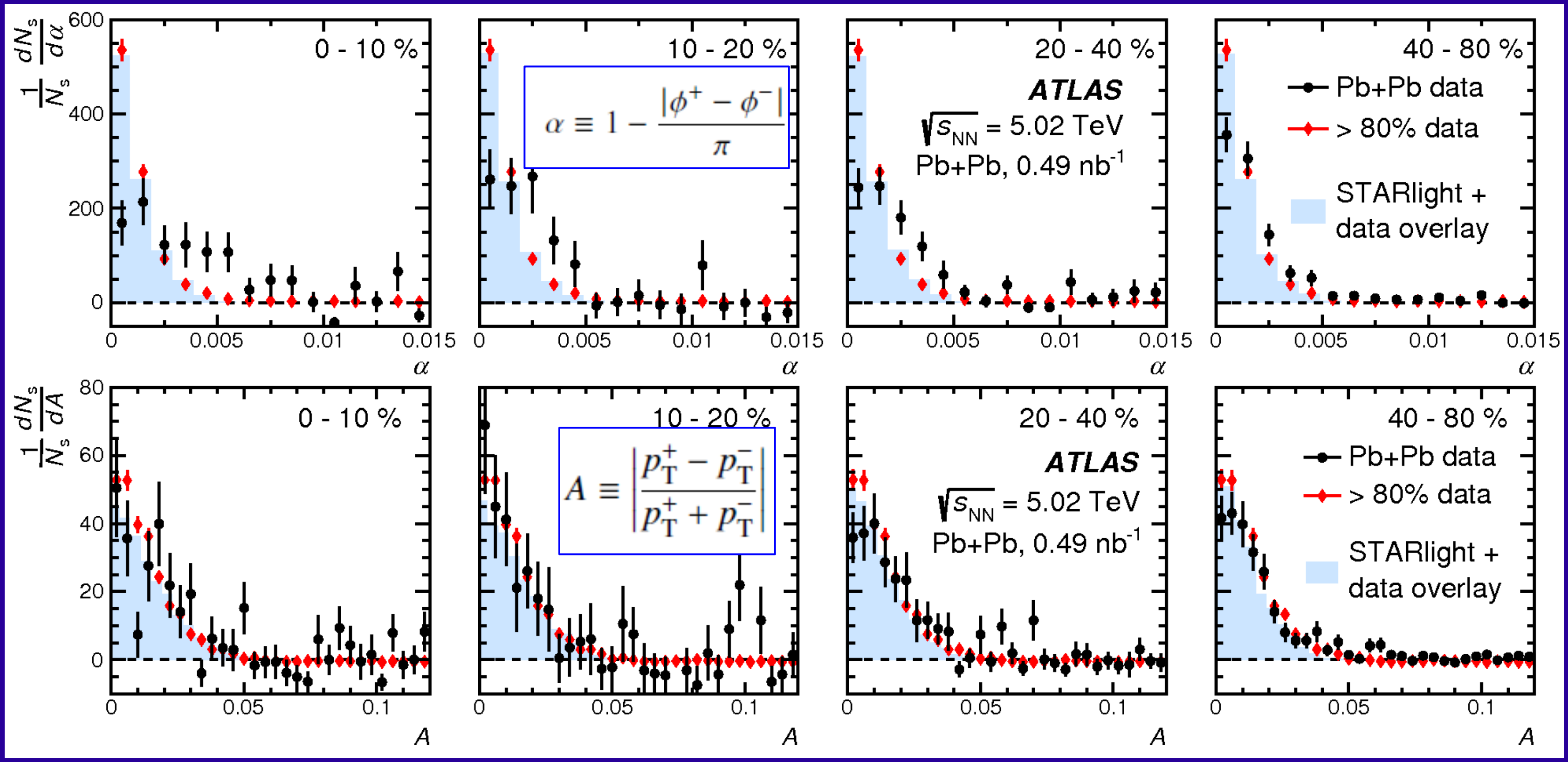

- Data reveals balance in energy, but acoplanarity is broadning with centrality.
- STARlight agrees in peripheral, but not in central collisions.

$\gamma\gamma \rightarrow \gamma\gamma$ in Non-Ultra Peripheral Collisions

Phys. Rev. Lett. 121 (2018) 212301

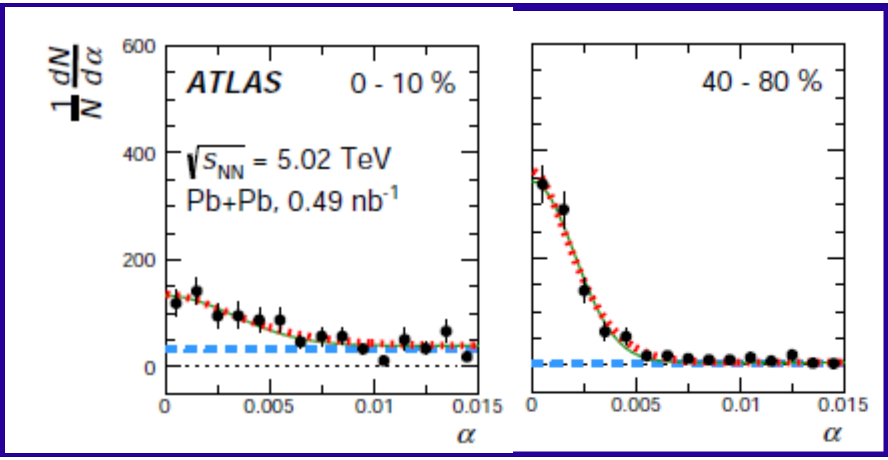

if broadening results ftom small k_T transfer:

$$\langle \alpha^2 \rangle = \langle \alpha^2 \rangle_0 + \frac{1}{\pi^2} \frac{\langle \vec{k}_T^2 \rangle}{\langle p_{T\,avg}^2 \rangle}$$

Centrality	$\langle N_{part} \rangle$	$p_{T\,avg}^{RMS}$ [GeV]	Gaussian fit			Convolution fit
			$\sigma_A(\times 10^3)$	$\sigma_\alpha(\times 10^3)$	k_T^{RMS} [MeV]	k_T^{RMS} [MeV]
0–10%	359±2	7.0±0.1	$17.9^{+1.0}_{-0.9}$	3.3±0.4	66±10	70±10
10–20%	264±3	7.7±0.4	$13.6^{+1.2}_{-1.0}$	2.3±0.3	40±7	42±7
20–40%	160±3	7.4±0.3	$17.2^{+0.4}_{-0.4}$	2.5±0.2	48±6	44±5
40–80%	47±2	6.8±0.3	$16.1^{+0.1}_{-0.1}$	2.0±0.1	35±4	32±2
> 80%	–	7.0±0.3	$15.5^{+0.1}_{-0.1}$	1.40±0.03	-	-

- Modifications are qualitatively consistent with re-scattering of the muons while crossing the QGP.

ATLAS Performance

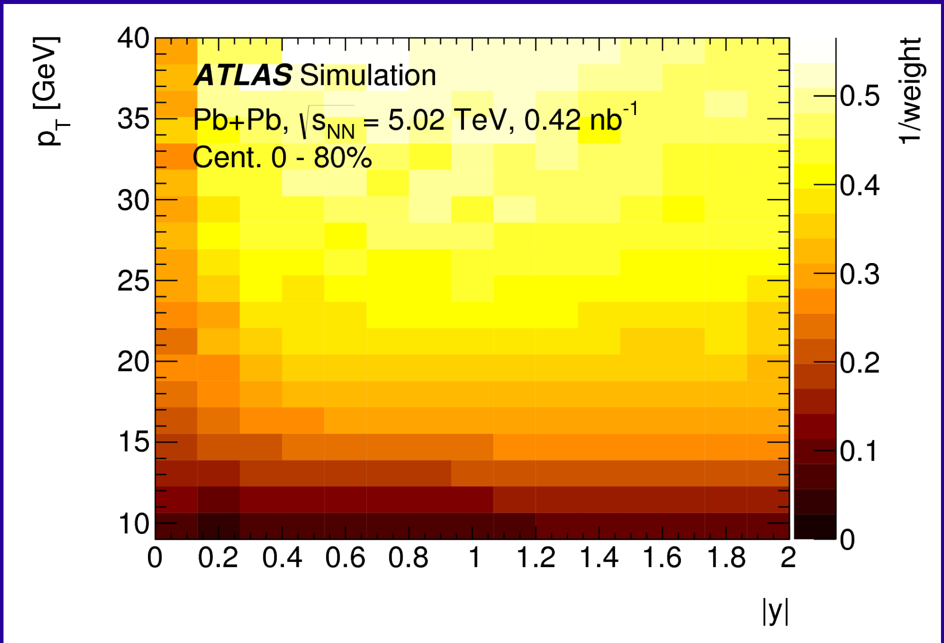

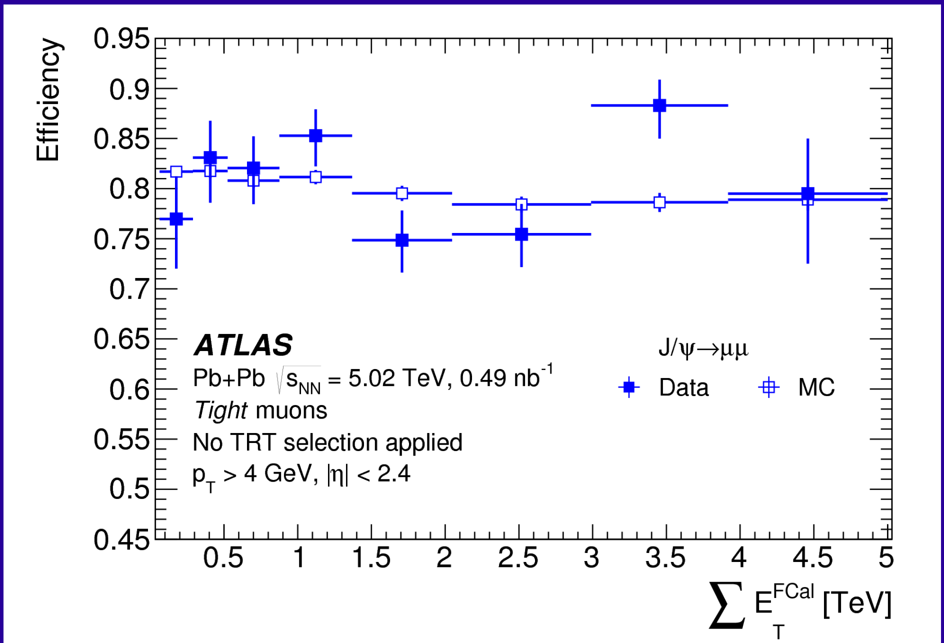

No dependence of the muon reconstruction efficiency on centrality.

J/ψ R_{pPb} and R_{AA} as a function of p_T

Eur. Phys. J. C 78 (2018) 762

Quarkonia in p+Pb collisions is a probe of cold nuclear matter effects

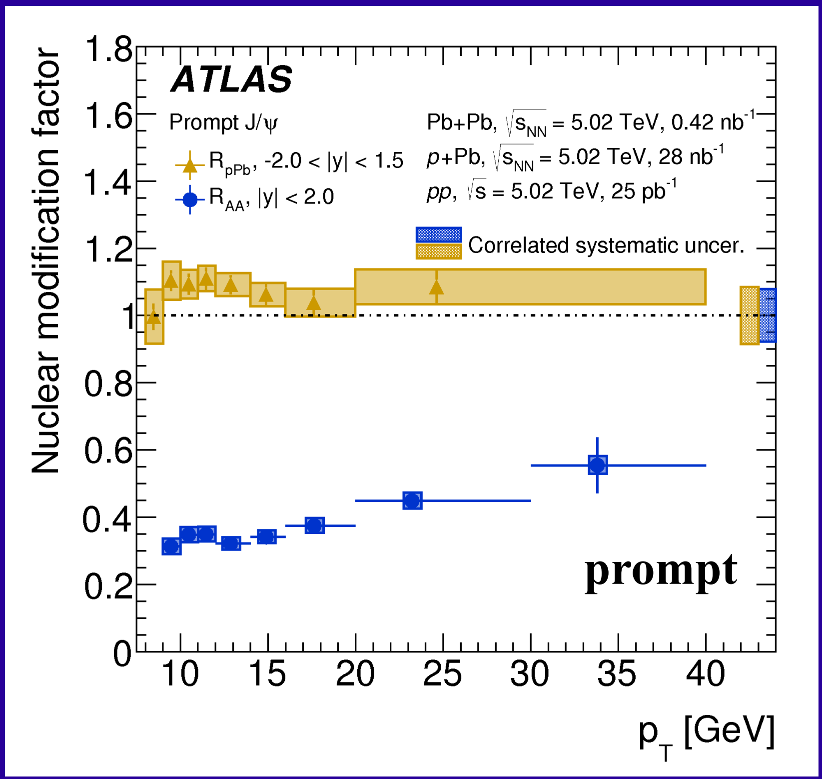

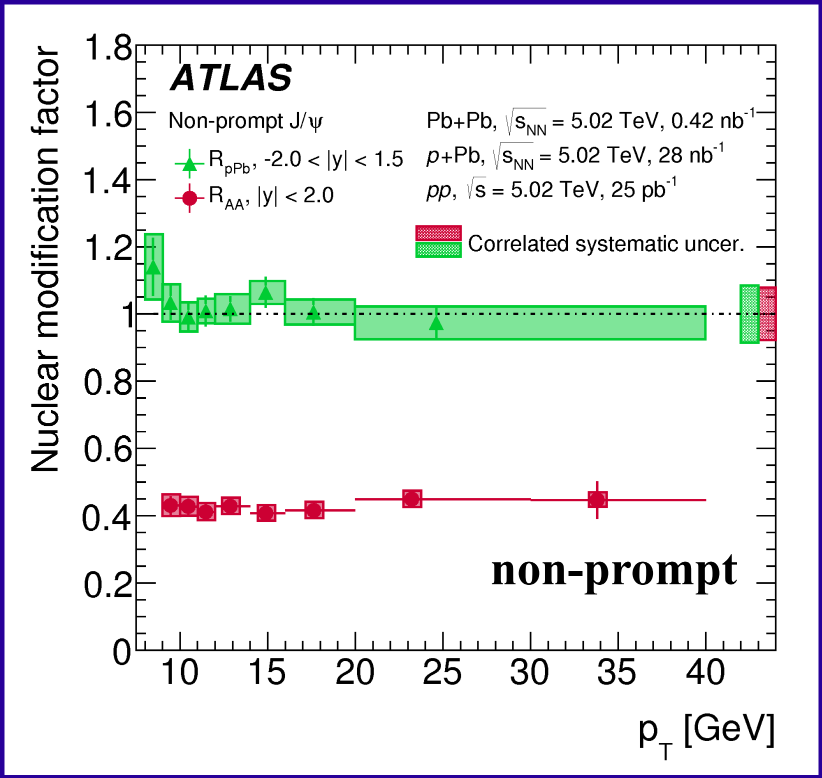

$$R_{pPb} = \frac{1}{208}\frac{\sigma^{\mathcal{O}(nS)}_{p+\mathrm{Pb}}}{\sigma^{\mathcal{O}(nS)}_{pp}},$$

- R_{pPb} is consistent with unity.
- J/ψ is strongly suppressed in Pb+Pb; prompt and non-prompt mechanisms have different p_T dependence.

J/ψ R_{AA} as a function of p_T

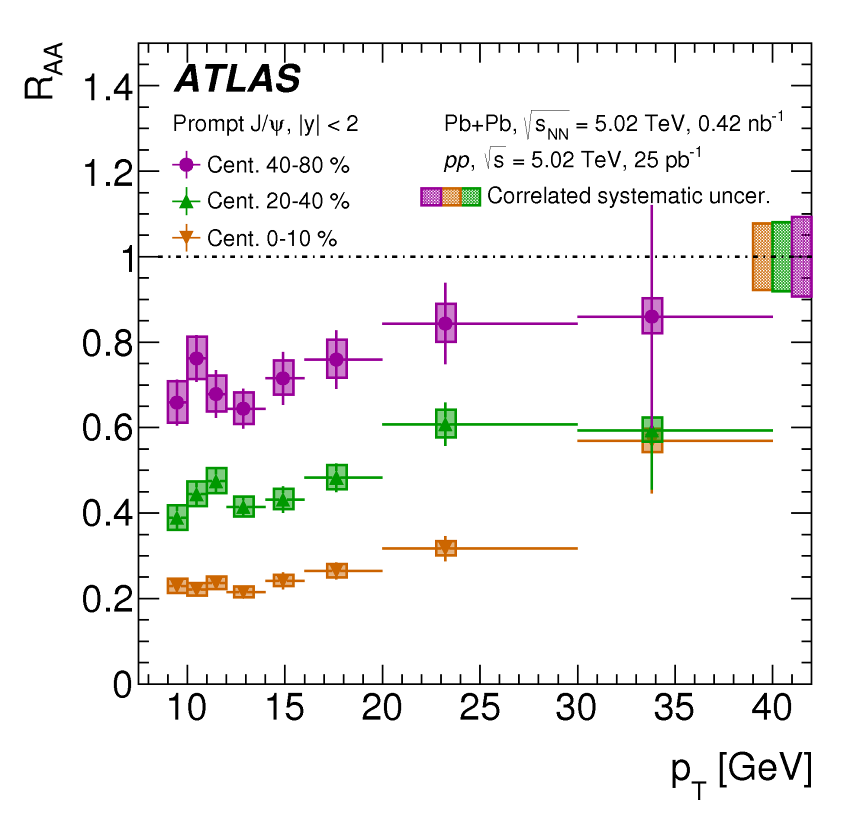

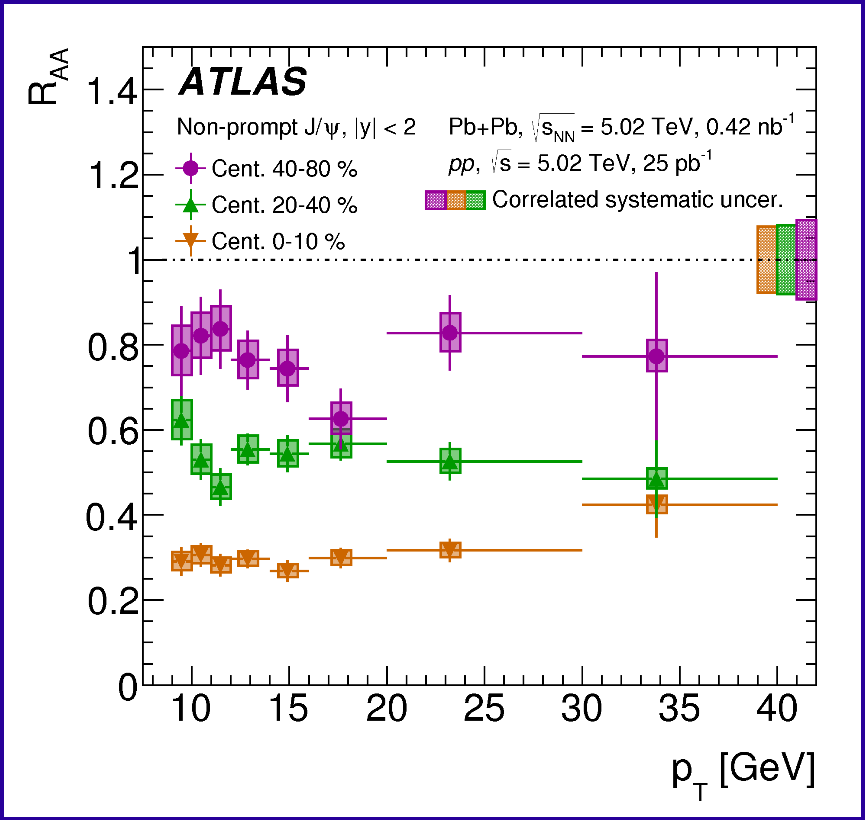

non-prompt fraction

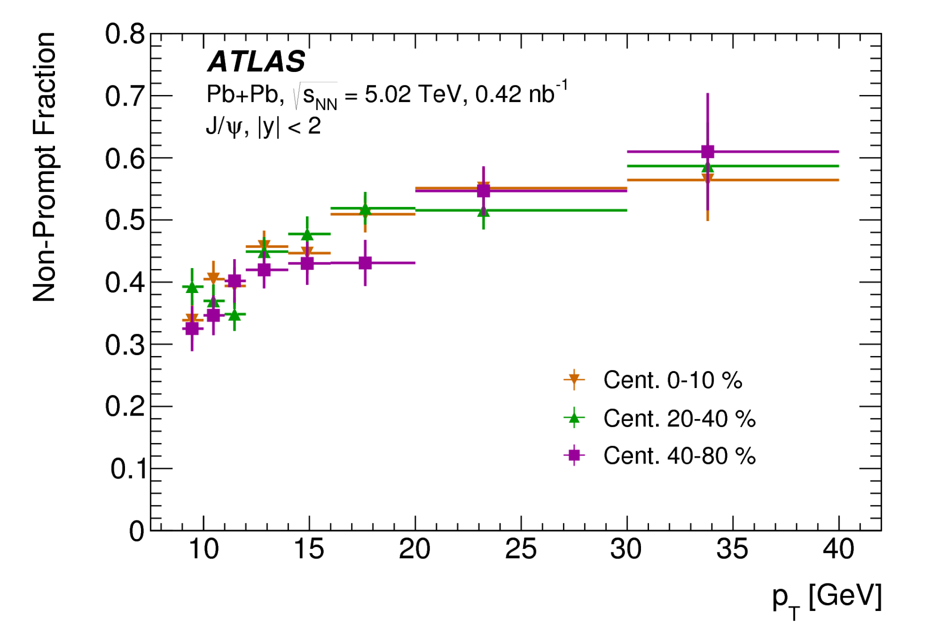

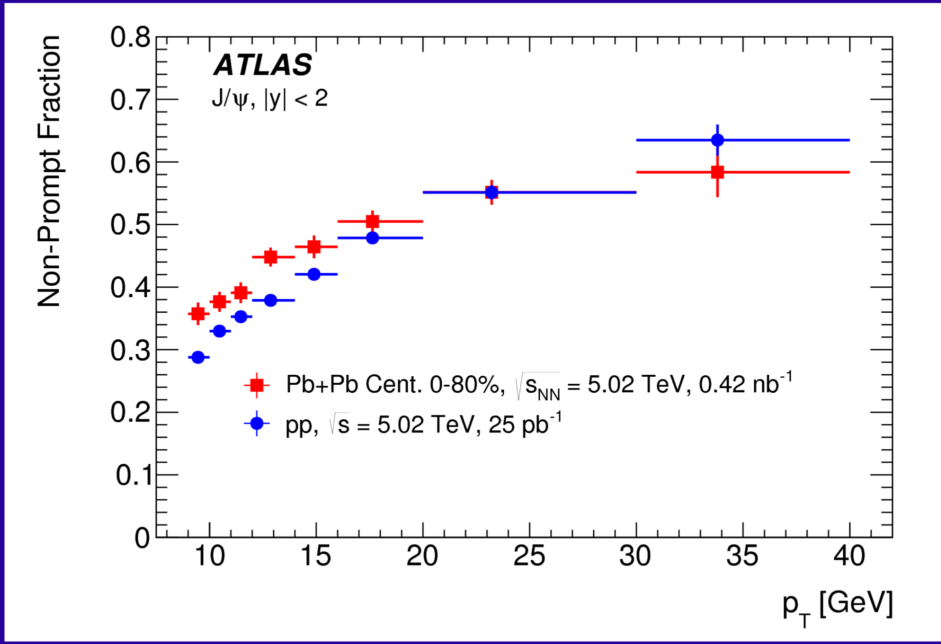

- Nearly independent on centrality.
- Slight difference from pp.

Upsilon R_{pPb}

arXiv1709.03089

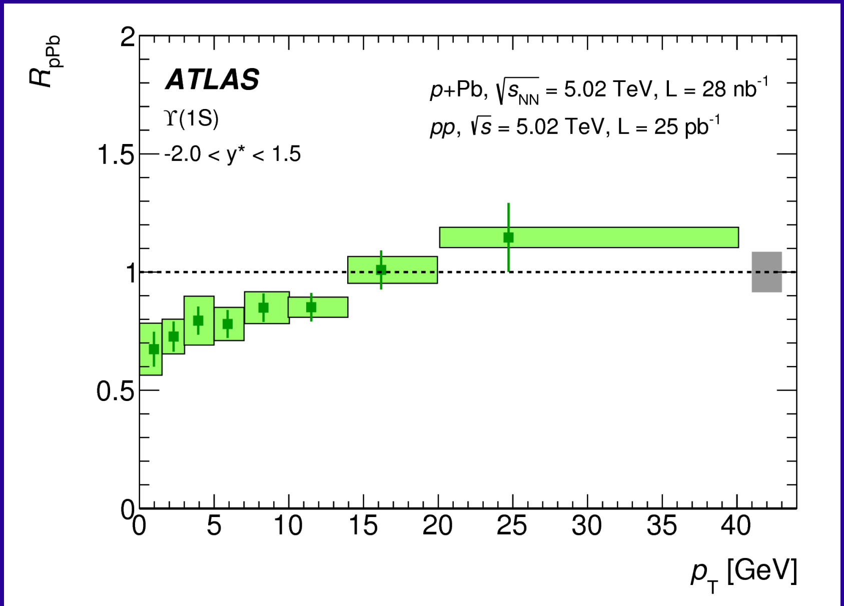

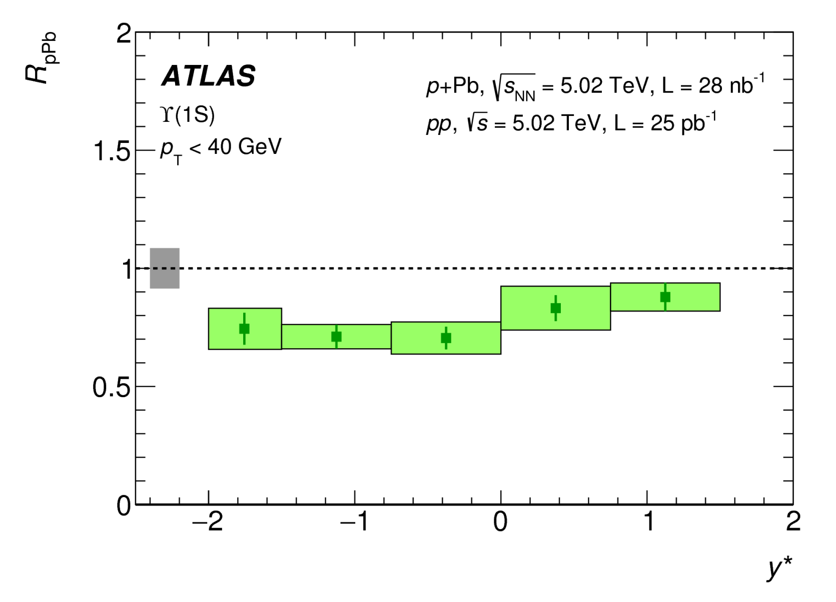

J/ψ R_{AA} as a function of |y| and centrality

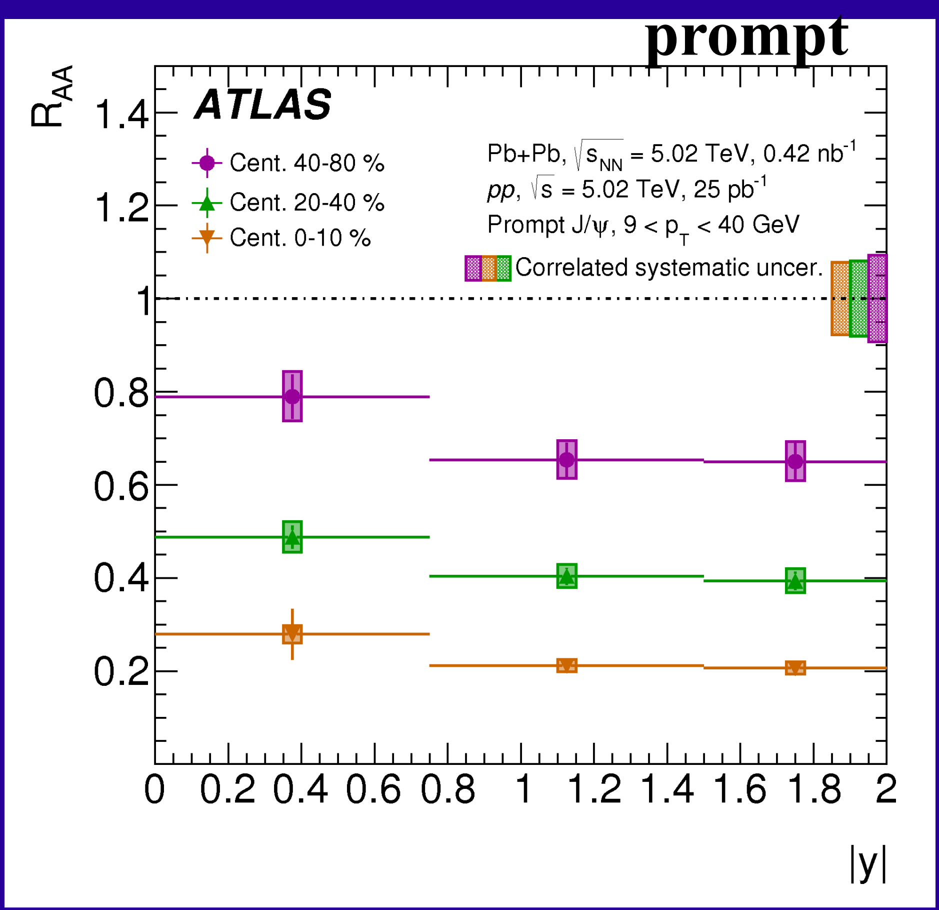

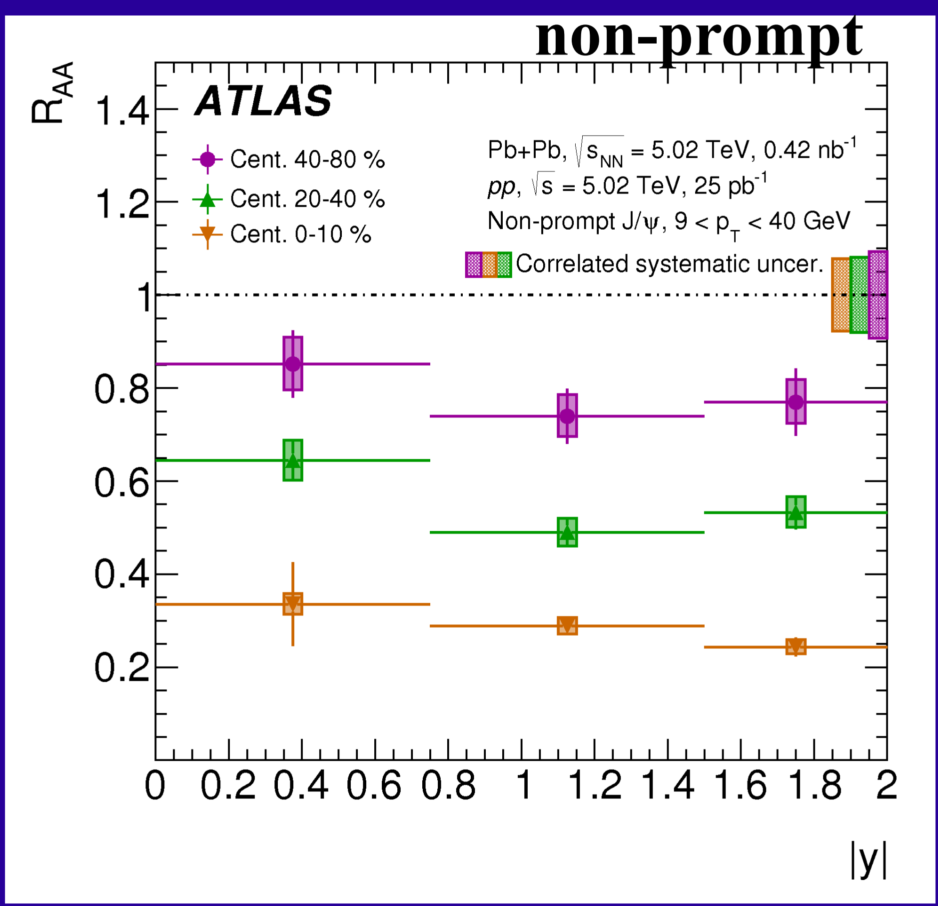

Modest dependence on rapidity for both prompt and non-prompt J/ψ.

Bottonium Fits to Dimuon Invariant Mass

$1.5 < p_T < 3.0$ GeV | $14.0 < p_T < 20.0$ GeV

pp

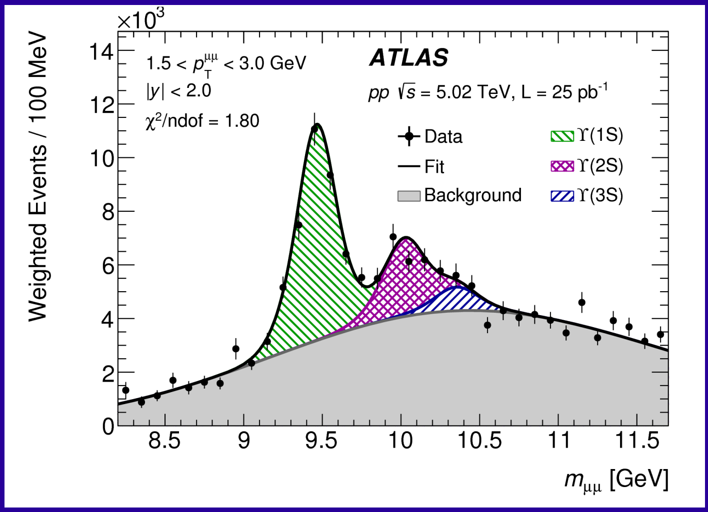

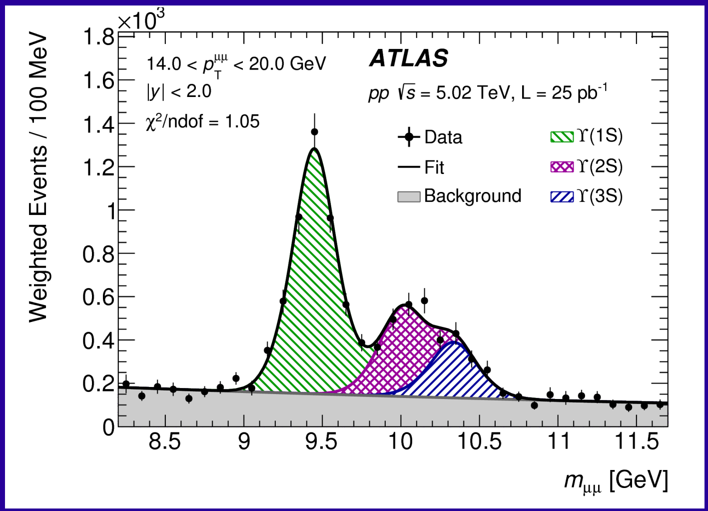

p+Pb

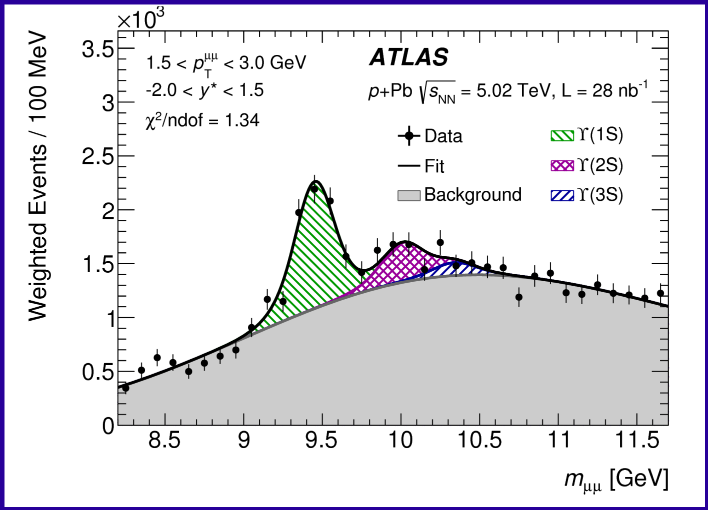

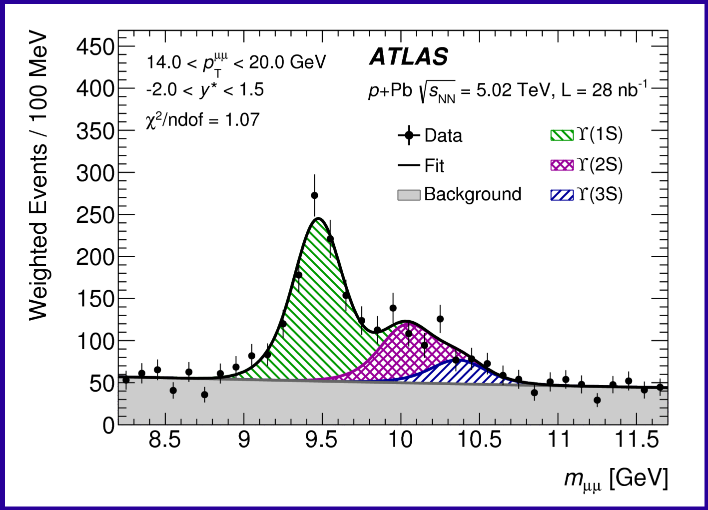

Quarkonia R_{pPb} as a function of p_T and y*

Eur. Phys. J. C 78 (2018) 171

p+Pb collisions are important to disentangle effects due to quarkonium interactions with QGP from those atributed to CNM.

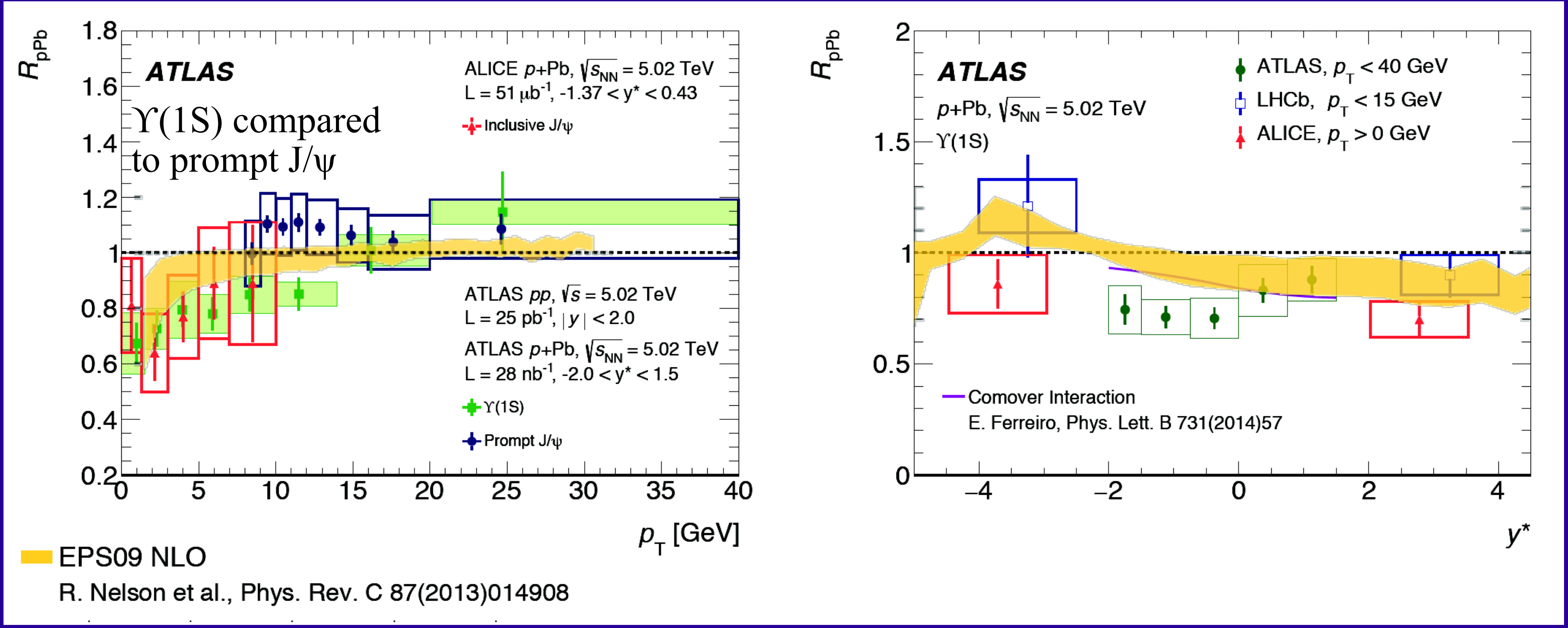

- R_{pPb} is consistent with unity for $p_T > 9$ GeV → important reference for the suppression at high p_T in larger collision systems (Pb+Pb and Xe+Xe).
- Models provide qualitatively good description.

Charged Hadron R_{AA} in Xe+Xe and Pb+Pb

ATLAS-CONF-2018-007

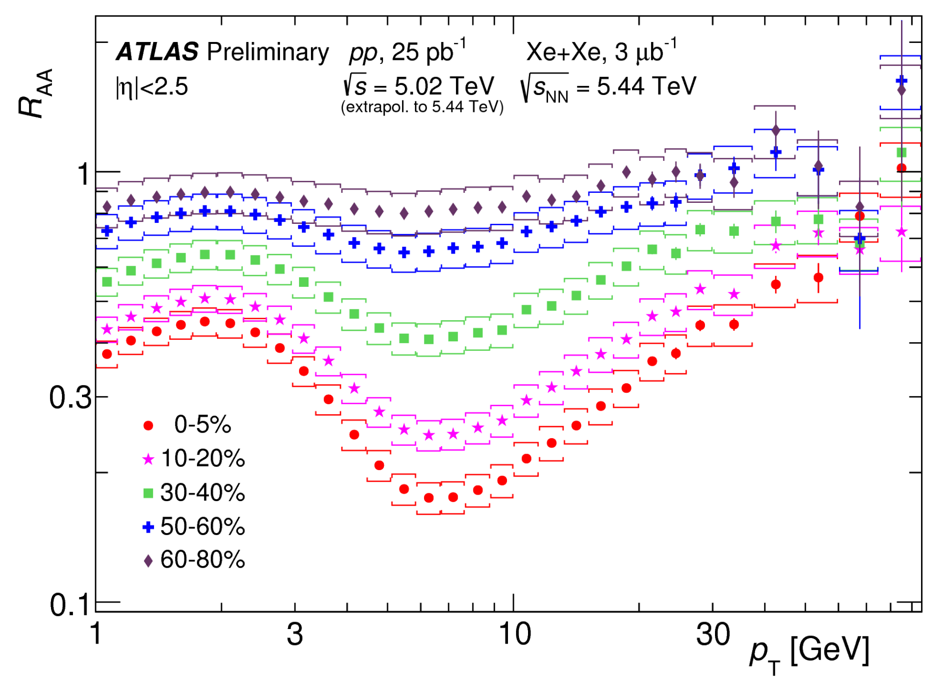

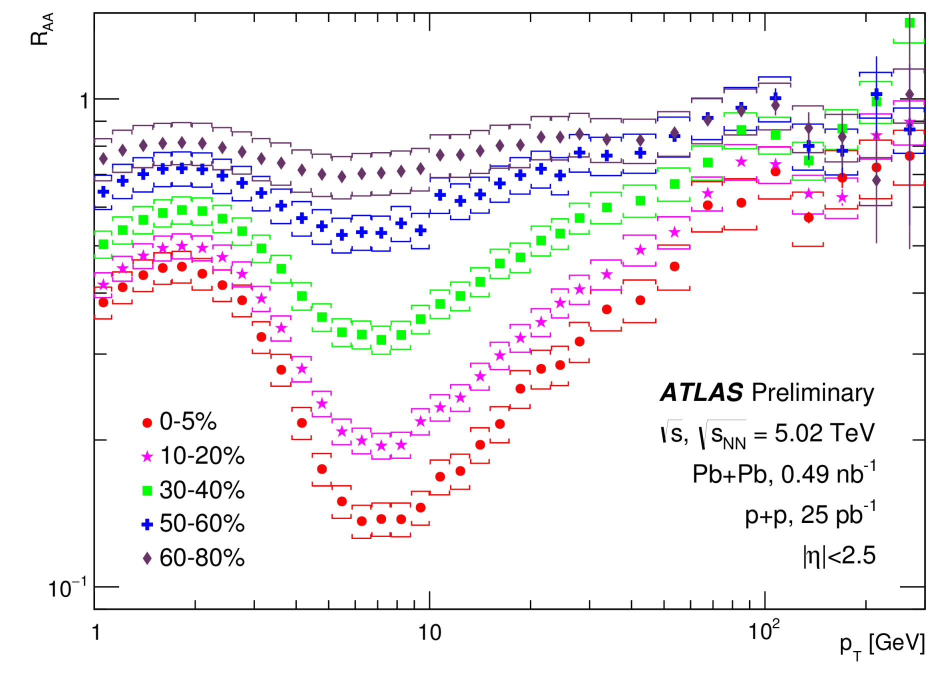

- Note different x-axis
- Qualitatively similar

Charged Hadron R_{AA} in Xe+Xe and Pb+Pb

ATLAS-CONF-2018-007

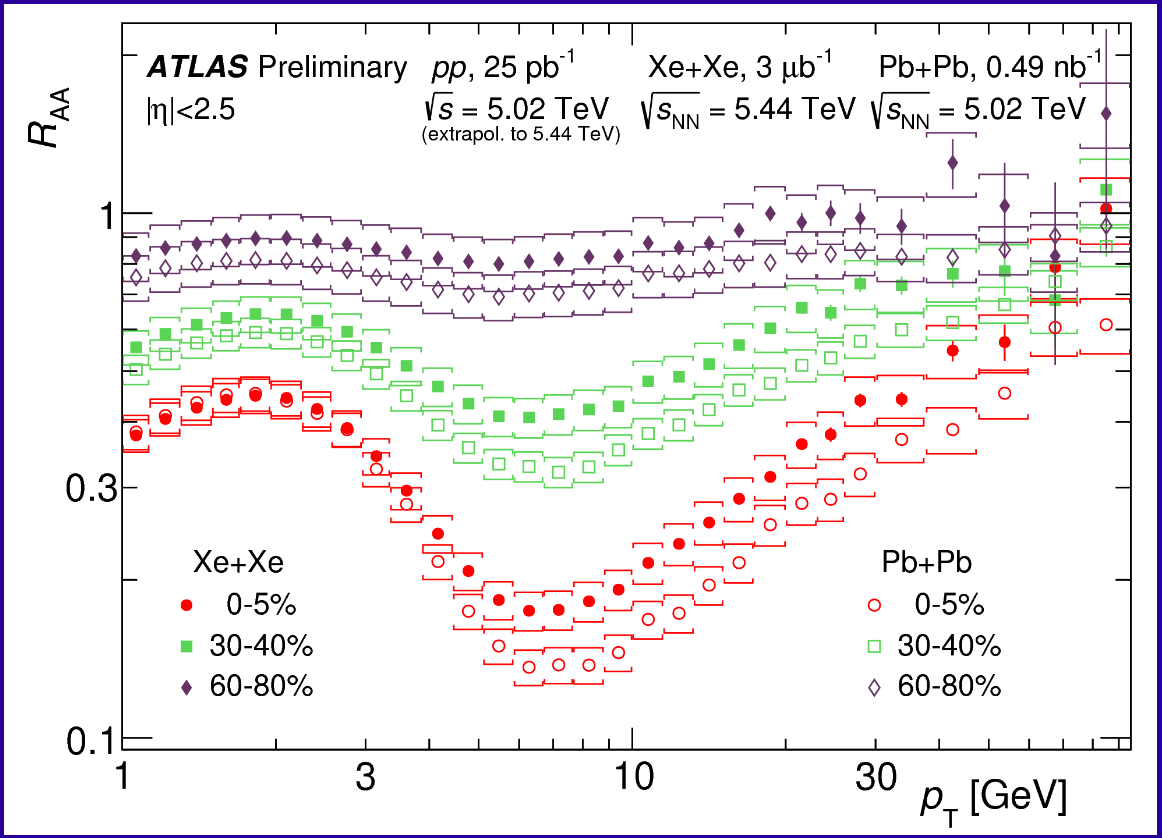

Same colours, same centrality

- R_{AA} is very similar at low pT in central collisions.
- Otherwise Xe+Xe is less suppressed than Pb+Pb.

Charged Hadron R_{AA} in Xe+Xe and Pb+Pb

ATLAS-CONF-2018-007

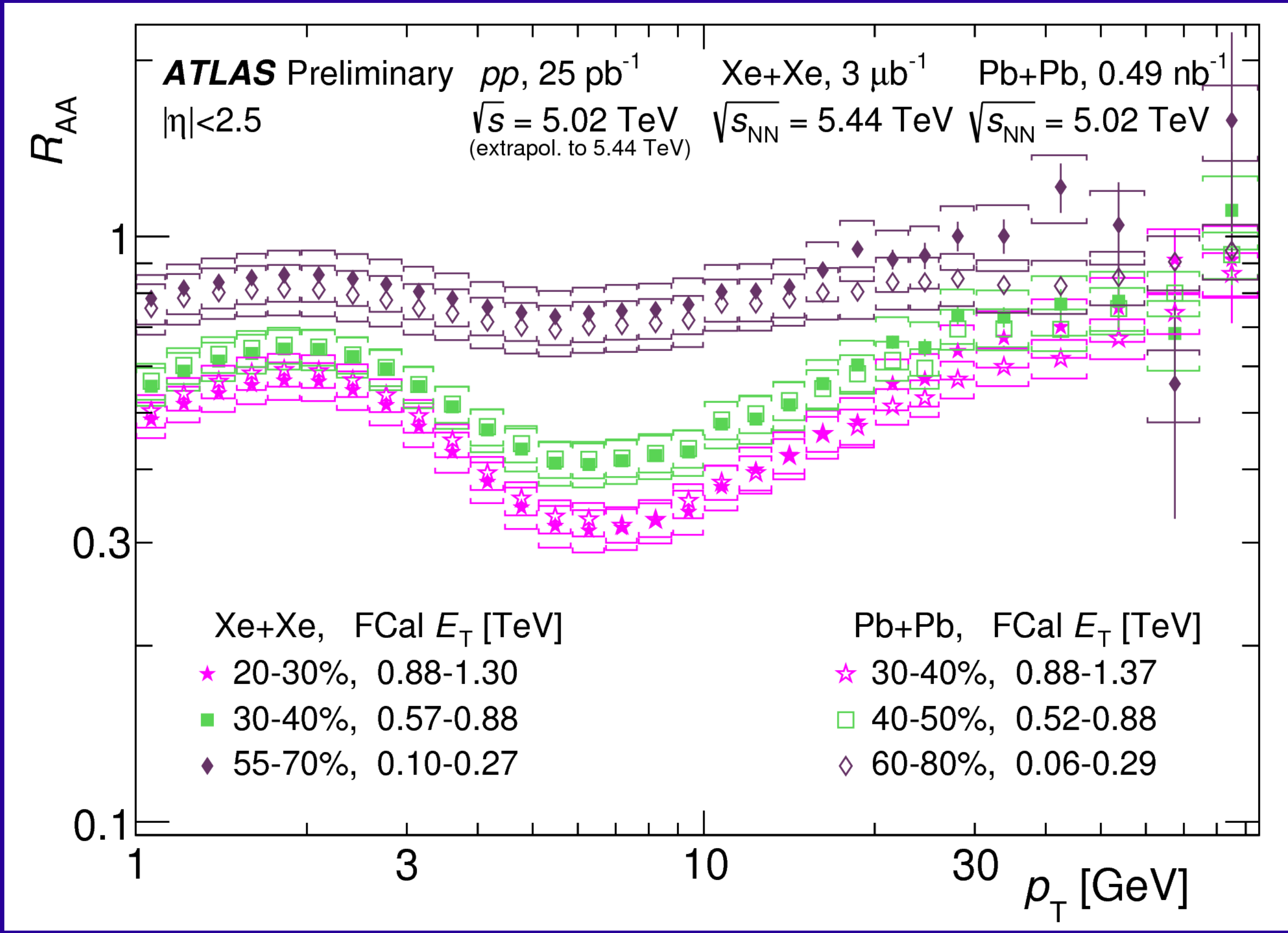

Same colours, same energy deposited in FCal

Two-particle correlations in Xe+Xe collisions

ATLAS-CONF-2018-011

Flow harmonics, v2—v5, have been measured in Xe+Xe at 5.44 TeV using 2-PC

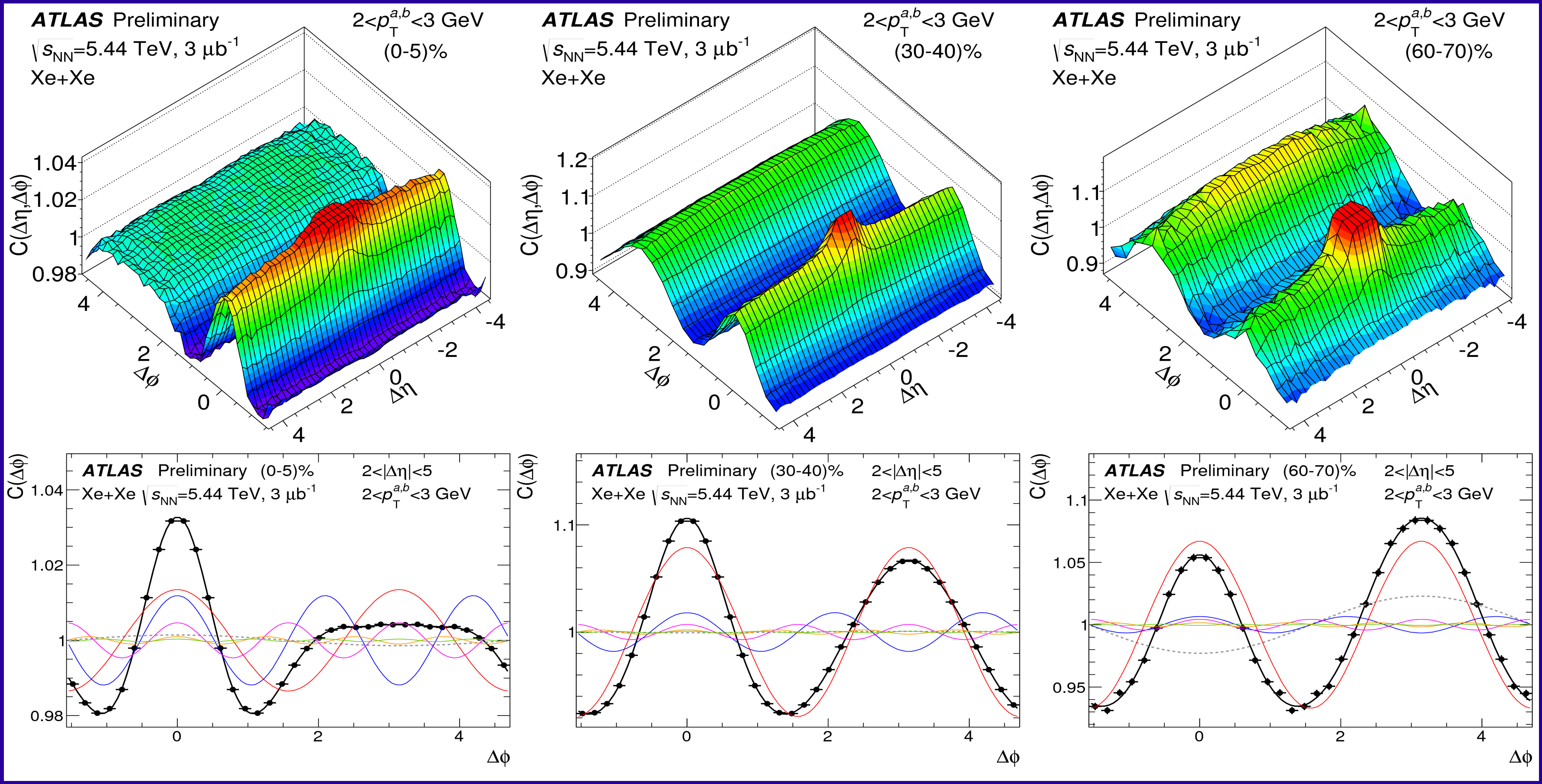

- Short-range ($\Delta\eta,\Delta\varphi$ ~ 0,0) correlations in all centralities are due to non-flow processes.
- Long-range ($\Delta\eta$ large) correlations are the result of the global anisotropy of the event.

Longitudinal flow decorrelations

Space-time evolution of the matter created is not boost-invariant in the longitudinal direction: $v_n(\eta_1) \neq v_n(\eta_2) \rightarrow$ FB asymmetry

$\Phi_n(\eta_1) \neq \Phi_n(\eta_2) \rightarrow$ sensitivity to twists

Harmonic flow vectors measured with charged particles over $|\eta| < 2.5$:

$$\vec{v}_n(\eta) = v_n(\eta) e^{in\Phi_n(\eta)}$$

Decorrelations → use $\boldsymbol{r}_{\mathbf{n|n,k}}$ between the ***k*th**-moment of the ***n*th**-order flow vectors in two different η intervals:

$$r_{n|n;k}(\eta) = \frac{\langle \boldsymbol{q}_n^k(-\eta)\boldsymbol{q}_n^{*k}(\eta_{\rm ref})\rangle}{\langle \boldsymbol{q}_n^k(\eta)\boldsymbol{q}_n^{*k}(\eta_{\rm ref})\rangle}$$

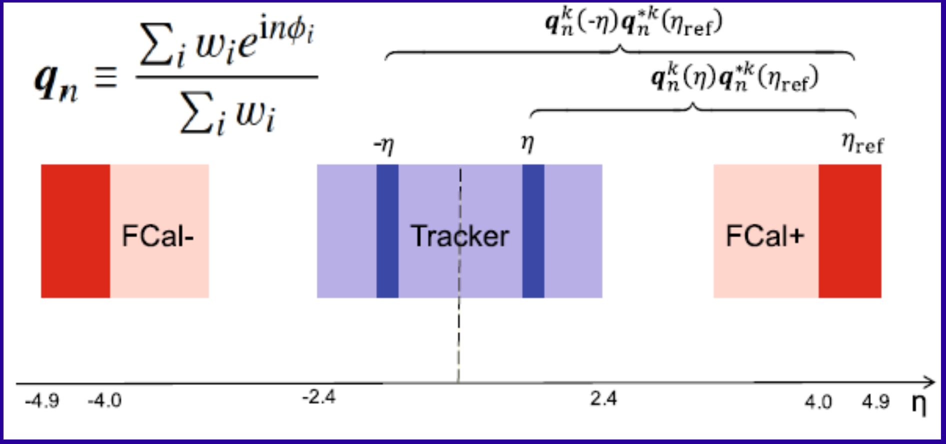

Longitudinal flow decorrelation in Pb+Pb collisions

Eur. Phys. J. C 76 (2018) 142

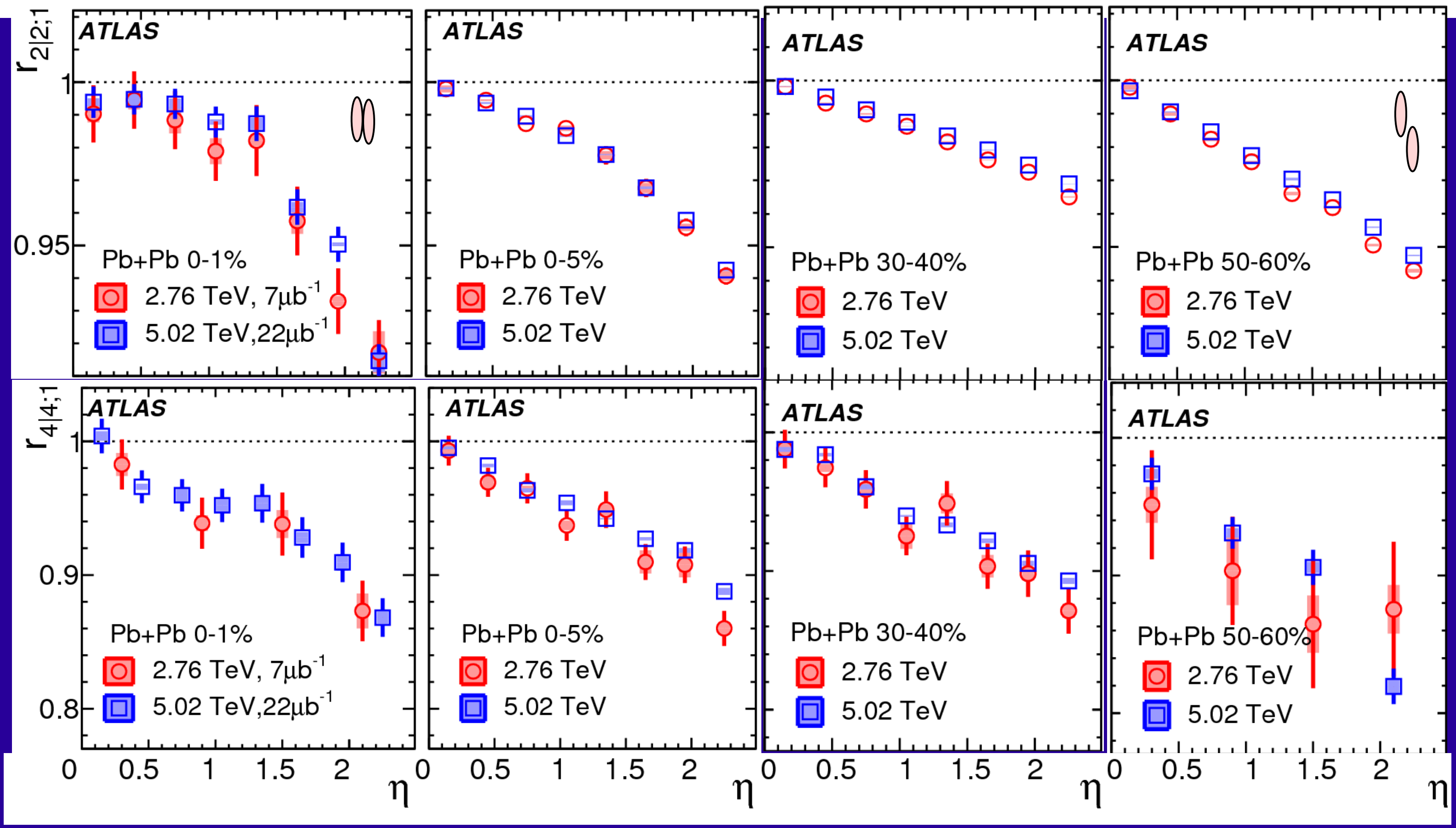

- $r_{n|n,k}$ shows a linear decrease with η_{ref}, except in the most central collisions.
- The decreasing trend of $r_{n|n,k}$ for n = 2—4 indicates significant breakdown of the factorisation of two-particle flow harmonics.
- The decreasing trend is slightly stronger at 2.76 TeV (collision system less boosted).

Jet Reconstruction in the Detector

- Jets are reconstructed by computational algorithms that group "towers" of energy deposited in the calorimeters.

- The Underlying Event ("background") is estimated event-by-event, excluding the jet candidate.

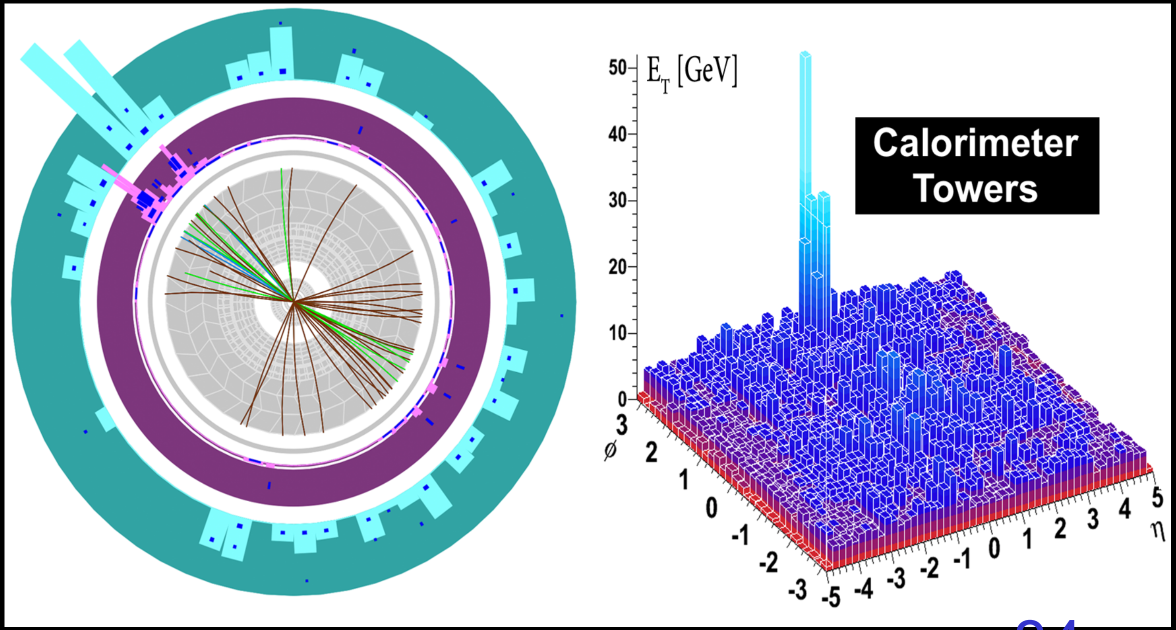

Jet Reconstruction

- Underlying event estimated and subtracted for each longitudinal layer and for 100 slices of $\Delta\eta = 0.1$:

$$E^{cell}_{T,sub} = E^{cell}_{T} - \rho \times A^{cell}$$

ρ is energy density estimated event-by-event from average over $0<\phi<2\pi$

• Two methods to avoid biasing ρ due to jets

1 - Sliding window exclusion
2 - Exclude cells in jets satisfying

$$D = E^{tower}_{T,max} / \langle E^{tower}_{T} \rangle > 5$$

- For R = 0.4, add an iteration step to ensure jets with E_T>50 GeV are always excluded from ρ estimate
- Correct for underlying event v_2

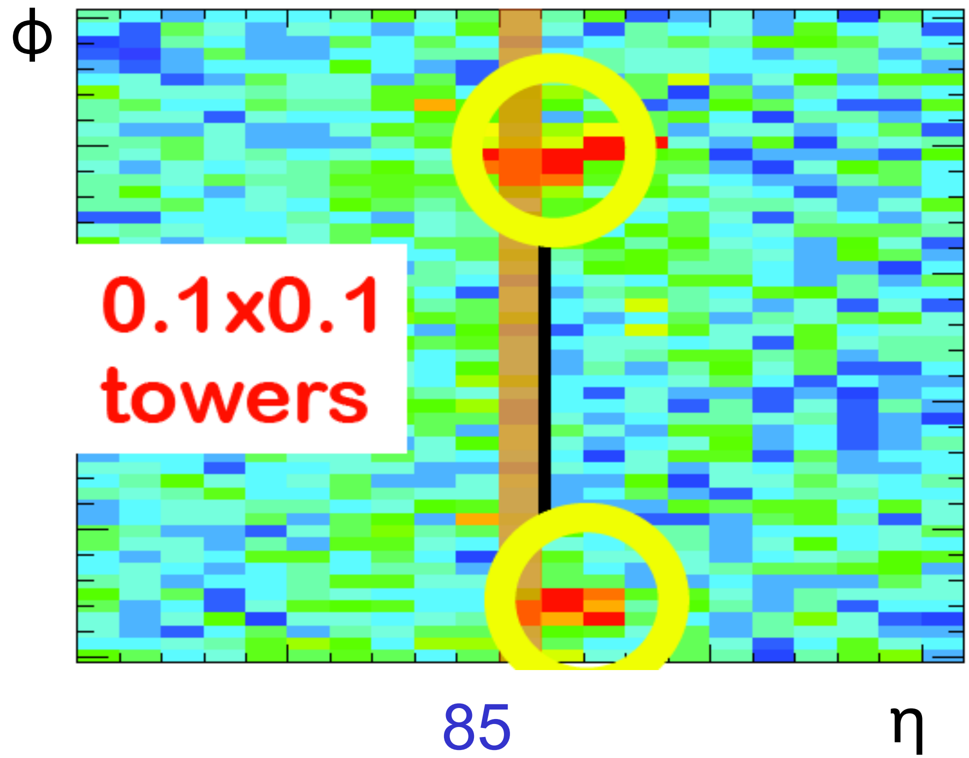

ATLAS

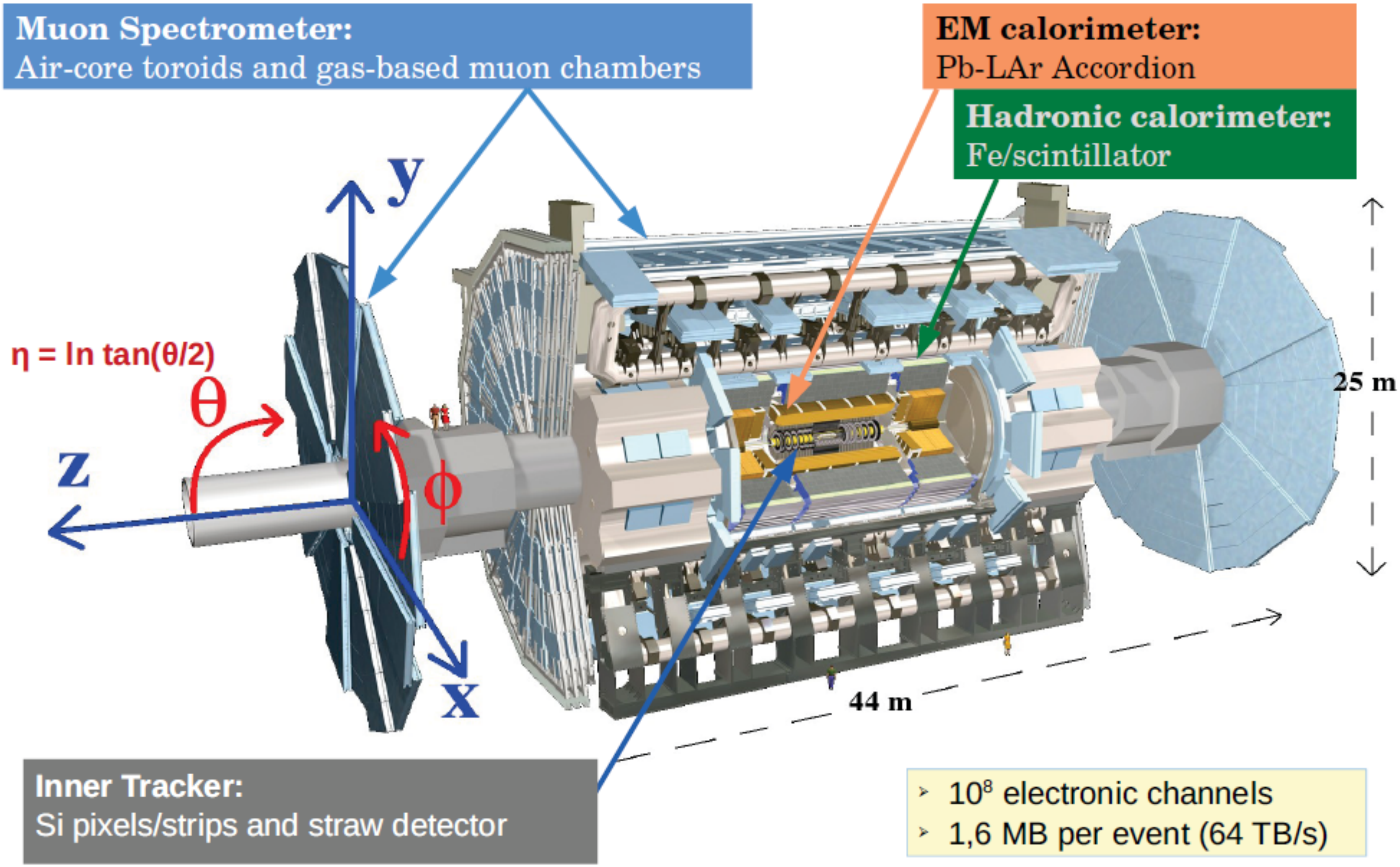

- 10^8 electronic channels
- 1,6 MB per event (64 TB/s)

Collisions Centrality

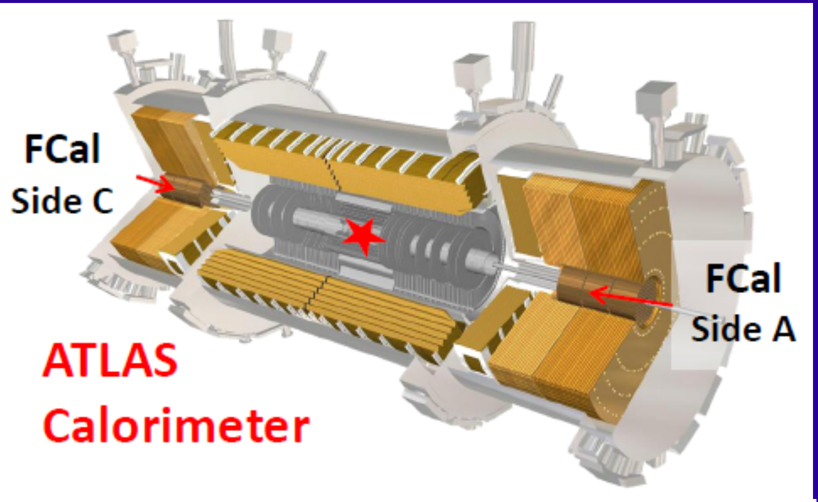

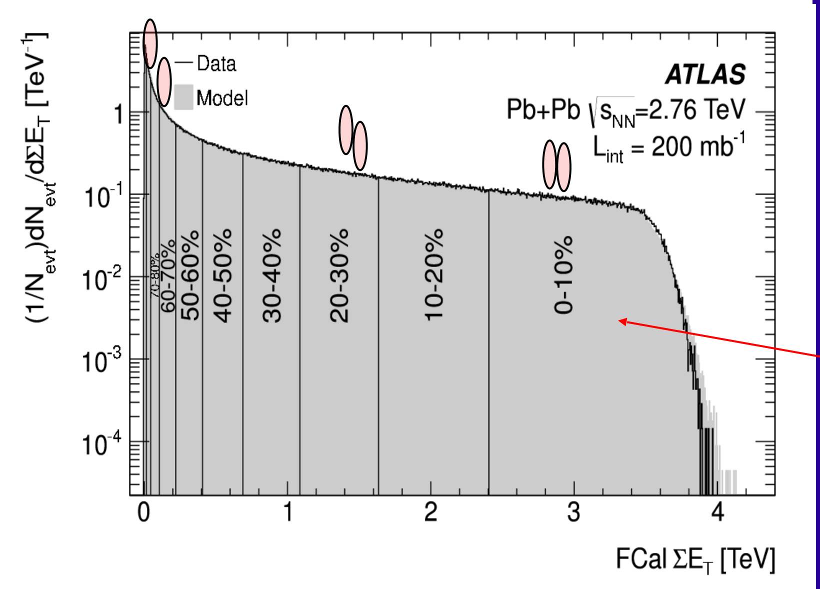

HI collision's dynamics controlled by impact parameter "*b*"

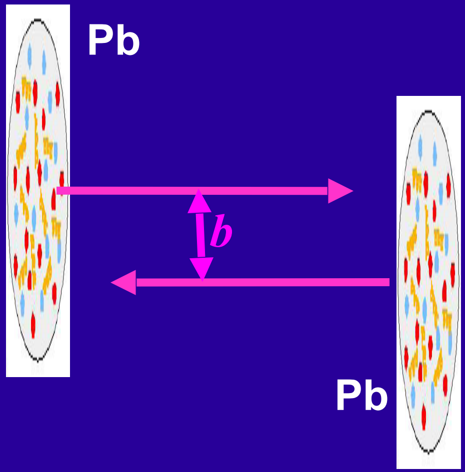

Transverse energy, E_T, deposited in Forward Calorimeter.

The number of binary nucleon-nucleon collisions, and number of participants in a collision for each centrality interval is estimated using a Glauber model.

Electroweak probes in p+Pb collisions – γ

ATLAS-CONF-2017-072

- Inclusive prompt photons in p+Pb collisions at 8.16 TeV.

E_T^γ **> 25 GeV**

E_T^{iso} **< 4.8 GeV + 4.2x10**$^{-3}E_T^\gamma$ **[GeV]**

- R_{pPb} consistent with unity at central and forward rapidity.
- R_{pPb}<1 for η* < –2 due to isospin effects.
- Data consistent within uncertainties with both free nPDF and with the small effects expected from a nuclear modification of the parton densities.
- Data disfavours large suppression due to E-loss.

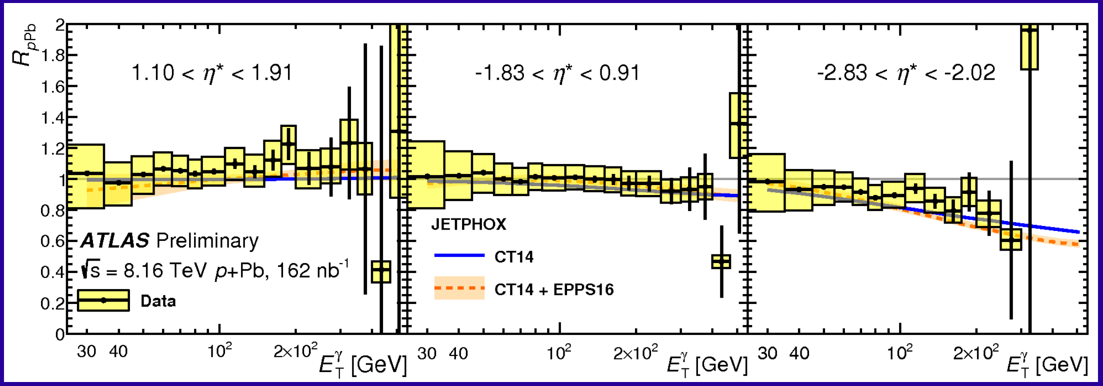

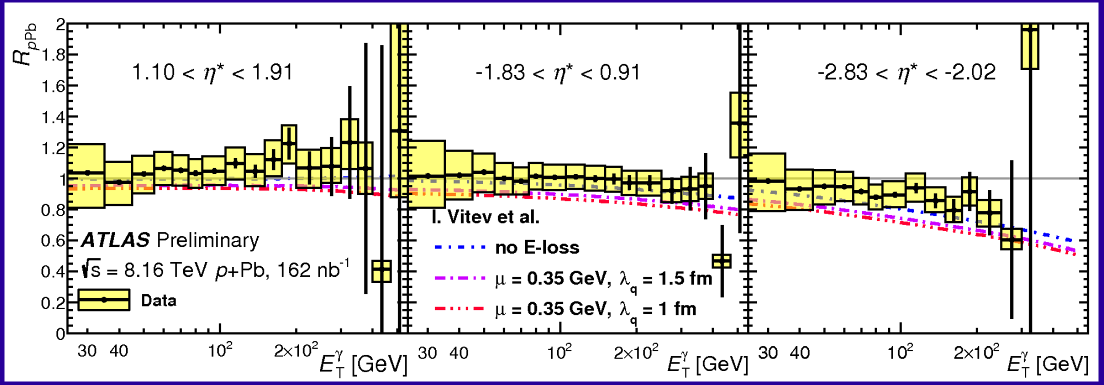

Electroweak probes: γ + jet p_T balance

Phys. Lett. B 789 (2019) 167

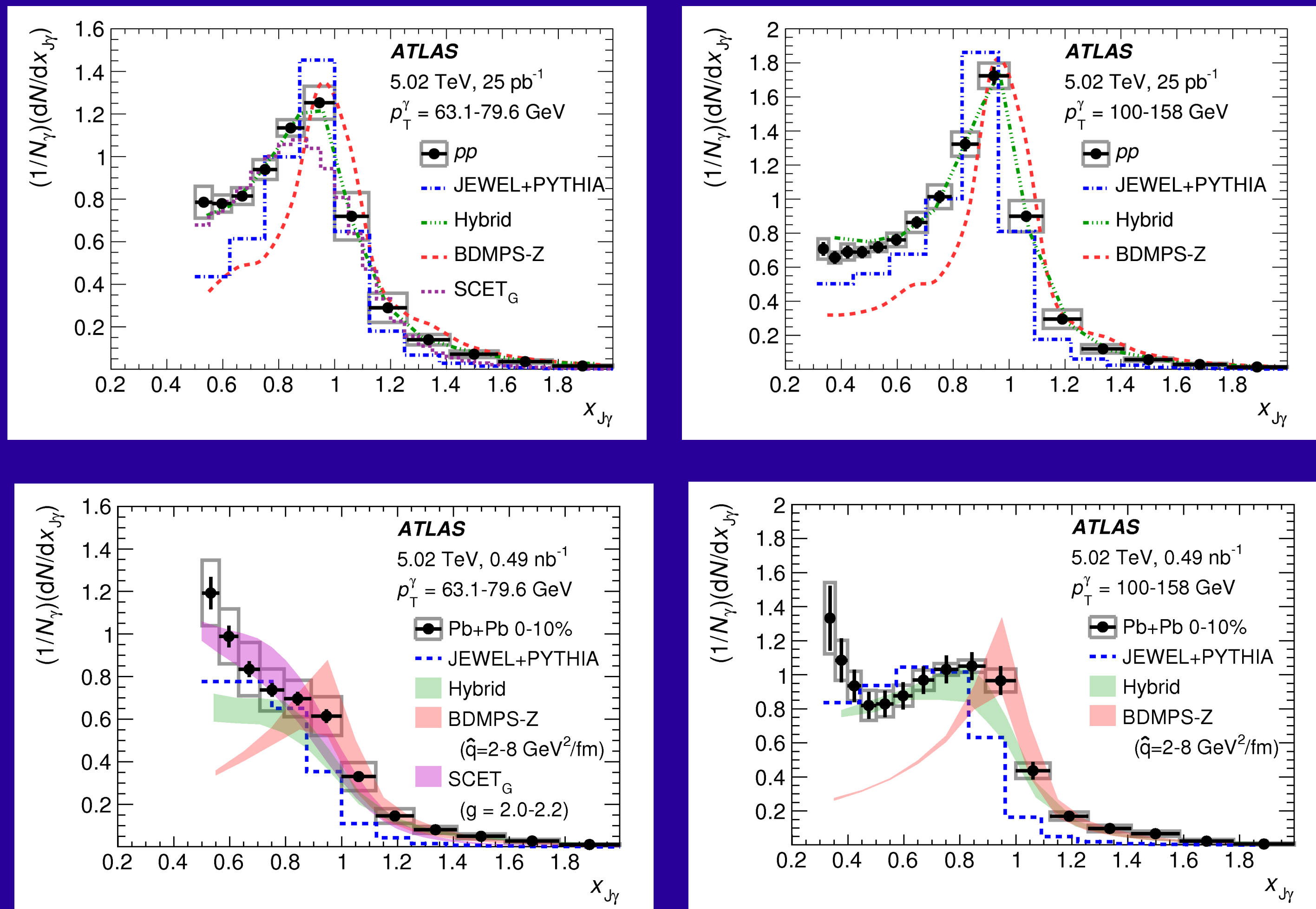

Jet v_n

ATLAS–CONF–2020–019

The v_2, v_3 and v_4 values for R=0.2 jets as a function of centrality

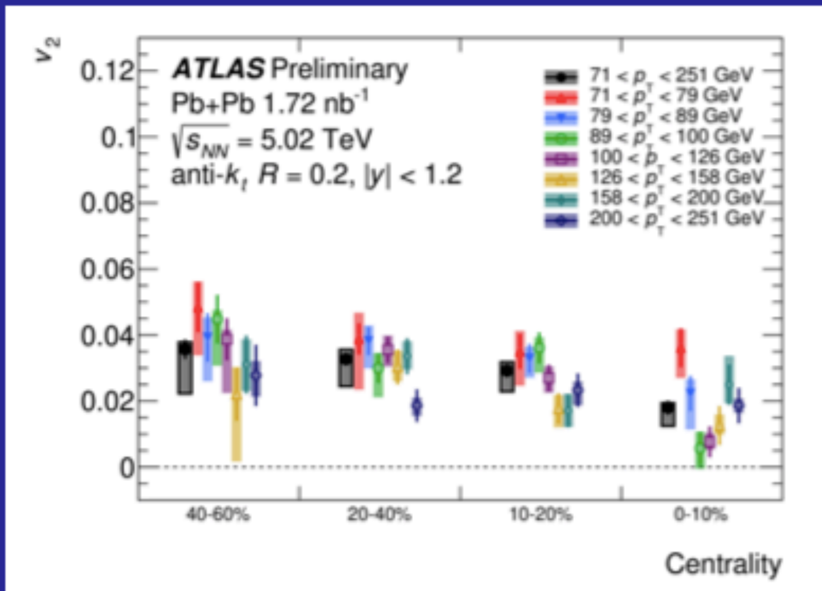

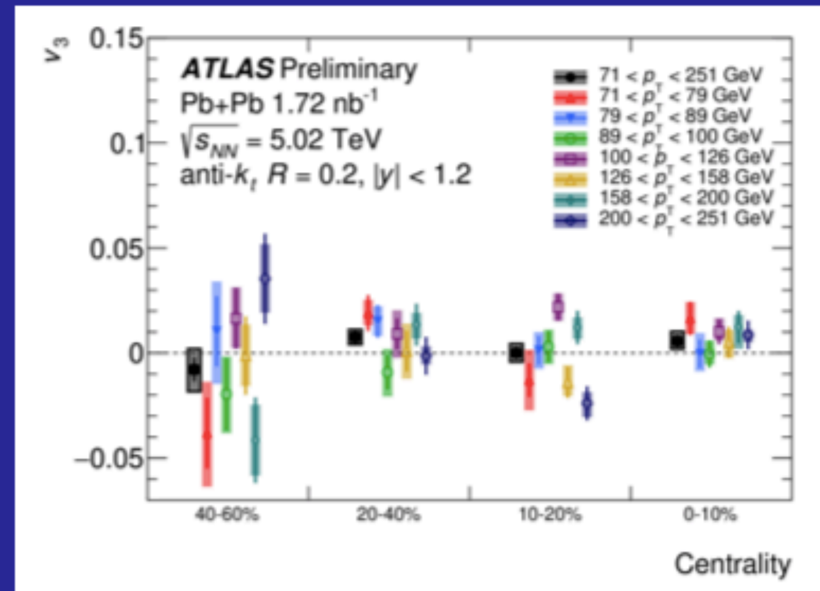

- Positive v_2, up to 4%.
- No dependence on the jet p_T within uncertainties.
- v_3 and v_4 compatible with 0.